

UNIVERSITY OF FLORIDA  
TRAINING REACTOR  
LICENSE NO. R-56  
DOCKET NO. 50-83

APPLICATION FOR CONVERSION FROM  
HIGH-ENRICHED TO LOW-ENRICHED  
URANIUM FUEL

REDACTED VERSION

SECURITY-RELATED INFORMATION REMOVED

Redacted text and figures blacked out or denoted by brackets



Nuclear Facilities  
Department of Nuclear and Radiological Engineering

202 Nuclear Sciences Center  
P.O. Box 118300  
Gainesville, Florida 32611-8300  
Tel: (352) 392-1408  
Fax: (352) 392-3380  
Email: vernet@ufl.edu

December 2, 2005

ATTN: Document Control Desk  
U.S. Nuclear Regulatory Commission  
Washington, DC 20555

Amendment 25  
UFTR Technical Specifications

UNIVERSITY OF FLORIDA TRAINING REACTOR  
FACILITY LICENSE: R-56, DOCKET NO. 50-83  
REQUEST FOR CHANGE IN TECHNICAL SPECIFICATIONS  
APPROVING HEU TO LEU CONVERSION

A proposed amendment to the UFTR Technical Specifications (R-56 License) for conversion from high enriched uranium (HEU) fuel to low enriched uranium (LEU) fuel affecting pages 4, 6, 13, 15 and 23 of the approved Tech Specs is attached. The proposed change will constitute Amendment 25 to the UFTR R-56 License as noted on the text pages. The changes are marked with the usual vertical line(s) in the right-hand margin with all amendments to date indicated on the bottom left on these five Tech Spec pages.

This change is requested to allow conversion of the UFTR to operate with low enriched uranium fuel. *Attachment I* to this letter contains the actual changed pages for the Tech Specs. *Attachment II* is the safety analysis on which the HEU to LEU conversion and the Tech Spec changes are based following the recommended format of NUREG-1537 (Guidelines for Preparing and Reviewing Applications for the Licensing of Non-Power Reactors) for such conversions.

For the UFTR HEU to LEU conversion, the only changes required for the UFTR Technical Specifications involve the fuel type and certain related specifications.

First, on page 4 of the Tech Specs, in Section 2.1, Safety Limits, specifications (1), (2) and (3), the safety limits on power level, primary coolant flow rate, and primary coolant outlet temperature from any fuel box are changed from their current specifications quoted as follows:

- (1) The steady-state power level shall not exceed 100 kWt.
- (2) The primary coolant flow rate shall be greater than 18 gpm at all power levels greater than 1 watt.
- (3) The primary coolant outlet temperature from any fuel box shall not exceed 200° F.

A020

to new specifications on power level, flow rate, and primary coolant outlet temperature from any fuel box, correlated with the existing limiting safety system setting (LSSS) (trip points) on power level of 125 kW, flow rate of 30 gpm and primary coolant outlet temperature of 200 F and the accident analysis results presented to assure conservative limits in Section 4.7 of *Attachment II* as follows:

- (1) The power level shall not exceed 190 kW.
- (2) The primary coolant flow rate shall be greater than 23 gpm at all power levels greater than 1 watt.
- (3) The primary coolant outlet temperature from any fuel box shall not exceed 160° F.

As noted in *Attachment II*, in the Section 4.7 analyses, the three parameters of power level, flow rate and primary coolant outlet temperature are interdependent so the safety limits are based on nominal as well as conservative analyses. For the nominal analyses, any two parameters are varied from nominal operating conditions to reach onset of nucleate boiling in the LEU core. In the conservative approach, any two parameters are varied from the LSSS point to reach onset of nucleate boiling. The actual proposed safety limits are based on a linear average of the two approaches as detailed in Section 4.7. In addition, the steady-state reference in specification (1) is removed as not applicable and the change from kWt to kW in specification (1) is simply to be consistent with the remainder of the Tech Specs. The resulting bases for specifications (1), (2) and (3) are then addressed together after the specifications in Section 2.1 as all three are interdependent with the objective now to prevent onset of nucleate boiling as a conservative objective and, as previously, to assure the fuel remains below temperatures at which fuel degradation would occur.

Second, on page 6 of the Tech Specs, in Section 3.1, Reactivity Limitations, paragraph (2), the core excess reactivity at cold critical, without xenon poisoning, is changed from not exceeding 2.3%  $\Delta k/k$  to not exceeding 1.4%  $\Delta k/k$ , again based on the accident analysis results presented in Section 13 of *Attachment II* and considering the actual realistic excess reactivity needed for operations.

Third, on page 13 of the Tech Specs, in Section 3.5, Limitations on Experiments, paragraph (3)(b), the limit on total absolute reactivity worth of all experiments is changed from not exceeding 2.3%  $\Delta k/k$  to not exceeding 1.4%  $\Delta k/k$  to be consistent with the change made on overall reactivity limitations per the previous paragraph.

Fourth, on page 15 of the Tech Specs, in Section 3.7, Fuel and Fuel Handling, paragraph (1), the description of fuel elements is changed from "fuel elements consisting of 11 plates each . . ." to "fuel elements consisting of 14 plates each . . ." This change is necessitated by the basic LEU fuel assembly design selected for the conversion as described in Section 4 of *Attachment II* for the LEU fuel.

Fifth, on page 23 of the Tech Specs, in Section 5.3, Reactor Fuel, in the first paragraph, line 2, the enrichment is changed to specify "no more than about 19.75% U-235" based on the LEU fuel selection. In lines 4 through 6, the allowable fabrication methodology is changed to allow high purity uranium silicide-aluminum dispersion fuel in addition to the currently allowed high purity

aluminum-uranium alloy. In the last line of the paragraph, the loading of U-235 per plate is changed to "nominally 12.5 g of U-235 per fuel plate." Again, these specifications are in agreement with the analysis provided in Section 4 of Appendix II for the LEU fuel.

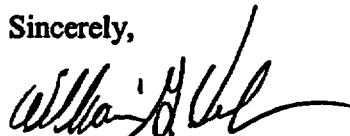
Sixth, on page 23 of the Tech Specs, in Section 5.4, Reactor Core, in the first paragraph, in line 1, the number of plates per assembly becomes 14 for LEU bundles versus 11 for HEU bundles. Similarly, in line 4, a full assembly shall be replaced with no fewer than 13 plates in a pair of partial assemblies versus 10 plates for the HEU core. Finally, in the second paragraph, the table giving the required nominal fuel element specifications is updated to provide the parameters for the LEU fuel per the analysis summarized in Section 4 of *Attachment II*.

This change as submitted is considered to have minor safety significance. This proposed change has been reviewed in progress by UFTR management and by the Reactor Safety Review Subcommittee (RSRS), as well as formally prior to submittal, with both concurring on this evaluation. In addition, as noted in the *Attachment II* safety analyses, a number of the members of the RSRS have been involved in developing this submittal.

This entire submittal consists of one signed original letter of transmittal plus *Attachment I* (Tech Spec changes) containing the proposed changes comprising the requested Amendment 25 to the UFTR Technical Specifications and *Attachment II* (safety analyses) containing details of supporting analyses per NUREG-1537. Thirteen additional photocopied sets are enclosed.

We appreciate your consideration of this amendment. Please advise if further information is needed.

Sincerely,



William G. Vernetson  
Director of Nuclear Facilities

WGV/dms

Attachments I & II plus  
Enclosures (13 sets of letter and attachments)

cc: Al Adams, NRC Project Manager  
Craig Bassett, NRC Inspector  
Reactor Safety Review Subcommittee

Sworn and subscribed this 2nd day of December 2005.



Notary Public



Terri L. Sparks  
Commission # DD346498  
Expires August 12, 2008  
Bonded Troy Fish - Insurance, Inc. 800-385-7010

**ATTACHMENT I**

**TECH SPEC CHANGES**

## **2.0 SAFETY LIMITS AND LIMITING SAFETY SYSTEM SETTINGS**

### **2.1 Safety Limits**

Safety limits for nuclear reactors are limits upon important process variables that are found to be necessary to reasonably protect the integrity of certain of the physical barriers that guard against the uncontrolled release of radioactivity. The principal physical barrier shall be the fuel cladding.

**Applicability:** These specifications apply to the variables that affect thermal, hydraulic, and materials performance of the core.

**Objective:** To ensure fuel cladding integrity.

**Specifications:**

- (1) The power level shall not exceed 190 kW.
- (2) The primary coolant flow rate shall be greater than 23 gpm at all power levels greater than 1 watt.
- (3) The primary coolant outlet temperature from any fuel box shall not exceed 160° F.
- (4) The specific resistivity of the primary coolant water shall not be less than 0.4 megohm-cm for periods of reactor operations over 4 hours.

**Bases:** Operating experiences and detailed calculations of Argonaut reactors have demonstrated that Specifications (1), (2) and (3) suffice to maintain core flow conditions to assure no onset of nucleate boiling within the core and the fuel and fuel cladding below temperatures at which fuel degradation would occur. Specification (4) suffices to maintain adequate water quality conditions to prevent deterioration of the fuel cladding and still allow for expected transient changes in the water resistivity.

### **2.2 Limiting Safety System Settings**

Limiting safety system settings for nuclear reactors are settings for automatic protective devices related to those variables having significant safety functions.

**Applicability:** These specifications are applicable to the reactor safety system set points.

**Objective:** To ensure that automatic protective action is initiated before exceeding a safety limit or before creating a radioactive hazard that is not considered under safety limits.

### 3.0 LIMITING CONDITIONS FOR OPERATIONS

Limiting conditions for operation are the lowest functional capabilities or performance levels required of equipment for safe operation of the facility.

#### 3.1 Reactivity Limitations

- (1) Shutdown Margin: The minimum shutdown margin, with the most reactive control blade fully withdrawn, shall not be less than 2%  $\Delta k/k$ .
- (2) Excess Reactivity: The core excess reactivity at cold critical, without xenon poisoning, shall not exceed 1.4%  $\Delta k/k$ .
- (3) Coefficients of Reactivity: The primary coolant void and temperature coefficients of reactivity shall be negative.
- (4) Maximum Single Blade Reactivity Insertion Rate: The reactivity insertion rate for a single control blade shall not exceed 0.06%  $\Delta k/k$  sec, when determined as an average over any 10 sec blade travel time from the characteristic experimental integral blade reactivity worth curve.
- (5) Experimental Limitations: The reactivity limitations associated with experiments are specified in Section 3.5 of this report.
- (6) Bases: These specifications are provided to limit the amount of excess reactivity to within limits known to be within the self-protection capabilities of the fuel, to ensure that a reactor shutdown can be established with the most reactive blade out of the core, to ensure a negative overall coefficient of reactivity, and to limit the reactivity insertion rate to levels commensurable with efficient and safe reactor operation.

#### 3.2 Reactor Control and Safety Systems

##### 3.2.1 Reactor Control System

- (1) Four cadmium-tipped, semaphore-type blades shall be used for reactor control. The control blades shall be protected by shrouds to ensure freedom of motion.
- (2) Only one control blade can be raised by the manual reactor controls at any one time. The safety blades shall not be used to raise reactor power simultaneously with the regulating blade when the reactor control system is in the automatic mode of operation.
- (3) The reactor shall not be started unless the reactor control system is operable.
- (4) The control-blade-drop time shall not exceed 1 sec from initiation of blade drop to full insertion (rod-drop time), as determined according to surveillance requirements.

Amendment 25

potential hazards, a determination will be made about the acceptable reactor power level and length of irradiation, taking into account such factors as: Isotope identity and chemical and physical form and containment, toxicity, potential for contamination of facility or environment, problems in removal or handling after irradiation including containment, transfer, and eventual disposition. Guidance should be obtained from the ANS 15.1 Standard. Experimental apparatus, material, or equipment to be inserted in the reactor shall be reviewed to ensure noninterference with the safe operation of the reactor.

**(2) Classification of Experiments**

**Class I** – Routine experiments, such as gold foil irradiation. This class shall be approved by the reactor manager; the radiation control officer may be informed if deemed necessary.

**Class II** – Relatively routine experiments that need to be documented for each new group of experimenters performing them, or whenever the experiment has not been carried out for one calendar year or more by the original experimenter, and that pose no hazard to the reactor, the personnel, or the public. This class shall be approved by the reactor manager and the radiation control officer.

**Class III** – Experiments that pose significant questions regarding the safety of the reactor, the personnel, or the public. This class shall be approved by the reactor manager and the radiation control officer, after review and approval by the Reactor Safety Review Subcommittee (RSRS).

**Class IV** – Experiments that have a significant potential for hazard to the reactor, the personnel, or the public. This class shall be approved by the reactor manager and radiation control officer after review and approval by the RSRS and specific emergency operating instructions shall be established for conducting the experiments.

**(3) Reactivity Limitations on Experiments**

- (a) The absolute reactivity worth of any single movable or nonsecured experiment shall not exceed 0.6%  $\Delta k/k$ .
- (b) The total absolute reactivity worth of all experiments shall not exceed 1.4%  $\Delta k/k$ .
- (c) When determining the absolute reactivity worth of an experiment, no credit shall be taken for temperature effects.
- (d) An experiment shall not be inserted or removed unless all the control blades are fully inserted or its absolute reactivity worth is less than that which could cause a positive 20-sec stable period.

**(4) Explosive Materials**

Explosive materials shall not be irradiated.



- (1) The evaluation alarm is actuated automatically when two area radiation monitors alarm high ( $\geq 25$  mrems/hr) in coincidence.
- (2) The evacuation alarm is actuated manually when an air particulate monitor is in a valid alarm condition.
- (3) The evacuation alarm is actuated manually when a reactor operator detects a potentially hazardous radiological condition and preventive actions are required to protect the health and safety of operating personnel and the general public.

**Bases:** To provide early and orderly evacuation of the reactor cell and the reactor building and to minimize radioactive hazards to the operating personnel and reactor building occupants.

### **3.7 Fuel and Fuel Handling**

**Applicability:** These specifications apply to the arrangement of fuel elements in core and in storage, as well as the handling of fuel elements.

**Objectives:** The objectives are to establish the maximum core loading for reactivity control purposes, to establish the fuel storage conditions, and to establish fuel performance and fuel-handling specifications with regard to radiological safety considerations.

#### **Specifications:**

- (1) The maximum fuel loading shall consist of 24 full fuel elements consisting of 14 plates each containing enriched uranium and clad with high purity aluminum.
- (2) Fuel element loading and distribution in the core shall comply with the fuel-handling procedures.
- (3) Fuel elements exhibiting release of fission products because of cladding rupture shall, upon positive identification, be removed from the core. Fission product contamination of the primary water shall be treated as evidence of fuel element failure.
- (4) The reactor shall not be operated if there is evidence of fuel element failure.
- (5) All fuel shall be removed and handled in accordance with approved procedures.
- (6) Fuel elements or fueled devices shall be stored and handled out of core in a geometry such that the  $k_{eff}$  is less than 0.8 under optimum conditions of moderation and reflection.
- (7) Irradiated fuel elements or fueled devices shall be stored so that temperatures do not exceed design values.

Amendment 15  
Amendment 25

prevent entrance during reactor operation. The freight door and panel shall not be used for general access to or egress from the reactor cell. This is not meant to preclude use of these doors in connection with authorized activities when the reactor is not in operation.

### 5.3 Reactor Fuel

Fuel elements shall be of the general MTR type, with thin fuel plates clad with aluminum and containing uranium fuel enriched to no more than about 19.75% U-235. The fuel matrix may be fabricated by alloying high purity aluminum-uranium alloy or the fuel matrix may be fabricated from uranium silicide-aluminum ( $U_3Si_2-Al$ ) using the powder metallurgy process. There shall be nominally 12.5 g of U-235 per fuel plate.

The UFTR facility license authorizes the receiving, possession, and use of

- (1) up to 4.82 kg of contained uranium-235
- (2) a 1-Ci sealed plutonium-beryllium neutron source
- (3) an up-to-25-Ci antimony-beryllium neutron source

Other neutron and gamma sources may be used if their use does not constitute an unreviewed safety questions pursuant to 10 CFR 50.59 and if the sources meet the criteria established by the Technical Specifications.

### 5.4 Reactor Core

The core shall contain up to 24 fuel assemblies of 14 plates each. Up to six of these assemblies may be replaced with pairs of partial assemblies. Each partial assembly shall be composed of either all dummy or all fueled plates. A full assembly shall be replaced with no fewer than 13 plates in a pair of partial assemblies.

Fuel elements shall conform to these nominal specifications:

Item	Specification
Overall size (bundle)	2.845 in. x 2.26 in. x 25.6 in.
Clad thickness	0.015 in.
Plate thickness	0.050 in.
Water channel width	0.111 in.
Number of plates	Standard fuel element – 14 fueled plates Partial element – no fewer than 13 plates in a pair of partial assemblies
Plate attachment	Bolted with spacers
Fuel content per plate	12.5 g U-235 nominal

Amendment 15  
Amendment 25

**ATTACHMENT II**

**SAFETY ANALYSES**

**SUBMITTAL REPORT  
To Cover Analyses of  
University of Florida Training Reactor (UFTR)  
Conversion from HEU to LEU Fuel**

**Submitted by**

**Alireza Haghighat, Ph.D.  
Prof. and Chair of the Nuclear and Radiological Engineering Department**

**University of Florida Training Reactor Facility  
Nuclear and Radiological Engineering Department  
College of Engineering  
University of Florida  
Gainesville, Florida**

**December 2005**

<b>Prepared by</b>	Benoit Dionne Alireza Haghighat
<b>Reviewed by</b>	Jim Matos (ANL) John Stillman (ANL) Glenn Sjoden William Vernetson
<b>Technical Contributors</b>	
Section 4.5	Benoit Dionne Ce Yi Robert Smith John Stillman (ANL) Kevin Manalo Gabriel Ghita Jangyong Huh Mike Wenner
Section 4.7	A. Olson E. Feldman Benoit Dionne Bobby Ahmed Anne Charneau
Section 13.1 to 13.3	John Stillman (ANL) Pat Garner (ANL)
Section 13.4 to 13.5	Phil Pfeiffer (ANL) Travis Mock V. Spring Cornelison
Sections 12,14 and 15	Benoit Dionne William Vernetson
Appendix A	Benoit Dionne Ce Yi
Appendix B	ANL
<b>UF Faculty Contributors</b>	Alireza Haghighat Glenn Sjoden William Vernetson Jim Baciak Samim Anghaie

Note that, unless specified otherwise, all contributors are part of the University of Florida Department of Nuclear and Radiological Engineering.

# Table of Contents

<b>TABLE OF CONTENTS</b>	<b>3</b>
<b>LIST OF FIGURES</b>	<b>6</b>
<b>LIST OF TABLES</b>	<b>7</b>
<b>SUMMARY</b>	<b>8</b>
<b>1. GENERAL DESCRIPTION OF THE FACILITY</b>	<b>8</b>
1.1 Introduction	8
1.2 Summary and Conclusions of Principal Safety Considerations	8
1.3 Summary of Reactor Facility Changes	8
1.4 Summary of Operating License, Technical Specifications, and Procedural Changes	8
1.5 Comparison with Similar Facilities Already Converted	9
<b>2. SITE CHARACTERISTICS</b>	<b>9</b>
<b>3. DESIGN OF STRUCTURES, SYSTEMS, AND COMPONENTS</b>	<b>9</b>
<b>4. REACTOR DESCRIPTION</b>	<b>9</b>
4.1 Reactor Facility	9
4.2 Reactor Core	11
4.2.1 Fuel Elements	12
Fuel Plate Description	12
Fuel Bundle Description	14
Fuel Box Description	15
4.2.2 Control Blades	16
4.2.3 Neutron Reflector	18
4.2.4 Neutron Source and Holder	18
4.2.5 In-Core Experimental Facilities	18
4.2.6 Reactor Materials	18
4.3 Reactor Tank and Biological Shielding	19
4.4 Core Support Structure	19
4.5 Dynamic Design	19
4.5.1 Calculation Model	19
Material Composition	19
Geometric Model	22
Benchmarking of the HEU Core Criticality Model	22
4.5.2 Critical Core Configuration	24
4.5.3 Excess Reactivity and Control Blade Worth	27
	3

Excess Reactivity for HEU and LEU Cores	27
Integral Control Blade Worth for HEU and LEU Cores	27
Maximum Reactivity Insertion Rate for HEU Core	28
Maximum Reactivity Insertion Rate for LEU Core	29
4.5.4 Shutdown Margin for HEU and LEU Cores	31
4.5.5 Other Core Physics Parameters	31
HEU Reactivity Coefficients and Kinetic Parameters	31
LEU Reactivity Coefficients and Kinetic Parameters	33
4.6 Functional Design of the Reactivity Control System	34
4.7 Thermal-hydraulic Analyses	34
4.7.1 Fuel Assembly and Fuel Box Geometry	34
4.7.2 PLTEMP/ANL v2.14 Code Description	36
4.7.3 Thermal-Hydraulic Analysis Results	38
<b>5. REACTOR COOLANT SYSTEM</b>	<b>41</b>
<b>6. ENGINEERING SAFETY FEATURES</b>	<b>41</b>
<b>7. INSTRUMENTATION AND CONTROL</b>	<b>41</b>
<b>8. ELECTRICAL POWER SYSTEM</b>	<b>41</b>
<b>9. AUXILIARY SYSTEM</b>	<b>41</b>
<b>10. EXPERIMENTAL FACILITY AND UTILIZATION</b>	<b>41</b>
<b>11. RADIATION PROTECTION AND RADIOACTIVE WASTE MANAGEMENT</b>	<b>41</b>
<b>12. CONDUCT OF OPERATION</b>	<b>42</b>
12.1 Organization and Staff Qualification	42
12.2 Procedures	42
12.3 Operator Training and Re-qualification	42
12.4 Emergency Plan	42
12.5 Physical Security	42
12.6 Reactor Reload and Startup Plan	43
<b>13. ACCIDENT ANALYSIS</b>	<b>43</b>
13.1 Reactivity Insertion Accidents	44
13.1.1 Step Insertion of 0.6% $\Delta k/k$	44
13.1.2 Slow Insertion of 0.06% $\Delta k/k$ /second	47
13.1.3 Sudden Insertion of the Maximum Allowed Excess Reactivity	49

<b>13.2 Loss-of-Coolant Accident</b>	<b>51</b>
<b>13.3 Fuel Handling Accident (FHA)</b>	<b>52</b>
13.3.1 Radionuclide Inventories	52
13.3.2 Methodology for Dose Calculations	53
Site Boundary (Occupational Exposure)	53
Urban Boundary (Public Exposure)	54
13.3.3 Dose Calculation Results for Fuel Handling Accident	55
<b>13.4 Maximum Hypothetical Accident (MHA)</b>	<b>57</b>
13.4.1 Radionuclide Inventories	58
13.4.2 Methodology for Dose Calculations	59
13.4.3 Dose Calculations for Maximum Hypothetical Accident	59
 <b>14. TECHNICAL SPECIFICATIONS</b>	 <b>62</b>
 <b>15. OTHER LICENSE CONSIDERATIONS</b>	 <b>62</b>
 <b>APPENDIX A</b>	 <b>64</b>
<b>A.1 Determination of Material Composition</b>	<b>64</b>
<b>A.2 Power History for the HEU Core</b>	<b>70</b>
<b>A.3 Impact of the Boron Content for the HEU Core</b>	<b>71</b>
<b>A.4 Determination of the Critical LEU Core</b>	<b>71</b>
<b>A.5 Detailed Flux Profiles for the HEU and LEU cores</b>	<b>73</b>
A.5.1 HEU Detailed Flux Profiles	74
A.5.2 LEU Detailed Flux Profiles	77
<b>A.6 Comparison of the parameters in the six-factor formula for HEU and LEU cores</b>	<b>80</b>
 <b>APPENDIX B</b>	 <b>82</b>
<b>B.1 ENGINEERING UNCERTAINTY FACTORS</b>	<b>82</b>
 <b>REFERENCES</b>	 <b>84</b>



## List of Figures

<i>Figure 4-1 Schematic Horizontal Cut of the UFTR Core</i>	11
<i>Figure 4-2 HEU and LEU Fuel Plate Dimensions</i>	13
<i>Figure 4-3 HEU Fuel Bundle XY Cut</i>	14
<i>Figure 4-4 LEU Fuel Bundle XY Cut</i>	14
<i>Figure 4-5 YZ Cut of a Fuel Box</i>	15
<i>Figure 4-6 XY Cut of One Quarter of a Fuel Box</i>	16
<i>Figure 4-7 Location of Control Blade Shrouds</i>	16
<i>Figure 4-8 XZ and YZ Cut of a Magnesium Shroud</i>	17
<i>Figure 4-9 Control Blade Dimensions</i>	17
<i>Figure 4-10 Cadmium Absorber Insert Dimensions</i>	17
<i>Figure 4-11 Reflector Regions Modeled in MCNP5</i>	18
<i>Figure 4-12 Schematic of the UFTR MCNP5 Model</i>	22
<i>Figure 4-13 Schematic of the Foil Positions within the CVP and Rabbit System</i>	23
<i>Figure 4-14 Fuel Pattern in the HEU Core</i>	25
<i>Figure 4-15 Fuel Pattern in the LEU Core</i>	25
<i>Figure 4-16 Integral Blade Worth versus Position for Safety 3 in the UFTR HEU Core.</i>	29
<i>Figure 4-17 Integral Blade Worth versus Position for Safety 2 in the UFTR LEU Core</i>	30
<i>Figure 13-1 Power and Clad Temperature Response to Slow Insertion of 0.06% <math>\Delta k/k/s</math> with SCRAM in HEU Core</i>	48
<i>Figure 13-2 Power and Clad Temperature Response to Slow Insertion of 0.06% <math>\Delta k/k/s</math> with SCRAM in LEU Core</i>	48
<i>Figure 13-3 Relationship Between Reactivity Coefficient and Inverse Period from D12/25 SPERT-I Tests</i>	50
<i>Figure 13-4 Thyroid Doses and Whole Body Doses for the Fuel Handling Accident</i>	57
<i>Figure 13-5 Thyroid Doses and Whole Body Doses for the Maximum Hypothetical Accident</i>	61

# List of Tables

<b>Table 4-1 Summary of Key Nominal Design Parameters of HEU (current) and LEU (expected) Cores</b>	<b>10</b>
<b>Table 4-2 Characteristics of the HEU and LEU Fuel Elements</b>	<b>12</b>
<b>Table 4-3 Fuel Bundle Characteristics of the HEU and LEU Cores</b>	<b>14</b>
<b>Table 4-4 Fuel Box Dimensions</b>	<b>15</b>
<b>Table 4-5 Composition of the HEU and LEU Fuel</b>	<b>19</b>
<b>Table 4-6 Selected Isotopes Considered for Criticality Calculation</b>	<b>20</b>
<b>Table 4-7 Other Materials Characteristics for HEU and LEU Cores</b>	<b>21</b>
<b>Table 4-8 Composition of LEU Fuel Cladding</b>	<b>21</b>
<b>Table 4-9 Comparison of Measured and Calculated Foil Reaction Rates in the CVP and Rabbit System</b>	<b>24</b>
<b>Table 4-10 Control blade positions for the HEU and LEU Cores</b>	<b>26</b>
<b>Table 4-11 Power Generated in Fuel for Depleted HEU and Reference LEU Cores</b>	<b>26</b>
<b>Table 4-12 Calculated Excess Reactivity for the HEU and LEU Cores (Fresh and Depleted)</b>	<b>27</b>
<b>Table 4-13 Comparison of Control Blades Worth for the HEU and LEU Cores</b>	<b>28</b>
<b>Table 4-14 Integral Reactivity Worth versus Position for Safety 3 in the HEU Core</b>	<b>28</b>
<b>Table 4-15 Integral Reactivity Worth Versus Position for Safety 2 in the LEU Core</b>	<b>30</b>
<b>Table 4-16 Shutdown Margins for the Current HEU Core and the Reference LEU Core</b>	<b>31</b>
<b>Table 4-17 Kinetics Parameters and Reactivity Coefficients for the UFTR HEU Core</b>	<b>33</b>
<b>Table 4-18 Kinetics Parameters and Reactivity Coefficients for the UFTR LEU Core</b>	<b>33</b>
<b>Table 13-1 Kinetics Parameters and Reactivity Coefficients Calculated for UFTR Accident Analyses.</b>	<b>44</b>
<b>Table 13-2 Selected Parameters for UFTR HEU and LEU Core Transient Analyses.</b>	<b>45</b>
<b>Table 13-3 RELAP5-3D Results for Step Insertion of 0.6% <math>\Delta k/k</math> in UFTR.</b>	<b>46</b>
<b>Table 13-4 RELAP5-3D Results for Slow Insertion of 0.06% <math>\Delta k/k</math>/second.</b>	<b>47</b>
<b>Table 13-5 Transient Response from a Sudden Reactivity Insertion</b>	<b>51</b>
<b>Table 13-6 Calculated Radionuclide Inventories (Ci) Released into the Reactor Cell from the FHA in the HEU and LEU Cores</b>	<b>53</b>
<b>Table 13-7 Dose Conversion Factors Utilized for Site and Urban Boundary Analyses</b>	<b>55</b>
<b>Table 13-8 Thyroid Doses and Whole Body Doses Calculated at the <u>Site Boundary</u> (30 m) for the FHA in the HEU and LEU Cores</b>	<b>56</b>
<b>Table 13-9 Thyroid Doses and Whole Body Doses Calculated at the <u>Urban Boundary</u> (400 m) for the FHA in the HEU and LEU Cores</b>	<b>56</b>
<b>Table 13-10 Thyroid and Whole Body Doses Calculated at Points of Interest Between the Site (30 m) and the Urban Boundary (400 m) for the FHA in the HEU and LEU Cores.</b>	<b>57</b>
<b>Table 13-11 Calculated Radionuclide Inventories (Ci) Released into the Reactor Cell from the Maximum Hypothetical Accident in the HEU and LEU Cores</b>	<b>59</b>
<b>Table 13-12 Thyroid Doses and Whole Body Doses Calculated at the <u>Site Boundary</u> (30 m) for the MHA in the HEU and LEU Cores.</b>	<b>60</b>
<b>Table 13-13 Thyroid Doses and Whole Body Doses Calculated at the <u>Urban Boundary</u> (400 m) for the MHA in the HEU and LEU Cores.</b>	<b>60</b>
<b>Table 13-14 Thyroid and Whole Body Doses Calculated at Points of Interest Between the Site Boundary (30 m) and the Urban Boundary (400 m) for the MHA in the HEU and LEU Cores.</b>	<b>61</b>
<b>Table 14-1 Summary of LEU Fuel Parameters to be Updated in the Technical Specifications</b>	<b>Error!</b>
<b>Bookmark not defined.</b>	

## **Summary**

This report contains the results of design and safety analyses performed by the University of Florida Nuclear and Radiological Engineering Department (NRE) and RERTR program at the Argonne National Laboratory (ANL) for conversion of the University of Florida Training Reactor (UFTR) from the use of highly-enriched uranium (HEU) fuel to low-enriched uranium (LEU) fuel. This study investigates the performance and safety margins of the proposed LEU core under nominal and accident conditions. It identifies any necessary changes to the UFTR Final Safety Analysis Report and Technical Specifications (FSAR, Ref. 1).

## **1. General Description of the Facility**

### **1.1 Introduction**

This section provides an overview of the changes to the physical, nuclear and operational characteristics of the facility required by the HEU to LEU conversion of the UFTR fuel.

The HEU to LEU conversion only requires the use of a different fuel type and core configuration, and does not require any changes to the remainder of the facility.

The proposed LEU critical core contains 22 fuel bundles, one partial fuel bundle (with 10 fuel plates and 4 dummy plates), and one dummy bundle. Based on this core configuration, it is concluded: i) the shutdown margin meets the required limit; ii) the reactivity coefficients remain negative; iii) fuel integrity is maintained under all operating conditions; and iv) dose to public from the Maximum Hypothetical Accident (MHA) and Fuel Handling Accident (FHA) remains below the maximum permissible limit.

The HEU to LEU conversion requires changes to the Technical Specifications, procedures, and emergency plan as discussed in Sections 9, 12, and 14.

### **1.2 Summary and Conclusions of Principal Safety Considerations**

The LEU core meets all the safety requirements as specified in FSAR.

### **1.3 Summary of Reactor Facility Changes**

The LEU fuel bundle has the same overall design as the present HEU fuel bundle; except that it contains 14 fuel plates with  $U_3Si_2$ -Al fuel meat instead of 11 fuel plates of U-Al alloy fuel meat. The cladding of the HEU fuel is composed of 1100 aluminum alloy while the LEU fuel cladding is composed of 6061 aluminum alloy. This LEU silicide fuel has been approved by the Nuclear Regulatory Commission (NRC) for use in non-power reactors (Ref. 2).

### **1.4 Summary of Operating License, Technical Specifications, and Procedural Changes**

In addition to the updated LEU fuel parameters, the safety limits presented in the Technical Specifications for power, flow rate and outlet temperature are changed (see Section 4.7 and 14) as well as the reactivity limitations on excess reactivity and experiment worth (see Section 13 and 14).

## **1.5 Comparison with Similar Facilities Already Converted**

In 1991, the Iowa State University successfully converted their Argonaut reactor (UTR-10) facility using the same type of fuel plate. The main differences between the UTR-10 and UFTR are the power level and the core configuration. Following closure of the Iowa State reactor fuel inspection revealed presence of unexpected corrosion. This issue has been analyzed in an INL/ANL report (Ref. 3). To minimize the possibility of corrosion, the manufacturer (BWXT) of the LEU fuel for the UFTR will apply a surface treatment resulting in a protective boehmite layer on the surface of the cladding. It is concluded that corrosion should not occur in the UFTR core and, in fact, the corrosion of the fuel at the UTR-10 was not expected to limit core usage.

## **2. Site Characteristics**

The HEU to LEU conversion does not impact the site characteristics. More details about this topic can be found in Ref. 1.

## **3. Design of Structures, Systems, and Components**

The HEU to LEU conversion does not require any changes to the design of structure, systems, and components. More details about this topic can be found in Ref. 1.

## **4. Reactor Description**

### **4.1 Reactor Facility**

The HEU to LEU conversion of the UFTR facility requires only changes in the core configuration and fuel type. All the following aspects of the facility remain unchanged:

- Control Blades
- Neutron Reflector
- Neutron Source and Holder
- In-Core Experimental Facilities
- Reactor Tank and Biological Shielding
- Core Support Structure
- Functional Design of the Reactivity Control System

The HEU and LEU cores contain different type of fuel meat, thickness of fuel meat and fuel plate, type of Al cladding, fuel enrichment, and fuel loading per plate. The current HEU core and the proposed LEU core also differ primarily in the number of fuel plates per fuel bundle with the number of full/partial fuel bundles, and number of dummy bundles. Note that the proposed LEU core configuration may differ when the actual fuel loading is performed.

Table 4-1 provides a comparison of the key design safety features of the HEU and LEU fuel bundles and a comparison of the key reactor and safety parameters that were calculated for each core. The results show that the UFTR reactor facility can be operated as safely with the new LEU fuel bundles as with the present HEU fuel bundles.

**Table 4-1 Summary of Key Nominal Design Parameters of HEU (current)  
and LEU (expected) Cores**

	<u>HEU</u>	<u>LEU</u>
<b><u>DESIGN DATA</u></b>		
Fuel Type	U-Al alloy	U <sub>3</sub> Si <sub>2</sub> -Al
Fuel Meat Size		
Width (cm)	5.96	5.96
Thickness (cm)	0.102	0.051
Height (cm)	60.0	60.0
Fuel Plate Size		
Width (cm)	7.23	7.23
Thickness (cm)	0.178	0.127
Height (cm)	65.1	65.1
Cladding	1100 Al	6061 Al
Cladding Thickness (cm)	0.038	0.038
Fuel Enrichment (nominal)	93.0 %	19.75%
"Meat" Composition (wt% U)		62.98
Mass of <sup>235</sup> U per Plate (nominal)		12.5 g
Number of Plates per Fuel Bundle	11	14
Number of Full Fuel Bundles (current/expected)	21	22
Number of Partial Fuel Bundles	1	1
	(5 fuel plates + 5 dummy plates)	(10 fuel plates + 4 dummy plates)
Number of Dummy Bundles	2	1
<b><u>REACTOR PARAMETERS</u></b>		
Fresh Core Excess Reactivity (% Δk/k)	1.09	0.925
Shutdown Margin (Δk/k)	3.11	3.17
Control blade worth,		
Regulating (% Δk/k)	0.87	0.65
Safety 1 (% Δk/k)	1.35	1.65
Safety 2 (% Δk/k)	1.63	1.81
Safety 3 (% Δk/k)	2.06	1.48
Maximum Reactivity Insertion Rate (% Δk/k/s)	0.042	0.045
Average Coolant Void Coefficient (% Δk/k/%void)	-0.148	-0.153
Coolant Temp. Coefficient (% Δk/k/°C)	-5.91E-03	-5.68E-03
Fuel Temp. Coefficient (% Δk/k/°C)	-2.91E-04	-1.40E-03
Effective Delayed Neutron Fraction	0.0079	0.0077
Neutron Lifetime (μs)	187.4	177.5
<b><u>THERMAL-HYDRAULIC PARAMETERS</u></b>		
Max. Fuel Temperature <sup>1</sup> (°C)	69.6	72.0
Max. Clad Temperature <sup>1</sup> (°C)	69.7	66.8
Max. Clad-to-Coolant Temperature Diff. <sup>1</sup> (°C)	31.6	19.3
Mixed Mean Coolant Outlet temperature (°C)	50.6	48.8
Minimum ONBR	1.75	1.93

<sup>1</sup> At nominal operating conditions

## 4.2 Reactor Core

This chapter provides a detailed description of the components and structures in the reactor core. Comparisons between the HEU and LEU cores are presented when the conversion requires changes in some characteristics.

The UFTR is a heterogeneous, graphite/water moderated and water cooled reactor fueled with 93% enriched plate-type U-Al fuel. In its current configuration, the core can contain up to 24 bundles (fuel or dummy) arranged in 2x2 arrays within six aluminum fuel boxes. It is possible to use bundles which contain a mix of dummy and fuel plates.

The reactor is controlled by means of four control blades (3 safety blades and 1 regulating blade) of swing-arm type. The blades are mounted on the side of the core and swing downward through the core between the fuel boxes. Each control blade is encased in a magnesium shroud.

The fuel boxes and the magnesium shrouds are surrounded by a stack of graphite stringers, which act as both moderator and reflector. Figure 4-1 shows the UFTR core. More detailed figures of the UFTR core can be found in Ref. 1.



Figure 4-1 Schematic Horizontal Cut of the UFTR Core

Heat removal is achieved during reactor operation by providing forced circulation into the core, i.e., by pumping water upward through fuel boxes in a closed loop and consequently between the plates and fuel bundles contained in each box.

### 4.2.1 Fuel Elements

The HEU and LEU fuel elements have similar overall designs, i.e., they are both plate-type elements composed of a "sandwich" of fuel "meat" and aluminum cladding. The plates are then assembled in bundles which, in turn, are inserted into the fuel boxes. More details about the specifications of the UFTR LEU fuel can be found in Ref. 4.

#### Fuel Plate Description

The HEU fuel meat consists of uranium-aluminum alloy with 93 wt% enriched uranium while the LEU fuel meat consists of  $U_3Si_2$ -aluminum dispersion fuel with 19.75 wt% enriched uranium. Table 4-2 compares various characteristic of the HEU and LEU fuel elements.

Table 4-2 Characteristics of the HEU and LEU Fuel Elements

	HEU <sup>1</sup>	LEU
Fuel plate,		
Width (cm)	7.23	7.23
Thickness (cm)	0.178	0.127
Height (cm)	65.1	65.1
Fuel meat,		
Width (cm)	5.96	5.96 <sup>2</sup>
Thickness (cm)	0.102	0.051
Height (cm)	60.0	60.0
Cladding,		
Along Width (cm)	0.635	0.635 <sup>2</sup>
Along Thickness (cm)	0.038	0.038
Coolant Channel Thickness (cm)	0.348	0.282
Volume ratios,		
Fuel-to-Coolant	0.08	0.05

<sup>1</sup> UFTR drawing #021-80-107 which corresponds to the 1957 design

<sup>2</sup> Drawing #441597 from INEEL shows tolerances between 5.89cm and 6.27cm for the width of the fuel meat (x-axis). The size was chosen to be the same as HEU for convenience until an "as-built" drawing is available.

The major difference in the fuel plates is that the LEU fuel meat is one half the thickness of the HEU fuel meat. Figures 4-2 a) and b), respectively, show the HEU and LEU plates, and provide the dimensions of the different segments of each plate type.

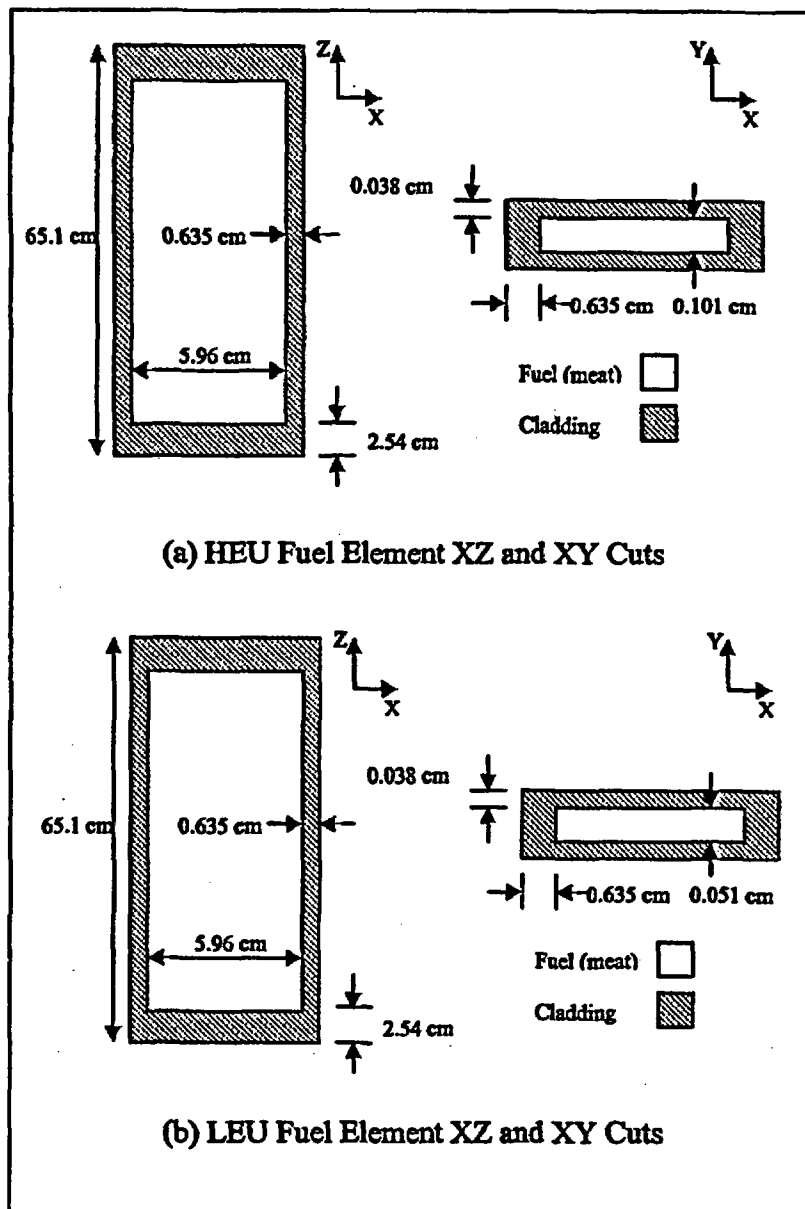


Figure 4-2 HEU and LEU Fuel Plate Dimensions

The axes displayed in Figure 4-2 represent the orientation of the elements in the model. The x-axis, y-axis, and z-axis are set along the east-west, north-south and bottom-top axes of the core, respectively.

The HEU and LEU dummy plates are identical to their respective fuel plates with the obvious exception of the "meat".



### Fuel Bundle Description

Each HEU fuel bundle is composed of 11 fuel plates. A water gap of 0.348 cm is provided between the fuel plates for coolant flow as illustrated in Figure 4-3.

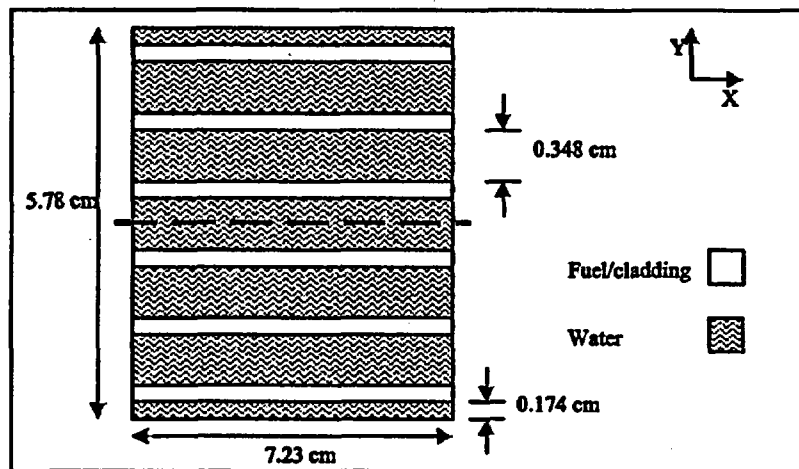


Figure 4-3 HEU Fuel Bundle XY Cut

The LEU fuel bundles are composed of 14 fuel plates with a water gap of 0.282 cm. Figure 4-4 depicts the layout of the fuel plates and water gaps in a LEU fuel bundle.

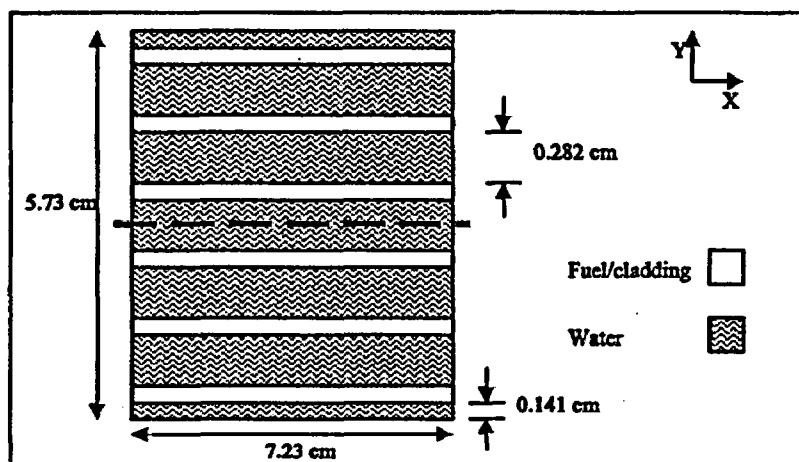


Figure 4-4 LEU Fuel Bundle XY Cut

Table 4-3 compares the bundle characteristics for HEU and LEU cores.

Table 4-3 Fuel Bundle Characteristics of the HEU and LEU Cores

	HEU	LEU
Number of Plates	11	14
Dimensions,		
x-axis (cm)	7.23	7.23
y-axis (cm)	5.78 <sup>1</sup>	5.73
z-axis (cm)	65.1	65.1

<sup>1</sup> The HEU fuel bundle as defined in the FSAR includes half a fuel element spacing of water at each side of the bundle (see Figures 4-3 and 4-4). The actual bundle size, without this extra water, is 5.4356 cm. The LEU fuel bundle was defined using the same approach.

### Fuel Box Description

The existing fuel boxes are planned to be used for the LEU fuel. Therefore, the dimensions of the fuel boxes for the HEU and LEU cores are identical. Table 4-4 provides dimensions of a fuel box.

Table 4-4 Fuel Box Dimensions

Inner Fuel Box, along x-axis (cm)	15.24
along y-axis (cm)	12.7
along z-axis (cm)	121.9
Fuel Box Wall Thickness (cm)	0.318
Fuel Box Spacing, along x-axis (cm)	2.54
along y-axis (cm)	30.48
½ Water Gap (between bundles), along x-axis (cm)	0.394
along y-axis (cm)	0.283

These dimensions are based on the current fuel size. The fuel region is vertically centered in the fuel box. Based on drawing #001-80-100, the water level is assumed to be at 5.08 cm below the top of the fuel box, i.e., at half the outlet pipe. This is confirmed by measurement of the water column height in the reactor building (measured at an average of 45.5" (115.57cm)). Figures 4-5 and 4-6 show the fuel box dimensions and the arrangement (as modeled) of the bundles inside the fuel boxes.

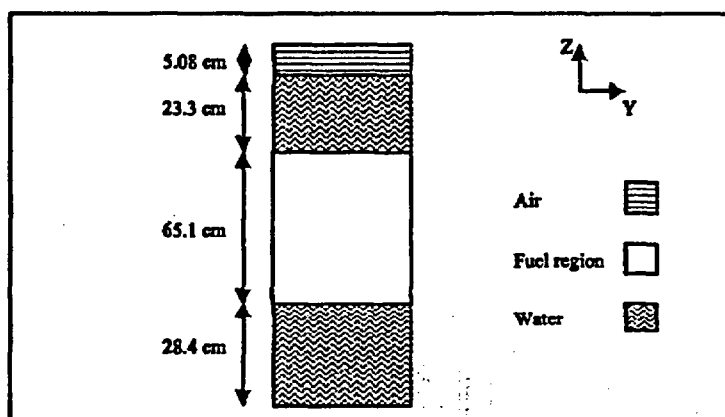


Figure 4-5 YZ Cut of a Fuel Box

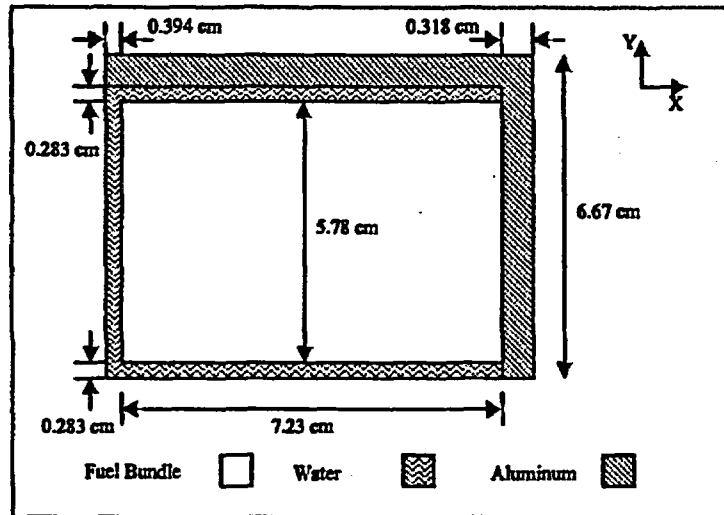


Figure 4-6 XY Cut of One Quarter of a Fuel Box

#### 4.2.2 Control Blades

The UFTR reactivity control system consists of three safety blades (labeled S1 to S3) and one regulating blade (labeled SR) rotating in and out of the core region along a vertical arc within the space provided between the fuel boxes. A cadmium insert is located at the tip of each blade. These blades are protected by magnesium shrouds. The control blades and shrouds are not expected to be replaced, therefore are identical for the HEU and LEU core. Figure 4-7 illustrates the location of the magnesium shrouds within the UFTR core.

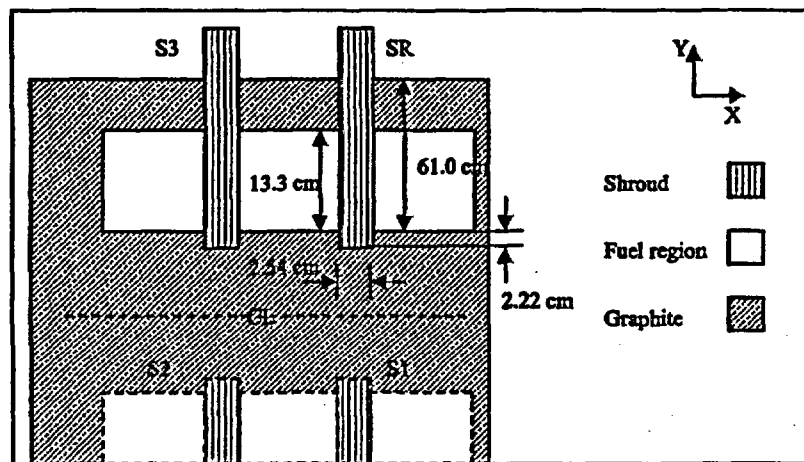


Figure 4-7 Location of Control Blade Shrouds

The dimensions of the shroud are based on UFTR drawing #89-31-118.

The blades have a fully-inserted nominal position of 2.5 degrees above the XY center plane and are moved out of the core by rotating them 45 degrees. The top of the shroud is located 10 cm above the top of the fuel box. Figure 4-8 shows the fully inserted and fully withdrawn location of the control blade with respect to one of the shrouds and the centerline of the core.

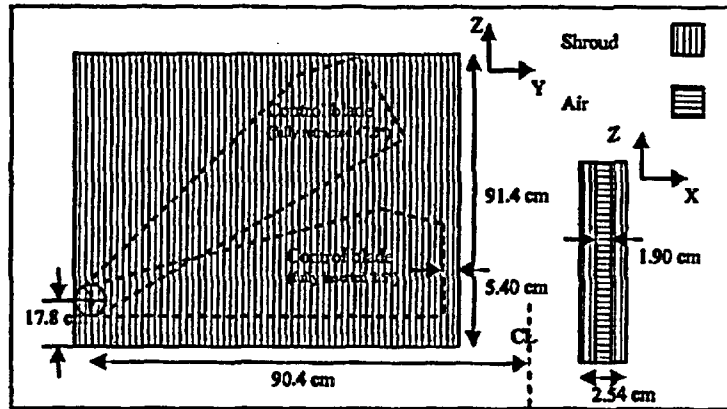


Figure 4-8 XZ and YZ Cut of a Magnesium Shroud

Figure 4-9 shows the dimensions and location of the blades as given in the UFTR drawings #021-80-100, #021-80-102 and #021-80-113.

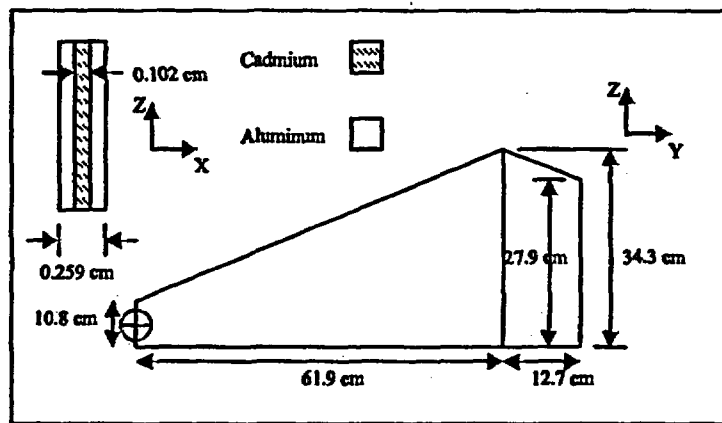


Figure 4-9 Control Blade Dimensions

Figure 4-10 shows the dimensions of the cadmium inserts for both the safety blades (all nominally identical) and the regulating control blade. These dimensions are obtained from drawing #89-31-121 and from x-ray radiographic images of the blades.

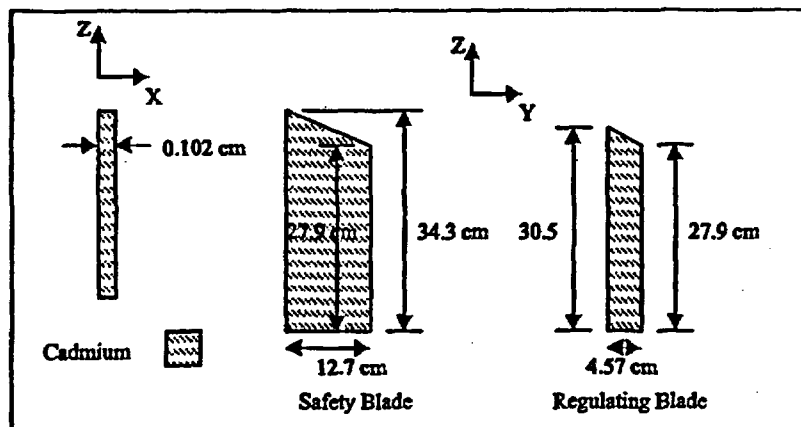


Figure 4-10 Cadmium Absorber Insert Dimensions

### 4.2.3 Neutron Reflector

Since there is no plan to change the reflector during the HEU to LEU conversion, the discussions presented here apply to both cores. The UFTR reactor uses nuclear-grade graphite (as well as water) as reflector. Figure 4-11 shows the different reflector regions as modeled.

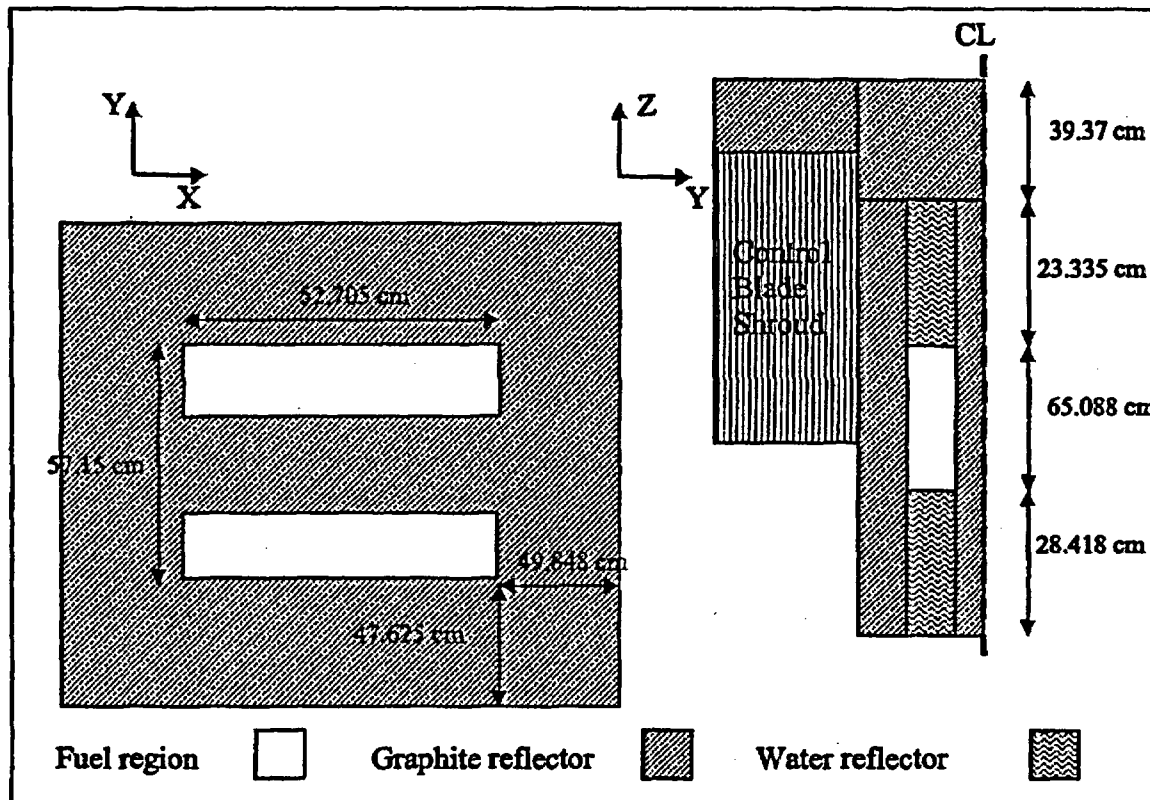


Figure 4-11 Reflector Regions Modeled in MCNP5

### 4.2.4 Neutron Source and Holder

The proposed HEU to LEU conversion of the UFTR core does not require any changes in the existing neutron source location. More details about the characteristics of the current design can be found in Ref. 1.

### 4.2.5 In-Core Experimental Facilities

The proposed HEU to LEU conversion of the UFTR core does not require any changes to the in-core experimental facilities. More details about the experimental characteristics of the current design can be found in Ref. 1.

### 4.2.6 Reactor Materials

The UFTR conversion to LEU requires changing the fuel and cladding compositions. The LEU silicide fuel has been approved by NRC for use in non-power reactors. More detailed information can be found in Ref. 2. Table 4-5 compares the material compositions of the HEU and LEU fuel plates.

**Table 4-5 Composition of the HEU and LEU Fuel**

	<b>HEU</b>	<b>LEU</b>
<b>Fuel "Meat"</b>		
Composition	U-Al alloy	U <sub>3</sub> Si <sub>2</sub> -Al
Enrichment	93%	19.75%
Mass of <sup>235</sup> U per Fuel Plate	████████	12.5 g
Weight Fraction of Uranium (%)	████████	62.98
<b>Cladding</b>		
Composition	1100 Al	6061 Al

<sup>1</sup> Average value (see Appendix A.1 for actual fuel loading)

### **4.3 Reactor Tank and Biological Shielding**

The proposed HEU to LEU conversion of the UFTR core does not require any changes in the reactor tank or biological shielding. More details about this topic can be found in Ref. 1.

### **4.4 Core Support Structure**

The proposed HEU to LEU conversion of the UFTR core does not require any changes in the core support structure. More details about this topic can be found in Ref. 1.

## **4.5 Dynamic Design**

### **4.5.1 Calculation Model**

In order to design the LEU core and determine the necessary operational and safety related parameters, a detailed calculational model for the HEU core was developed and benchmarked against experimental data. A similar model was then developed for the LEU core. These calculations utilized the MCNP5 (Ref. 5) Monte Carlo code with the ENDF/B-VI continuous energy cross section library (when these cross-sections are available, otherwise the latest cross-section library is used), and the SAS2 sequence of the SCALES package (Ref. 6) for fuel depletion calculations.

This section provides information on the material composition (fresh and depleted) for both cores, discusses the MCNP5 model developed for these analyses and the benchmark calculations for the HEU core, and determines a reference critical LEU core.

#### **Material Composition**

The HEU reactor core was modeled at two different burnups; beginning-of-life (BOL, fresh fuel) and current (depleted fuel at about 21.2 MWD for the oldest bundles). For the beginning-of-life core, the isotopic compositions and densities are presented in Table A.1-1, Appendix A.1.

To perform the required depletion calculations for the HEU core, the beginning-of-life peak-to-average ratios presented in Table A.1-2 (appendix A.1) and the power histories presented in Appendix A.2 are used. Further discussions on determination of peak-to-average power ratios are presented in Appendix A.1.

Similar to the HEU core, two burnup states were also considered for the LEU core: BOL (fresh fuel); expected end-of-life (depleted fuel at about ~86.67 MWD; this is based on operation load of 4hr/day, 5day/week, 20 years at 100 kW). This power history results in a burnup that is about four times larger than the current HEU core.

The LEU  $U_3Si_2$  fuel composition at BOL was obtained by averaging 6 sets of concentrations obtained from the manufacturer BWXT (Ref. 7). The fuel matrix aluminum alloy and aluminum cladding compositions were obtained from the same package. Further, it is important to note that in case the impurity concentration is not exact, rather bounded, we have used the maximum value. The detailed isotopic compositions and densities for the LEU core are presented in Tables A.1-3a, A.1-3b, and A.1-3c of Appendix A.1. The formulation for estimating fuel porosity was obtained from an IAEA document (Ref. 8).

For the fuel meat, the calculated density is  $5.55 \text{ g/cm}^3$  with a  $^{235}\text{U}$  loading of 12.5 g per plate and fuel enrichment of 19.75 wt%. This means that the nominal mass of  $^{235}\text{U}$  is 175.0 g per full fuel bundle. Table A.1-4 presents the peak-to-average power ratios at BOL used for the LEU depletion calculations.

As mentioned earlier, the depletion calculations required to model the current core were performed using the SAS2 sequence of the SCALE5 package which tracks a large number of fission products. However, it is only necessary to obtain the concentrations of the most important fission products, i.e., those that have the most effect on the reactivity of the core. The fission products were selected based on their poisoning ratio, i.e., the ratio of neutrons absorbed by the fission product to the neutrons absorbed by fuel. Consequently, in addition to the various uranium and plutonium isotopes, the highly neutron-absorbing fission products were considered as well as some long-lived isotopes. Table 4-6 presents the selected isotopes.

Table 4-6 Selected Isotopes Considered for Criticality Calculation <sup>1</sup>

Element	Isotope
Uranium	234, 235, 236, 238
Plutonium	239, 240, 241
Iodine	129, 131
Xenon	131, 133, 135
Samarium	149, 151
Promethium	147
Technetium	99
Neodymium	143, 145
Rhodium	103

<sup>1</sup> Due to the low burnup of the fuel and the spectrum characteristics of the UFTR, some of these isotopes may not be present in all the bundles.

Other materials used in the HEU and LEU cores are aluminum for cladding and other structures, graphite for moderator and reflector, cadmium tips for the control blades and magnesium for the control blade shrouds. Table 4-7 presents the characteristics of these various materials.

**Table 4-7 Other Materials Characteristics for HEU and LEU Cores**

Material	Composition		Density	
	HEU	LEU	HEU	LEU
Aluminum - cladding	Al + 10ppm of natural boron	See Table 4-8	2.70 g/cc	2.70 g/cc
Aluminum - other structures	Al + 10ppm of natural boron	Al + 10ppm of natural boron	2.70 g/cc	2.70 g/cc
Graphite -nuclear-grade	C + 5ppm of natural boron	C + 5ppm of natural boron	1.60 g/cc	1.60 g/cc
Cadmium (abundance in %) - natural cadmium	106Cd (1.25) 108Cd (0.89) 110Cd (12.49) 111Cd (12.80) 112Cd (24.13) 113Cd (12.22) 114Cd (28.73) 116Cd (7.49)	106Cd (1.25) 108Cd (0.89) 110Cd (12.49) 111Cd (12.80) 112Cd (24.13) 113Cd (12.22) 114Cd (28.73) 116Cd (7.49)	8.75 g/cc	8.75 g/cc
Magnesium	Mg	Mg	1.74 g/cc	1.74 g/cc

The 10ppm of natural boron-equivalent in the HEU aluminum cladding and structure material correspond to the best estimate of the impact of the impurities. The 5 ppm of natural boron-equivalent in the graphite corresponds to our best estimate of the impurities based on INL chemical analysis (Ref. 9) of several graphite samples.

**Table 4-8 Composition of LEU Fuel Cladding**

Isotope	Weight Fraction (%)
Al	97.599
Si	0.500
Fe	0.354
Cu	0.294
Mn	0.070
Mg	0.924
Cr	0.135
Zn	0.089
V	0.010
Zr	0.003
B	0.001
Co	0.001
Ga	0.005
Cd	0.001
Li	0.001



### Geometric Model

Detailed MCNP5 models were developed for the HEU and LEU cores. Both models represent the reactor core, the moderator and reflector regions as well as part of the thermal column. MCNP5 capabilities allowed modeling of the geometry described in Section 4.2. The major differences between the geometric models of the HEU and LEU cores are the size and number of fuel plates, and the number of fuel bundles, dummy bundles and dummy plates.

Figures 4.12(a) and 4.12(b) show the axial and radial projections of the UFTR model.



Figure 4-12 Schematic of the UFTR MCNP5 Model

### Benchmarking of the HEU Core Criticality Model

In order to benchmark the HEU core model, experiments were performed by placing uncovered and cadmium-covered gold foils at the center vertical port and rabbit system of UFTR.

Figure 4-13 shows the experimental setup for determination of reaction rates in the center vertical port (CVP) and the rabbit system which is located in the east-west throughport.

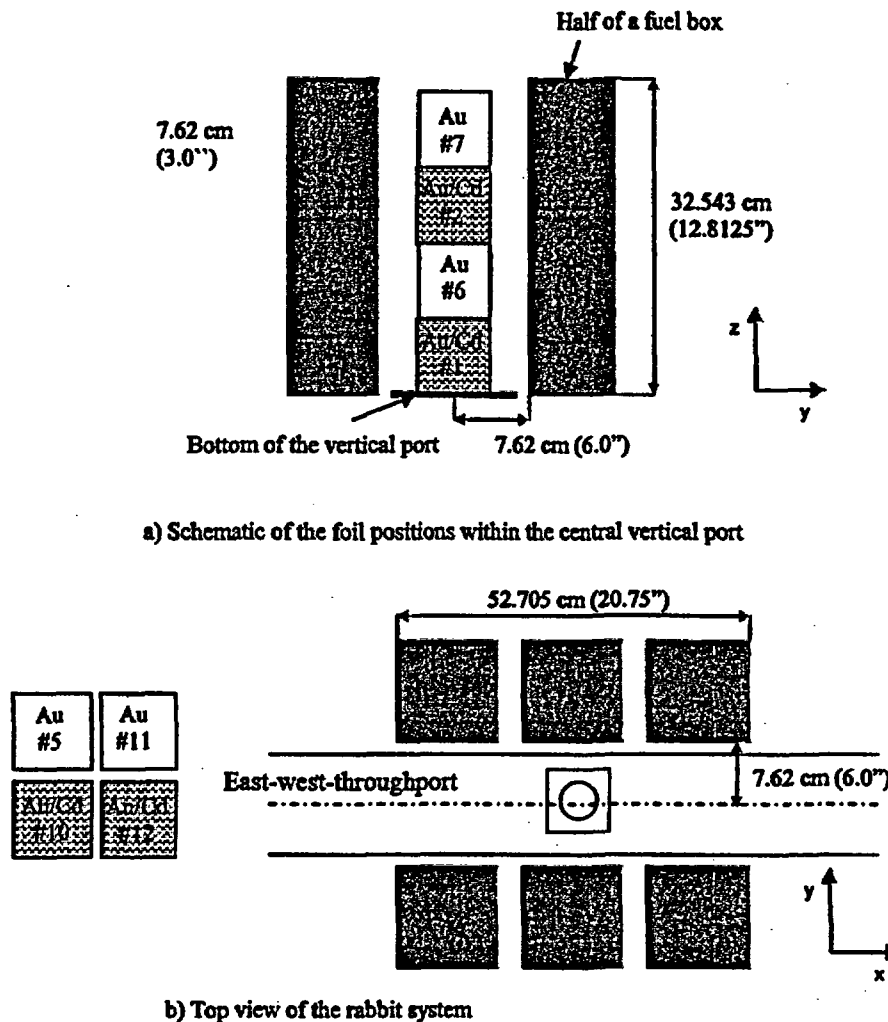


Figure 4-13 Schematic of the Foil Positions within the CVP and Rabbit System

Gold and Cd-covered gold Au foils were placed alternately along the axis of the center vertical port. The foils used in the rabbit system were positioned at the center of the core, which is right below the bottom of the center vertical port.

Table 4-9 presents measured and calculated reaction rates in gold and Cd-covered gold foils located at different axial positions within the center vertical port of UFTR and the center of core within the rabbit system.

**Table 4-9 Comparison of Measured and Calculated Foil Reaction Rates in the CVP and Rabbit System**

Foil ID	Foil Type	Foil Position	Measured Reaction Rate	Calculated Reaction Rate (relative error) <sup>3</sup>	Ratio Measured to Calculated
1	Cd-covered Au	Vertical port	6.77E+09	6.78E+09 (7.47%)	1.00
6	Au	Vertical port	2.39E+10	2.43E+10 (3.79%)	0.98
2	Cd-covered Au	Vertical port	6.91E+09	5.80E+09 (8.25%)	1.19
7	Au	Vertical port	2.23E+10	1.82E+10 (4.70%)	1.23
10,12 <sup>1</sup>	Cd-covered Au	Rabbit system	5.96E+09 <sup>2</sup>	6.05E+09 (6.10%)	0.99
5,11 <sup>1</sup>	Au	Rabbit system	2.17E+10 <sup>2</sup>	2.29E+10 (3.22%)	1.06

<sup>1</sup> Measured twice at the same position with two foils

<sup>2</sup> Averaged value for the two measurements at the same position

<sup>3</sup> 1- $\sigma$  statistical uncertainty

For first two axial segments from the bottom of the central vertical port, the measured and calculated relative differences are within 1%, and for the next two axial positions the differences are within ~20%.

For the Cd-covered Au foil positioned at the center of the rabbit system, the measured and calculated reaction rates are within 1%. For the Au foil at the same position, the measured and calculated reaction rates are within 6%.

#### 4.5.2 Critical Core Configuration

The current HEU core is composed of 21 fuel bundles, 1 partial fuel bundle and 2 dummy bundles. As mentioned in Section 4.2.1, each full fuel bundle contains 11 fuel plates, while the partial (or half fuel bundle) contains 5 fuel plates and only five dummy plates. The remaining two dummy bundles contain 11 dummy plates each. Figure 4.14 shows the pattern of the fuel and dummy bundles for the HEU core.



Figure 4-14 Fuel Pattern in the HEU Core

The two dummy bundles are located in north-east and south-east corners, and the partial fuel bundle is located in the south-west corner.

To develop a reference LEU core, criticality calculations were performed for different core configurations. Based on these results, the reference critical LEU core is composed of 22 fuel bundles with 14 fuel plates each, 1 partial fuel bundle of 10 fuel plates and 3 dummy plates, and one dummy bundle with 14 dummy plates. Figure 4-15 shows the reference LEU core fuel pattern.



Figure 4-15 Fuel Pattern in the LEU Core

The partial fuel bundle and the dummy bundle are located at the south-east and north-east corners, respectively.

The positions of the control blades for the HEU critical core were measured and used to demonstrate that the MCNP5 model achieves a critical core. For the LEU core, the positions for the control blades were determined by performing criticality calculations. Table 4-10 compares the positions of the control blades for the HEU and LEU critical cores.

**Table 4-10 Control blade positions for the HEU and LEU Cores**

Control Blade	Position (degree)	
	HEU	LEU
Safety 1 (SE)	38.5	26.3
Safety 2 (SW)	38.5	26.3
Safety 3 (NW)	38.5	26.3
Regulating (NE)	18.7	16.9

Since the LEU core contains fresh fuel, the safety blades are inserted farther into the core. The critical positions of the control blades for the LEU core are similar to the positions for the HEU core at BOL. The impact of impurities on the HEU core is discussed in Appendix A.3, and variations in the  $k_{eff}$  of the LEU for other core configurations are discussed in Appendix A.4. Table 4-11 compares the power distribution in each fuel bundle of the current HEU and reference LEU cores.

**Table 4-11 Power Generated in Fuel for Depleted HEU and Reference LEU Cores**

Bundle Number	Power (kW)		Relative Difference (%)
	HEU	LEU	
1-1	1.96	3.86	97.2
1-2	4.17	4.33	3.8
1-3	4.05	4.25	5.0
1-4	4.65	4.82	3.6
2-1	4.46	4.60	3.2
2-2	4.34	4.56	5.0
2-3	5.01	5.13	2.3
2-4	4.88	5.09	4.2
3-1	3.72	4.03	8.3
3-2	0.0 (dummy)	2.72	n/a
3-3	4.06	4.45	9.8
3-4	3.58	3.85	7.7
4-1	4.62	4.01	-13.3
4-2	5.21	4.49	-13.8
4-3	4.20	3.58	-14.6
4-4	4.75	3.96	-16.7
5-1	5.36	4.68	-12.8
5-2	5.01	4.45	-11.1
5-3	4.84	4.10	-15.4
5-4	4.52	3.91	-13.4
6-1	4.11	3.71	-9.7
6-2	3.64	3.36	-7.6

6-3	3.76	3.30	-12.2
Total <sup>2</sup>	94.89	95.25	0.376

In the reference LEU core, bundle 1-1 (see Fig. 4-15 for its location) is a full fuel bundle instead of a half fuel bundle in the HEU core (see Fig. 4-14 for its location), the bundle 3-2 is a partly loaded fuel bundle with 10 fuel plates and 3 Al dummy plates, instead of a dummy bundle in the HEU core, and the bundle 6-4 is a dummy bundle in both HEU and LEU cores. The total power generated in the fuel of the LEU core is ~0.38% higher than in the fuel of HEU core. Further, there is a shift of power from north to south. Both cores have a total power of 100 kW. This is expected because the LEU core contains more fuel plates in the south part of core as compared to the HEU core.

Finally, the energy group flux profiles for the HEU and LEU cores are compared in Section A.5.

### 4.5.3 Excess Reactivity and Control Blade Worth

#### Excess Reactivity for HEU and LEU Cores

The MCNP5 code was used to calculate the excess reactivity for both fresh and depleted fuel for both HEU and LEU cores. The excess reactivity was evaluated by rotating the control blades to their fully withdrawn positions (47.5 degrees from horizontal) and calculating the corresponding  $k_{eff}$ .

Table 4-12 compares the calculated excess reactivity for the fresh and depleted HEU and LEU cores.

Table 4-12 Calculated Excess Reactivity for the HEU and LEU Cores (Fresh and Depleted)

Status	HEU ( $\Delta k/k$ %)	Reference LEU ( $\Delta k/k$ %)	Relative Difference (%)
Fresh	1.09	0.93	-15.1
Depleted	0.47	-0.42 <sup>1</sup>	n/a

<sup>1</sup> The power history used for the depletion calculation is different from the HEU power history. The LEU power history was selected in order to investigate the lifetime of the new core. (see Appendices A.2 and A.4). This implies that it will be necessary to insert additional fuel bundles in the available location before the end of this selected power history.

The calculated excess reactivity of the current core is 0.47% (+/- 0.03%). This value is consistent with the last measured excess reactivity of 0.38% performed in February 2005, but indicates a small bias of about 0.1%  $\Delta k/k$ , which can be partially attributed to experimental uncertainties.

#### Integral Control Blade Worth for HEU and LEU Cores

To evaluate the worth of each control blade,  $\Delta k/k$  was calculated between the case where all the blades are fully withdrawn and the case where a given blade is fully inserted

Table 4-13 compares the worth of control blades as measured and calculated for HEU depleted core, and for the fresh and depleted LEU core.

<sup>2</sup> For the HEU and LEU cores, 5.11 kW and 4.75 kW, respectively, is deposited in the coolant, graphite moderator and core structures materials.

Table 4-13 Comparison of Control Blades Worth for the HEU and LEU Cores

Control Blade	HEU (calculated)	HEU (measured)	LEU-fresh (calculated)	LEU-depleted (calculated)
Regulating	0.87%	0.82%	0.63%	0.66%
Safety 1	1.35%	1.21%	1.62%	1.65%
Safety 2	1.63%	1.36%	1.77%	1.76%
Safety 3	2.06%	1.88%	1.42%	1.46%

For the HEU core, the calculated and experimental data differ in a range of 6.1% to 19.9%. These differences can be attributed to experimental uncertainty and inconsistency between the experimental procedure to measure the blade worth and the modeling procedure.

Further, the two control blades on the south part of the reference LEU core (safety 1 and 2) have higher worths as compared to the HEU core, while the two control blades on the north part of the LEU core (safety 3 and regulating) have lower worth than in the HEU core. This finding is expected because of the observed power shift presented in Table 4-10. This power shift is expected since more fuel is added to the south part of the core.

#### Maximum Reactivity Insertion Rate for HEU Core

In addition to calculations of the total reactivity worth for the UFTR control blades, an analysis of the integral worth as a function of position was performed for the most reactive blade. In the prior calculations, Safety Blade 3 was determined to be the most reactive blade. An MCNP model of the UFTR fueled with 21.5 HEU fuel bundles was utilized. The calculations were performed by positioning the Safety 1, Safety 2, and Regulating Blades at a critical position for the core, and then moving Safety Blade 3 through its full range of motion (2.5° to 47.5°). Results are provided in Table 4-14 and Figure 4-16. The total blade worth calculated here is 2.03%  $\Delta k/k$ , which is almost the same as the prior calculation for the total blade worth (2.06 %  $\Delta k/k$ ). In the prior calculations, the other blades were fully-withdrawn, while in the calculations presented in Table 4-14, the safety blades were inserted at 38.5° and the regulating blade was at 18.7°.

Table 4-14 Integral Reactivity Worth versus Position for Safety 3 in the HEU Core

Time (s) <sup>1</sup>	Blade Position		$k_{eff}$	Reactivity (% $\Delta k/k$ )	Reactivity Insertion Rate (% $\Delta k/k/s$ )
	Degrees	Units			
0.0	2.5	0	0.98747 $\pm$ 0.04%	0.00%	n/a
5.6	5	56	0.98936 $\pm$ 0.03%	0.19%	0.034%
16.7	10	167	0.99330 $\pm$ 0.04%	0.59%	0.036%
27.8	15	278	0.99789 $\pm$ 0.04%	1.06%	0.042%
38.9	20	389	1.00158 $\pm$ 0.02%	1.43%	0.034%
50.0	25	500	1.00423 $\pm$ 0.02%	1.70%	0.024%
61.1	30	611	1.00576 $\pm$ 0.02%	1.85%	0.014%
72.2	35	722	1.00664 $\pm$ 0.02%	1.94%	0.008%
83.3	40	833	1.00704 $\pm$ 0.02%	1.98%	0.004%
100.0	47.5	1000	1.00747 $\pm$ 0.02%	2.03%	0.003%

<sup>1</sup> Assumes 100 seconds withdrawal time

Figure 4-16 shows calculated the Safety Blade 3 (most reactive blade for HEU core) worth as a function of position.

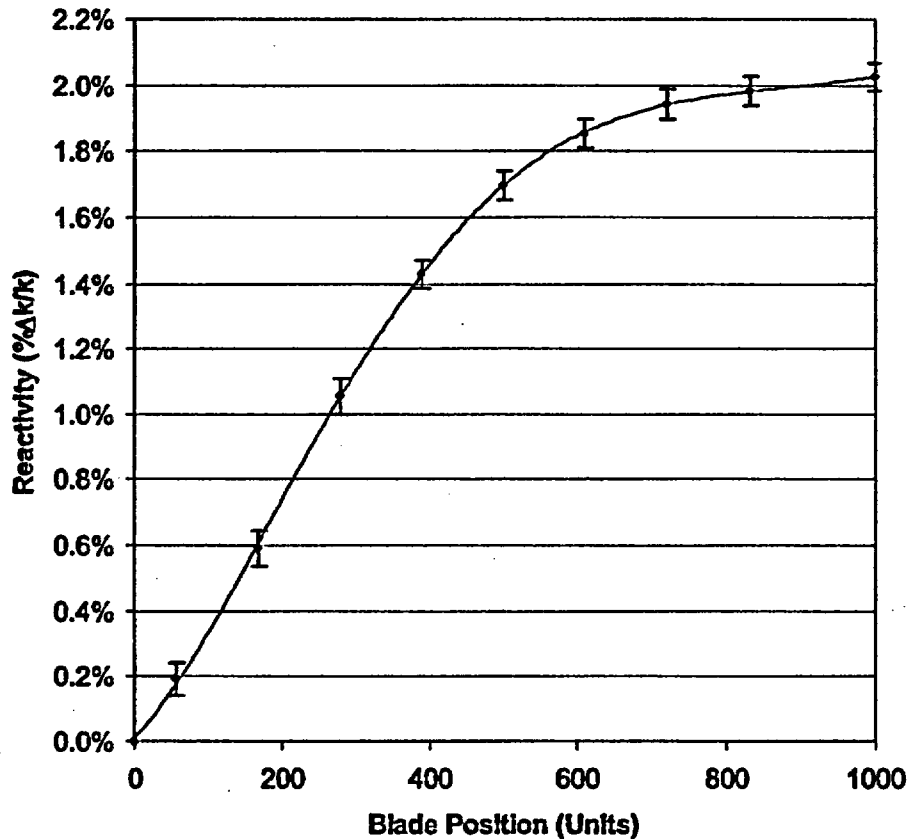


Figure 4-16 Integral Blade Worth versus Position for Safety 3 in the UFTR HEU Core.

The UFTR Technical Specifications require that the reactivity insertion rate from control blade withdrawal must be less than 0.06%  $\Delta k/k/s$  when averaged over a 10 second interval. The rate of reactivity insertion resulting from withdrawal of the highest worth blade was approximated by assuming a 100 second (minimum allowed) blade withdrawal time. As shown in Table 4-14, the highest rate of reactivity insertion from withdrawal of Safety Blade 3 is 0.042%  $\Delta k/k/s$ , which meets the requisite UFTR Technical Specification.

#### Maximum Reactivity Insertion Rate for LEU Core

The integral reactivity worth as a function of position was determined for Safety Blade 2 (most reactive blade for the LEU core) based on MCNP calculations in a manner similar to that employed for the HEU core calculations. The position of Safety Blade 1 and Safety Blade 3 was fixed at 26.3° and the Regulating Blade was positioned at 16.9°, while Safety Blade 2 was rotated from 2.5° to 47.5°. Results are provided in Table 4-15 and Figure 4-17. The total worth for Safety Blade 2 calculated in this manner is similar to that obtained in the prior calculations with the other blades fully-withdrawn.



**Table 4-15 Integral Reactivity Worth Versus Position for Safety 2 in the LEU Core**

Time (s) <sup>1</sup>	Blade Position		$k_{eff}$	Reactivity (% $\Delta k/k$ )	Reactivity Insertion Rate (% $\Delta k/k/s$ )
	Degrees	Units			
0.0	2.5	0	0.98455 $\pm$ 0.04%	0.00%	n/a
5.6	5	56	0.98612 $\pm$ 0.03%	0.16%	0.029%
16.7	10	167	0.98954 $\pm$ 0.03%	0.51%	0.031%
27.8	15	278	0.99448 $\pm$ 0.04%	1.01%	0.045%
38.9	20	389	0.99701 $\pm$ 0.02%	1.27%	0.023%
50.0	25	500	0.99969 $\pm$ 0.02%	1.54%	0.024%
61.1	30	611	1.00114 $\pm$ 0.02%	1.69%	0.013%
72.2	35	722	1.00213 $\pm$ 0.02%	1.79%	0.009%
83.3	40	833	1.00238 $\pm$ 0.02%	1.81%	0.002%
100.0	47.5	1000	1.00229 $\pm$ 0.02%	1.80%	-0.001%

<sup>1</sup> Assumes 100 seconds withdrawal time

Figure 4-17 shows the calculated Safety Blade 2 (most reactive blade for LEU core) worth as a function of position.

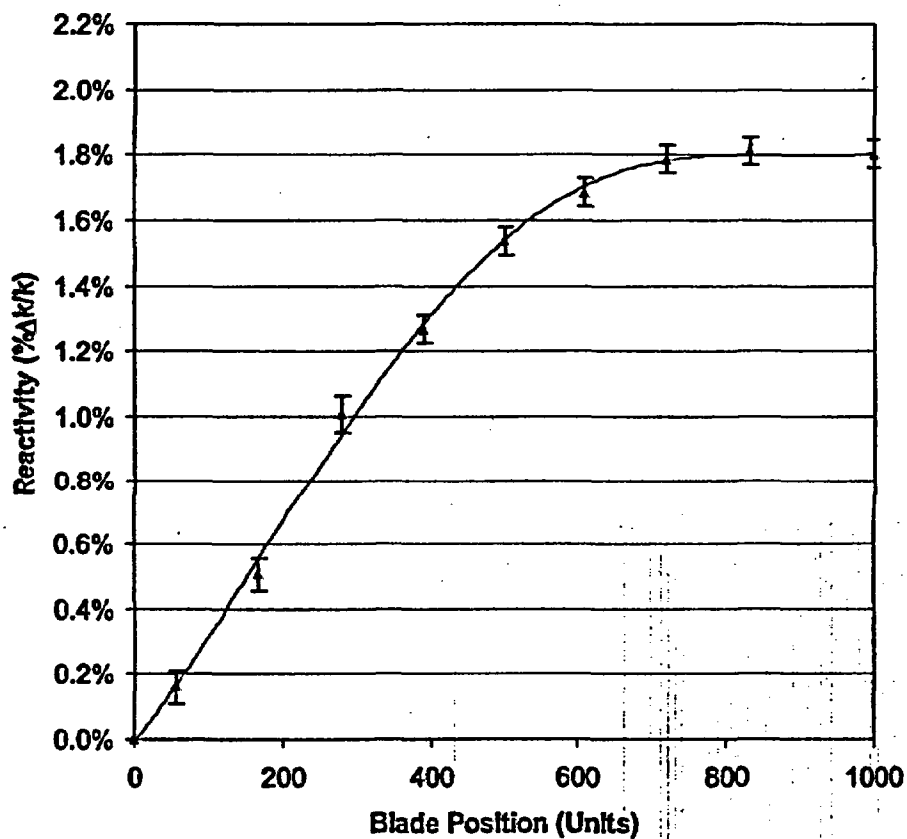


**Figure 4-17 Integral Blade Worth versus Position for Safety 2 in the UFTR LEU Core**

The UFTR Technical Specifications require that the reactivity insertion rate from control blade withdrawal must be less than 0.06%  $\Delta k/k/s$  when averaged over a 10 second interval. The rate of reactivity insertion resulting from withdrawal of the highest worth blade was again approximated by assuming a 100 second blade withdrawal time. As shown in Table 4-15, the highest rate of reactivity insertion from withdrawal of Safety 2 is 0.045%  $\Delta k/k/s$ , which also meets the Technical Specification for the reactor.

#### 4.5.4 Shutdown Margin for HEU and LEU Cores

For the HEU core, the shutdown margin is evaluated by fully inserting (2.5 degrees from horizontal) the Safety Blades 1 and 2 and the Regulating Blade and withdrawing the Safety Blade 3 to its fully withdrawn position (47.5 degrees from horizontal). For the LEU core, the Safety Blade 2 is kept fully withdrawn while the others blades are fully inserted. Table 4-16 compares the shutdown margins of the HEU and LEU cores.

Table 4-16 Shutdown Margins for the Current HEU Core and the Reference LEU Core

	Depleted HEU Core (calculated)	HEU Core (measured)	Reference LEU Core
Shutdown Margin ( $\Delta k/k$ %)	3.11	3.01	3.17

Since the measured shutdown margin for the HEU depleted core is 3.01% the calculated and experimental shutdown margins differ by about 3%. The LEU shutdown margins meet the Technical Specification requirement that the shutdown margin be at least 2%  $\Delta k/k$  with the most reactive blade stuck out.

#### 4.5.5 Other Core Physics Parameters

##### HEU Reactivity Coefficients and Kinetic Parameters

Reactivity coefficients and neutron kinetics parameters were calculated for the HEU-fueled UFTR. These provide a measure of the core reactivity response to changes in the water properties or fuel temperature changes under both off-nominal (e.g., changes to inlet coolant conditions) and accident conditions (e.g., inadvertent reactivity insertion accidents). The Technical Specifications for the UFTR require that the primary coolant temperature and void coefficients be negative.

The reactivity coefficients are used to estimate the core reactivity change due to a change in some state property value. So,

$$\Delta \rho = \alpha_x \cdot \Delta x \quad (4.1)$$

where  $\alpha_x$  is the reactivity coefficient due to a unit change in state property  $x$  and  $\Delta x$  is the value change for  $x$ . The reactivity coefficients are calculated assuming that reactivity effects resulting from simultaneous changes in multiple state properties are separable. These are calculated from core eigenvalue calculations with independent perturbations to the state properties. Consequently,

$$\alpha_x = \frac{\Delta \rho}{\Delta x} = \frac{k_1 - k_0}{k_1 k_0} \cdot \frac{1}{(x_1 - x_0)} \quad (4.2)$$

For the UFTR, reactivity coefficients were calculated for perturbations to the water temperature, water density (coolant void), and fuel temperature. Core eigenvalue calculations were performed with the MCNP5 code using the same core model that was used to evaluate the steady-state neutron flux distribution, excess reactivity, and control blade reactivity worth.

The kinetics parameters evaluated for the UFTR were the effective delayed neutron fraction,  $\beta_{\text{eff}}$ , and the prompt neutron lifetime,  $\lambda$ . The effective delayed neutron fraction is calculated using two eigenvalue calculations. The normal calculation of  $k_{\text{eff}}$  will include both prompt and delayed neutrons. A second calculation with prompt neutrons only yielded from fission gives  $k_{\text{eff}}^{\text{prompt}}$ . The effective delayed neutron fraction is then defined as

$$\beta_{\text{eff}} = 1 - \frac{k_{\text{eff}}^{\text{prompt}}}{k_{\text{eff}}} \quad (4.3)$$

The prompt-neutron lifetime is calculated using the "1/v insertion method," in which a uniform concentration of a 1/v absorber such as  $\text{B}^{10}$  is included at a very dilute concentration everywhere in the core and reflector. Consequently, the lifetime is calculated by the formulation

$$\lambda = \lim_{N \rightarrow 0} \left[ \frac{\frac{k_1 - k_0}{k_1}}{N_1 \sigma_a v} \right] \quad (4.4)$$

where  $k_1$  is the  $k_{\text{eff}}$  of the system with a uniform concentration,  $N_1$ , of a 1/v absorber, and  $\sigma_a$  is the infinitely-dilute absorption cross section of the absorber for neutrons at speed  $v$ . In this work, the  $^{10}\text{B}$  absorption cross section was assumed to be  $\sigma_a = 3837$  barns at a neutron speed of  $v = 2200$  m/s.

Table 4-17 provides the reactivity coefficients and kinetics parameters calculated for the UFTR HEU core. The calculations were performed for the fresh HEU core with 21.5 bundles. This core has an excess reactivity of 1.09%  $\Delta k/k$ , and the control blades were positioned to achieve a critical condition. The reactivity coefficients are all negative, which meets the requirements of the Technical Specifications. The fuel temperature (Doppler) coefficient is quite small for the HEU fuel (93 wt.% U-235) because of the very small fraction of U-238.

**Table 4-17 Kinetics Parameters and Reactivity Coefficients for the UFTR HEU Core**

Parameter		Calculated Result
$\beta_{eff}$		7.92E-03 $\pm$ 1%
$\lambda$ ( $\mu$ s)		187.4 $\pm$ 3%
$\alpha_{void}$ ( $\Delta\rho/\%$ void)	(0 to 5% void)	-1.48E-03 $\pm$ 1%
	(5 to 10% void)	-1.69E-03 $\pm$ 1%
$\alpha_{water}$ ( $\Delta\rho/^\circ$ C)	(21 to 127 $^\circ$ C)	-5.91E-05 $\pm$ 1%
$\alpha_{fuel}$ ( $\Delta\rho/^\circ$ C)	(21 to 127 $^\circ$ C)	-6.49E-06 $\pm$ 18%
	(21 to 227 $^\circ$ C)	-2.91E-06 $\pm$ 12%

The ranges on coolant voiding (change of density) and temperature selected here cover perturbations that will occur during normal operations. The calculated coefficients show that there is some non-linearity in the reactivity response to coolant voiding and temperature, and fuel temperature changes. When performing coupled thermal/hydraulic-neutronics analyses for transients, the expected range of the coolant and fuel conditions should be taken into account when selecting the coefficients to employ. The RELAP5-3D code (Ref. 10) which was used for transient analyses does not easily allow the input of temperature dependent coefficients, so a single value must be selected.

#### LEU Reactivity Coefficients and Kinetic Parameters

Kinetics parameters and reactivity coefficients were calculated for the reference fresh LEU core. The excess reactivity for the LEU core is 0.93%  $\Delta k/k$ , and the control blades were positioned to achieve a critical core condition. The calculated parameters are summarized in Table 4-18.

**Table 4-18 Kinetics Parameters and Reactivity Coefficients for the UFTR LEU Core**

Parameter		Calculated Result
$\beta_{eff}$		7.71E-03 $\pm$ 1%
$\lambda$ ( $\mu$ s)		177.5 $\pm$ 5%
$\alpha_{void}$ ( $\Delta\rho/\%$ void)	(0 to 5% void)	-1.53E-03 $\pm$ 1%
	(5 to 10% void)	-1.75E-03 $\pm$ 1%
$\alpha_{water}$ ( $\Delta\rho/^\circ$ C)	(21 to 127 $^\circ$ C)	-5.68E-05 $\pm$ 2%
$\alpha_{fuel}$ ( $\Delta\rho/^\circ$ C)	(21 to 127 $^\circ$ C)	-1.29E-05 $\pm$ 10%
	(21 to 227 $^\circ$ C)	-1.40E-05 $\pm$ 4%

As expected, the LEU fuel has a much larger fuel temperature (Doppler) coefficient relative to the HEU-fueled UFTR. The LEU core has a harder neutron spectrum, which slightly decreases the prompt-neutron lifetime, increases the magnitude of the coolant void coefficient, and slightly reduces the magnitude of the coolant temperature coefficient. All coefficients are negative, as required by the Technical Specifications.

The ranges on coolant voiding and temperature selected here cover any perturbations that will occur during normal operations and accident conditions. Just as for the HEU fuel, the calculated coefficients show that there is some non-linearity in the reactivity response to coolant voiding and temperature, and fuel temperature changes. When performing coupled thermal/hydraulic-neutronics analyses for transients, the expected range of the coolant and fuel conditions should be taken into account when selecting the applicable coefficients.

#### **4.6 Functional Design of the Reactivity Control System**

The proposed HEU to LEU conversion of the UFTR core does not require any changes in the functional design of the reactivity control system. More details about this topic can be found in Ref. 1.

#### **4.7 Thermal-hydraulic Analyses**

In this section, the results of thermal-hydraulic analyses are discussed in order to demonstrate that the UFTR thermal-hydraulic LEU design provides the cooling conditions necessary to ensure fuel integrity under all anticipated reactor operating conditions. Analyses for operation under accident scenarios are presented in Section 13.

##### **4.7.1 Fuel Assembly and Fuel Box Geometry**

Fuel is loaded into six "fuel boxes," each containing up to four fuel assemblies. In these thermal-hydraulic analyses, only the fuel box containing the fuel assembly with the maximum power was considered. In addition, each of the four fuel assemblies in the box was assumed to produce that same maximum power. The axial power distribution for the hottest plate was obtained from the results of the criticality calculations and was assumed to apply to all fuel plates in an assembly.

The relative sizes of the HEU and LEU fuel assemblies are shown in Figure 4-18. The arrangement of four fuel assemblies inside a fuel box is shown in Figure 4-19.

**Figure 4-18 Comparing drawings of the LEU and HEU assemblies**

**Figure 4-19 Arrangements of the HEU and LEU Fuel Assemblies in a Fuel Box**  
(Each drawing shows the smallest fuel assemblies allowed by the dimensional tolerances inside the largest fuel box.)

In order to analyze the most conservative geometry from a thermal-hydraulics point of view, the smallest fuel assemblies allowed by the manufacturing tolerances were modeled inside the largest fuel box (5 1/8" x 6 1/8" interior dimensions). These dimensions were used in the HEU and LEU thermal-hydraulic models and are shown in Table 4-19.

**Table 4-19 Key Geometrical Parameters Used in the HEU and LEU Models**

Model Geometrical Parameter	HEU	LEU
Fuel box cross section, Interior Dimensions, mm	130.175 x 155.575 (5 1/8" x 6 1/8")	130.175 x 155.575 (5 1/8" x 6 1/8")
Fuel plate thickness, mm	1.7018	1.2192
Gap thickness, channel against fuel box, mm	3.4544	9.3345
Central slot channel thickness, mm	16.7386	4.7244
Vertical bypass gap thickness, mm	11.3030	11.3030
Coolant channel width, mm	3.4544	2.794
Grid hydraulic diameter, mm	12.202	12.202
Bolt head height, mm	3.4544	2.3622

The bolt-to-bolt, or stack height, dimension for the LEU assembly was designed to be smaller than that for the HEU assemblies. This was done so that the largest LEU fuel assemblies allowed by the manufacturing tolerances will fit more easily into the smallest fuel box than did the HEU assemblies. The HEU assembly configuration uses a central tapered wedge pin to force the four assemblies to the corners of the fuel box, as shown in Figure 4-19. The analysis assumes that the assemblies are in contact with the fuel box. This leaves a wide East-West channel in the center of the fuel box. If four of the smallest HEU assemblies allowed by the manufacturing tolerances are placed in the largest fuel

box, the central East-West channel is 0.659" (16.7 mm) wide (bolt heads in contact with the fuel box).

The LEU design uses two semi-circular wedge pins to position the fuel assemblies in each fuel box, as shown in Figure 4-19. Triangular, rather than semi-circular, wedge pins are also an option. The two-pin LEU configuration with the smallest assemblies in the largest box produces two wide East-West channels of width 0.3675" (9.33 mm). Had the single pin HEU design been employed here, there would have been one large central East-West channel of width 0.735" (18.7 mm). This very wide channel would have consumed a disproportionate amount of the total coolant flow, leaving less to cool the other fuel plates in the fuel box. Therefore, the two-pin configuration is hydraulically superior to the single pin configuration in that it causes more flow into the narrower coolant channels where it is needed most. In both the HEU and the two-pin LEU designs the 0.445" central North-South channel is maintained, as shown in Figure 4-19.

The grid plate, which supports the four fuel assemblies in each fuel box, is included in the hydraulic analysis because it makes the velocity distribution in each fuel box more uniform. The hydraulic model in the code assumes that the hydraulic resistance for each coolant path, from the bottom of the grid plate to the region above the fuel plates, has two components, a form- or k-loss and a frictional loss. For each of these parallel paths or channels the pressure drop,  $\Delta P$ , is given by  $\Delta P = (K + fL/D) \times \rho V^2 / 2$ , where  $K$  is the k-loss value,  $f$  is the friction factor for smooth-walled channels,  $L$  is the channel length,  $D$  is the channel hydraulic diameter,  $\rho$  is the coolant density, and  $V$  is the average coolant velocity in the channel. For laminar flow the value of  $f$  is affected by the shape of the channel. The single value of  $K$  represents not only the form losses at the inlet and exit to the fuel plates, but also the hydraulic resistance due to the grid plate. The minimum total flow area in the grid plate is considerably smaller than the total flow area in the fuel region. A value of 5.0 was assumed for the value of  $K$  and is considered to be conservatively small. A larger value of  $K$  would result in larger margins to the limiting conditions, such as the onset of nucleate boiling, by causing the thinner channels to have more flow. In the following section, we will elaborate on the thermal-hydraulics code used for performing these analyses.

#### 4.7.2 PLTEMP/ANL v2.14 Code Description

The thermal-hydraulic analyses were performed using the computer code PLTEMP/ANL V 2.14 (Ref. 11). This code provides a steady-state thermal-hydraulics solution for research reactor fuel assemblies with plate-type or tube-type geometries. The code accounts for pressure drops axially in one dimension including any bypass flows, and accounts for thermal effects in two dimensions. Friction factors and mass flow rates are determined through a network of parallel channels, some of which are not heated. Both laminar and turbulent flow regimes are accommodated.

The heat source from fission is assumed to be flat across the meat and along the width of a fuel plate, but varies axially in a step-wise nodal approximation. All of the fuel plates in a fuel assembly are modeled, each with different peak power densities. PLTEMP determines the friction factors and coolant mass flow rates in each channel, and then calculates the steady-state temperature distribution in the meat, clad, and coolant at each axial node.

The code accounts for one-sided heating of a channel, as occurs for the channel next to the fuel box. In laminar flow, the heat transfer coefficient is different for a channel heated on one side than for a channel heated on two sides. Also, Version 2.14 accounts for pressure drop friction factors over the full Reynolds number range from laminar, through the critical zone, and on through turbulent flow.

Safety-related parameters such as the Onset of Nucleate Boiling Ratio (ONBR) and Departure from Nucleate Boiling Ratio (DNBR) are calculated along with fuel, clad, and coolant temperatures in each channel.

The major thermal-hydraulic correlation options in PLTEMP that were selected for use in these analyses are:

1.  $Nu = hD/k = 7.63$ , if laminar forced convection, or  $Nu = 4.86$ , if laminar forced convection and the channel is heated on one side only (Ref. 12). Note: turbulent flow does not take place. If it did, the Petukhov & Popov (Ref. 13) single-phase heat transfer correlation would be used.
2. Bergles-Rohsenow correlation (Ref. 14) for ONB thermal margin.
3. Groeneveld Lookup Table for Critical Heat Flux Prediction (Ref. 15).

Table 4-20. HEU and LEU Random Hot-Channel Factors

Uncertainty	Type	HEU Core			LEU Core		
		$F_q^3$	$F_b$	$F_h$	$F_q$	$F_b$	$F_h$
Fuel Meat Thickness (local) <sup>a</sup>	random	1.05	-	-	1.05	-	-
<sup>235</sup> U Loading Per Plate <sup>b</sup>	random	1.03	1.015	-	1.03	1.015	-
<sup>235</sup> U Homogeneity (local) <sup>c</sup>	random	1.03	-	-	1.20	-	-
Coolant Channel Spacing <sup>d</sup>	random	-	-	-	-	-	-
Calculated Power Density <sup>a</sup>	random	1.10	1.05	-	1.10	1.05	-
Statistical Combination of Random Factors		1.12	1.05	1.00	1.23	1.05	1.00

<sup>a</sup> HEU and LEU: Assumed values.

<sup>b</sup> HEU: Assumed to be the same as for the LEU plate. Derived from fuel plate loading specification of  $12.5 \pm 0.35$  g <sup>235</sup>U.

<sup>c</sup> HEU: Estimated for U-Al alloy fuel meat. LEU: From fuel plate homogeneity specification.

<sup>d</sup> No factor was included here because the analysis was done for the thinnest coolant channel spacing allowed by the manufacturing specifications.

However, the systematic uncertainties in the measurements of the reactor power level and the coolant flow rate were not included explicitly in the calculations. These systematic uncertainties will be included in the interpretation of the results.

<sup>3</sup> These hot-channel factors are defined in more details in Appendix B



The code requires specification of the fuel plate to which the hot channel factors will be applied. The side of the plate (or channel) to be affected also needs to be specified. A series of cases were examined to be certain that the safety-limiting case is identified. For a given mass flow rate and design case, eleven explicit cases were examined in order to determine the most limiting safety case with hot channel factors included. The factor  $F_q$  was applied to the most limiting axial node, the uppermost axial node as a local hot channel factor. The factor  $F_h$  was applied to the entire fuel assembly, while the factor  $F_b$  was applied to a specific channel.

#### 4.7.3 Thermal-Hydraulic Analysis Results

In this section, the PLTEMP/ANL V 2.14 code is used to determine the thermal hydraulics conditions of UFTR at full power of 100 kW for both HEU and LEU cores. The code is also used to determine the safety limits for the new core, considering the existing Limiting Safety System Setting (LSSS) (or trip points).

The nominal operating conditions and the Limiting Safety System Setting are listed in Table 4-21

Table 4-21 Nominal Operating Conditions and Limiting Safety System Settings (LSSS)

	Nominal Condition	LSSS
Inlet Temperature, C	30	-
Inlet mass flow rate, kg/s	2.688 (43 gpm)	1.875 (30 gpm)
Power, kW	100	125
Outlet Temperature, C	-	68.3 (155F)

Table 4-22 compares the thermal-hydraulics conditions of the LEU and HEU cores at nominal conditions and the maximum power of 100 kW. These calculations include all hot channel factors, except for uncertainties in measurements of the power level and coolant flow rate.

Table 4-22 Thermal-hydraulics Conditions of the HEU and LEU Cores at nominal conditions and full power

Parameter	HEU	LEU
Max. Fuel Temp. (C)	62.4	60.7
Max. Clad Temp. (C)	62.4	60.7
Mixed Mean Coolant, outlet temperature (C)	44.2	43.8
Max. Coolant Channel, outlet temperature (C)	54.6	56.3
Min. ONBR	2.20	2.33
Min. DNBR	359	367

The data in the above table show that the maximum coolant outlet temperature is about 55 °C in the HEU core and 56 °C in the LEU core. The minimum ratios for Departure

from Nucleate Boiling (DNB) are calculated to be 359 and 367 in the HEU and LEU cores, respectively. Thus, both the HEU and LEU cores have adequate thermal-hydraulic safety margins under normal operating conditions. It is worth noting that, for both LEU and HEU cores, the maximum fuel temperature and the maximum clad temperatures occurred at a height of 57.5 cm from the bottom of the fuel meat.

To further examine the safety margin of UFTR at nominal conditions and trip points, Table 4-22 compares the necessary power levels at which the onset of nucleate boiling occurs for the HEU and LEU cores.

**Table 4-22 Calculated Power Level At Which ONBR = 1.0 for the HEU and LEU Cases with the Smallest Allowed Fuel Assembly in the Largest Fuel Box.**

Flow Rate	Power (kW)	
	HEU	LEU
30 gpm	182.5	194.4
43 gpm	251.5	285.0

Results in Table 4-22 indicate that for the nominal coolant flow rate of 43 gpm, for HEU and LEU cores, initiation of onset of nucleate boiling (ONB) occurs at power levels of 251 kW and 285 kW, respectively. This means that the power required for initiation of ONB is far, (factors of 2.5 and 2.8) from the maximum power level of 100 kW at which the reactor is licensed to operate. Similar statements can be made if the flow rate is reduced to its trip point value (30 gpm); factors of 1.8 and 1.9 of the maximum power of 100 kW is necessary for ONB. Since there would be no possibility of bubble formation due to boiling, there is no possibility for flow instability to develop at this coolant flow rate.

In the UFTR, the first and principal physical barrier protecting against release of radioactive material is the cladding of the fuel. The criterion normally used to evaluate safety limits is the margin to flow-instability-induced burnout to ensure the integrity of the fuel cladding. In this analysis, a more restrictive criterion was used since the safety limits are based on preventing any localized boiling by ensuring that the ONBR doesn't get below 1.0 at the safety limits. Since there would be no possibility of bubble formation due to boiling, flow instability cannot develop.

In this section, the safety limits, and consequently the safety margins to the current limiting safety system setting (LSSS), are evaluated for the major thermal-hydraulics physical variables related to the integrity of the fuel. These physical variables include the power, the inlet mass flow rate and the bulk (mixed mean) temperature at the outlet of each fuel box.

To determine the safety limit for each variable, we consider the following. For the power level safety limit, we set the inlet temperature and inlet flow rate, and determine the power at which the ONBR is about 1.0. For the inlet flow rate safety limit, we set the inlet temperature and the power level, and determine the inlet flow rate at which the ONBR is about 1.0. Finally, for the safety limit on the outlet temperature, we set the

power level and the inlet flow rate, and vary the inlet temperature until the ONBR is about 1.0; the resulting outlet temperature is the safety limit.

To be conservative but realistic, we consider two set of input parameters; i) the nominal conditions, and ii) the LSSS points, and find an average of the two sets. Note that the second set of input parameters (LSSS points) is highly conservative since the license doesn't allow the UFTR to operate at steady-state power above 100 kW.

Table 4-23 gives the results of the thermal-hydraulic calculations performed to evaluate the safety limits of the LEU core using the two set of input parameters.

**Table 4-23 Results of the Analyses Performed to Evaluate the LEU Core Thermal-Hydraulics Safety Limits**

Parameter	Safety Limit					
	Power		Mass Flow Rate		Outlet Temperature	
	Set 1	Set 2	Set 1	Set 2	Set 1	Set 2
Reactor Power, kW	<u>250</u>	<u>135</u>	100	125	100	125
Coolant Flow Rate, gpm	43	30	<u>18</u>	<u>27</u>	43	30
Coolant Inlet Temp., °C (F)	30 (86)	43.3 (110)	30 (86)	43.3 (110)	72.5 (162.5)	49 (120.2)
Max. Fuel Temp. °C (F)	102.4 (216.3)	99.7 (211.5)	101.1 (214.0)	101.6 (214.9)	101.4 (214.5)	101.1 (214.0)
Max. Cladding Temp., °C (F)	102.4 (216.3)	99.7 (211.5)	101.1 (214.0)	101.6 (214.9)	101.4 (214.5)	101.0 (213.8)
Mixed Mean Outlet Temp., °C (F)	55.8 (132.4)	63.3 (145.9)	54.6 (130.3)	63.8 (146.8)	<u>82.7</u> (180.9)	<u>67.4</u> (153.3)
Max. Coolant Channel Outlet Temp., °C (F)	90.1 (194.2)	93.2 (199.8)	97.6 (207.7)	95.8 (204.4)	96.5 (205.7)	95.1 (203.2)
Minimum ONBR	0.998	1.038	1.007	1.004	1.011	1.02
Minimum DNBR	93	151	157	150	195	156

To determine the safety limits, the linear average of the two sets (underlined numbers in Table 4-23) is calculated. These averages are then rounded up conservatively assuming two significant digits to represent conservative yet realistic values for the safety limits. Table 4-24 gives the safety limits for the LEU core. Note that the outlet temperature is set in Fahrenheit.

**Table 4-24 LEU Core Safety Limits**

Safety Limit		
Power	Mass Flow Rate	Outlet Temperature
190 kW	23 gpm	160 F

## **5. Reactor coolant system**

The HEU to LEU conversion does not require any changes to the reactor coolant system. More details about this topic can be found in Ref. 1.

## **6. Engineering Safety Features**

The HEU to LEU conversion does not require any changes to engineering safety features. More details about this topic can be found in Ref. 1.

## **7. Instrumentation and control**

The HEU to LEU conversion does not require any changes to instrumentation and control. More details about this topic can be found in Ref. 1.

## **8. Electrical power system**

The HEU to LEU conversion does not require any changes to electrical power systems. More details about this topic can be found in Ref. 1.

## **9. Auxiliary system**

Existing procedure will be used for fuel storage.

## **10. Experimental Facility and utilization**

The HEU to LEU conversion does not require any changes to experimental facility and utilization of UFTR. More details about this topic can be found in Ref. 1.

## **11. Radiation Protection and Radioactive Waste Management**

The HEU to LEU conversion does not require any changes to the radiation protection and radioactive waste management of UFTR facility. More details about this topic can be found in Ref. 1.

## **12. Conduct of Operation**

### **12.1 Organization and Staff Qualification**

The HEU to LEU conversion does not require any changes to the organization and staff qualification of UFTR personnel. More details about this topic can be found in Ref. 1.

### **12.2 Procedures**

Few procedural changes are required for the HEU to LEU fuel conversion. The expected changes are outlined in the following paragraphs.

In SOP-A.7 (Determination of Control Blade Integral or Differential Reactivity Worth) the reference to 2.3%  $\Delta k/k$  core excess reactivity limit will be changed in Section 3.1.1.1(2) to 1.4%  $\Delta k/k$  per Technical Specification changes. The same change from 2.3%  $\Delta k/k$  to 1.4%  $\Delta k/k$  will be made for the total reactivity worth allowed for all experiments in Section 3.1.1.2(2). In addition, the power ratio curves in Appendix II of this procedure for evaluation of control blade reactivity worth by the blade drop method will need to be regenerated for the LEU fuel if this method of blade worth measurement is utilized.

In SOP-C.2 (Fuel Loading) the excess reactivity limit will be changed to 1.4% versus 2.3% in Section 3.2, Section 4.5, in the note for Section 7.2.2.5, in Section 7.4.1.1.3 and Section 7.4.2.1.3.

In SOP-C.3 (Fuel Inventory Procedure) the fuel inventory forms should be changed to account for the presence of LEU uranium-silicide fuel. Though this change is not required, it is recommended to assure ease of assuring the presence and location of all special nuclear material (fuel).

### **12.3 Operator Training and Re-qualification**

The HEU to LEU conversion requires no changes to the requalification training program itself. Some changes will be required where fuel description, fuel loading, reactivity limitations and safety limits as well as accident analyses are addressed in the various training modules. These will be changed as the modules are updated for the respective training topics.

### **12.4 Emergency Plan**

The only changes anticipated for the approved UFTR Emergency Plan are the fuel description on page 1-1 in Section 1.3.1; in the Credible Accidents and Consequences in Section 1.5 on pages 1-6, 1-12 and 1-13; in the definition of Site Boundary on page 2.3; and possibly in Section 5.0 Emergency Action Levels on page 5-1 and Section 6.0 Emergency Planning Zone on page 6-1; though the latter two do not seem necessary at this point based on the analyses in Section B.

### **12.5 Physical Security**

The HEU to LEU conversion does not necessitate any changes at this point; changes are anticipated to be proposed but will be submitted under separate cover and withheld from public disclosure.

## 12.6 Reactor Reload and Startup Plan

Existing procedures will control unloading HEU and loading LEU fuel. The primary applicable procedures are SOP-C.1 (Irradiated Fuel Handling), SOP-C.2 (Fuel Loading), SOP-D.2 (Radiation Work Permit), and SOP-E.2 (Alterations to Reactor Shielding and Graphite Configuration). Of these, the only changes needed are that the core excess reactivity limit specified in SOP-C.2 will be changed from 2.3%  $\Delta k/k$  to 1.4%  $\Delta k/k$ . All other procedural steps remain unchanged as stated.

## 13. Accident Analysis

The accident categories that were evaluated for the HEU and LEU cores in this section were reactivity insertion transients during UFTR operations, a loss-of-coolant accident during full-power operation, a fuel handling accident involving possible release of fission products (considered as the maximum credible accident) and the maximum hypothetical accident (MHA), resulting in large-scale release of radioactivity. Accidents involving explosive chemical reactions and graphite fires that were evaluated in Ref. 16 were not addressed here because these accidents do not depend on whether HEU or LEU fuel is used in the reactor core.

The following three hypothetical reactivity insertion scenarios were postulated analyzed:

- A step insertion of 0.6%  $\Delta k/k$  reactivity. The Technical Specifications state that the absolute reactivity worth of any single moveable or non-secured experiment shall not exceed 0.6%  $\Delta k/k$ . This scenario represents the reactivity insertion resulting from the rapid ejection of a maximum worth experiment from the reactor. Cases were analyzed both without and with reactor emergency shutdown system (SCRAM).
- A reactivity ramp insertion of 0.06%  $\Delta k/k$ /second. This scenario represents the insertion of reactivity due to control blade withdrawal at the maximum rate allowed by the Technical Specifications. Reactor SCRAM was initiated at the overpower trip setting of 125 kW. No limit was set for the amount of reactivity prior to SCRAM.
- A sudden insertion of the maximum excess reactivity allowed by the Technical Specifications without reactor SCRAM. The existing Technical Specification limits the excess reactivity in the UFTR to a maximum of 2.3%  $\Delta k/k$ . This value is analyzed for comparison of the HEU and LEU cores. However, 2.3%  $\Delta k/k$  has not and would not be loaded into the core. This is simply an historical value used as a limit.

A loss-of-coolant accident was summarized but not re-analyzed here because the LEU core has a lower power per fuel plate and a larger coolant volume fraction that will result in a fuel temperature increase that is lower in the LEU core than in the HEU core.

Further, in this section, a fuel handling accident (FHA) and the maximum hypothetical accident (MHA) were analyzed for both HEU and LEU cores as follows:

- FHA: In this accident, it is assumed that one irradiated fuel element is dropped during a core reload or other fuel handling operation.
- MHA: A core-crushing accident is considered in which the core is assumed to be severely crushed in either the horizontal or vertical direction by postulating that a ~~concrete~~ concrete shield block is inadvertently dropped onto the core.

Calculations were performed for both the HEU and reference LEU cores. Reactivity coefficients and neutron kinetics parameters calculated as part of the reactor dynamic design section (see Section 4.5) were employed to account for inherent reactivity feedback mechanisms. Because of the non-linearity of the feedback coefficients with increasing temperature or water void, the calculated coefficients with the smallest magnitude were employed for conservatism in the transient analyses. The coefficients that were calculated are summarized in Table 13-1.

Table 13-1 Kinetics Parameters and Reactivity Coefficients Calculated for UFTR Accident Analyses.

Parameter	HEU	LEU
$\beta_{\text{eff}}$	0.0079	0.0077
$\lambda$ ( $\mu\text{s}$ )	187.4	177.5
$\alpha_{\text{void}} (\Delta\rho/\%\text{void})$	-1.48E-03	-1.53E-03
$\alpha_{\text{water}} (\Delta\rho/^{\circ}\text{C})$	-5.91E-05	-5.68E-05
$\alpha_{\text{fuel}} (\Delta\rho/^{\circ}\text{C})$	-0.29E-05	-1.40E-05

The total reactivity worth of the safety and regulating blades calculated for the HEU and LEU cores was assumed to be inserted under reactor SCRAM conditions. The total blade reactivity worths calculated in Section 4.5 are for insertion from a fully-withdrawn position. However, it is difficult to envision a situation where all blades are fully-withdrawn when fuel is in the core. Therefore, the reactivity worth of inserting all blades from a critical core condition was used for the SCRAM reactivity in this scenario. The worth of all blades when inserted from a critical core condition was calculated to be 5.44%  $\Delta k/k$  for the HEU core and 5.09%  $\Delta k/k$  for the LEU core.

The reactor trip setting for these accident analyses is the reactor overpower setting of 125 kW. When the core power reaches this power level, a signal is sent to release the blades and drop them into a fully-inserted position. A delay time of 100 ms (0.1 seconds) was used to represent the delay from the time the SCRAM signal is sent to when the blades actually start to fall. The blade drop time is currently required to be less than 1 second in the UFTR Technical Specifications. Blade drop times of both 1.0 and 1.5 seconds were considered in these analyses.

## 13.1 Reactivity Insertion Accidents

### 13.1.1 Step Insertion of 0.6% $\Delta k/k$

This hypothetical accident was analyzed using the RELAP5-3D code (Ref. 10). The reactor was modeled as two fuel-plate channels. One channel represented the fuel plate and associated coolant for the plate with peak power in the core, and the other channel represented the average of the remainder of the core. The fuel power densities for the peak and average channels were taken from MCNP results for the core operating at 100 kW under steady-state conditions. Fuel plate and channel dimensions corresponding to the fuel assembly design were utilized. The effect of engineering uncertainties (hot channel factors) was not included in these analyses. A comparison of key parameters for the HEU and LEU cores is provided in Table 13-2.

**Table 13-2 Selected Parameters for UFTR HEU and LEU Core Transient Analyses.**

<b>Parameter</b>	<b>HEU</b>	<b>LEU</b>
Fuel meat thickness, cm	0.1016	0.0508
Fuel plate thickness, cm	0.1778	0.1270
Fuel plate width, cm	7.226	7.226
Fuel plate heated length, cm	60.0	60.0
Coolant channel thickness, cm	0.348	0.282
Number of axial nodes in fuel plate	12	12
Fraction of core represented by peak power channel	0.42%	0.31%
Coolant inlet temperature, °C	30	30
Coolant exit pressure, kPa	101.3	101.3
Channel inlet velocity, cm/s	3.29	3.18
Initial total core power, kW	100	100
Peak-to-average power density	1.62	1.78
Fraction of heat deposited directly into coolant	5.2%	4.7%

Results for the RELAP5-3D analyses of a step insertion of 0.6%  $\Delta k/k$  in 0.1 seconds on the HEU and LEU cores are presented in Table 13-3. In the unprotected transient cases, the core power rises to 1.30 MW in the HEU core and 1.25 MW in the LEU core before inherent reactivity feedback mechanisms suppress the transient power spike. There is a much larger prompt fuel temperature (Doppler) feedback in the LEU fuel, which suppresses the power spike earlier.



Table 13-3 RELAP5-3D Results for Step Insertion of 0.6%  $\Delta k/k$  in UFTR.

Case	HEU Core			LEU Core		
	No SCRAM	SCRAM (1.0s drop)	SCRAM (1.5s drop)	No SCRAM	SCRAM (1.0s drop)	SCRAM (1.5s drop)
$P_o$ (kW)	100			100		
Reactivity Insertion	0.60%			0.60%		
	\$0.76			\$0.78		

Length of Transient Modeled (s)	300.0	30.0	30.0	21.2	30.0	30.0
Time to Peak Power (s)	2.57	0.17	0.17	2.46	0.14	0.14
Peak Power (MW)	1.30	0.29	0.30	1.25	0.32	0.32
$T_{fuel,max}$ (°C) (at Peak Power)	89	54	54	96	52	52
$T_{fuel,max}$ (°C)	108	54	55	107	52	52
$T_{clad,max}$ (°C)	108	54	55	107	52	52
$T_{cool,max}$ (°C)	101	44	44	101	45	45

The peak fuel temperature in the HEU core reaches 89°C at the time of peak power and continues to rise to a maximum of 108°C. In the LEU core, the peak fuel temperature at the time of the power peak is 96°C, but it reaches a lower maximum temperature of 107°C due to the fuel temperature coefficient. The LEU fuel heats up more rapidly because the LEU  $U_3Si_2$ -Al dispersion fuel meat has a lower thermal conductivity than the HEU U-Al alloy fuel meat.

The unprotected insertion of 0.6%  $\Delta k/k$  was modeled for 300 seconds to show that the power does not rise again after suppression of the initial power spike. However, the core does reach an equilibrium power level of about 600 kW. Under these conditions, the coolant reaches the saturation temperature and boiling occurs in the uppermost nodes of the coolant channel. The peak temperatures of about 108°C in the fuel and cladding for both the HEU and LEU cores are well below the incipient melting temperatures of 660°C for the 1100 aluminum cladding of the HEU fuel and 582°C for the 6061 cladding of the LEU silicide fuel. Thus, even without action of the reactivity control system, the UFTR can tolerate the sudden ejection of a maximum reactivity worth experiment, or equivalent reactivity insertion, without any fuel damage in either the HEU or LEU fuel assembly designs.

Cases with reactor SCRAM were evaluated for the HEU and LEU cores. In each case, the reactor is tripped at 125 kW, with an assumed 0.1 second delay before the control blades begin dropping into the core. In these cases, the core reaches a maximum power of about 300 kW and the peak fuel temperature increases to 54 °C in the HEU core and 52°C in the LEU core. Based on the RELAP5 steady-state analysis, this transient results in a fuel temperature rise of only 1°C. If the control blade drop time is increased from 1.0 second (the current Technical Specification upper limit allowed for the UFTR) to 1.5 seconds, there is practically no impact on the maximum fuel and clad temperatures as shown in Table 13-3.

### 13.1.2 Slow Insertion of 0.06% $\Delta k/k$ /second

The UFTR Technical Specifications require that the reactivity addition from control blade withdrawal must be less than 0.06%  $\Delta k/k$ /second when averaged over any 10 second interval. In this hypothetical accident, a reactivity insertion at this maximum rate initiates the transient and continues until the reactor is tripped at the overpower trip setting of 125 kW. The results of RELAP5-3D calculations in the HEU and LEU cores are summarized in Table 13-4.

Table 13-4 RELAP5-3D Results for Slow Insertion of 0.06%  $\Delta k/k$ /second.

Case	HEU Core		LEU Core	
	SCRAM (1.0s drop)	SCRAM (1.5s drop)	SCRAM (1.0s drop)	SCRAM (1.5s drop)
P <sub>o</sub> (kW)	100		100	
Reactivity Insertion	0.06%/second		0.06%/second	
	7.6¢/second		7.8¢/second	

Length of Transient Modeled (s)	30.0	30.0	30.0	30.0
Time to Peak Power (s)	2.26	2.26	2.21	2.21
Peak Power (MW)	0.13	0.13	0.13	0.13
T <sub>fuel,max</sub> (°C) (at Peak Power)	54	54	52	52
T <sub>fuel,max</sub> (°C)	54	54	52	52
T <sub>clad,max</sub> (°C)	54	54	52	52
T <sub>cool,max</sub> (°C)	44	44	45	45

The cores reach the overpower trip setting of 125 kW within about 2.1 seconds, at which time a reactivity of only 0.126%  $\Delta k/k$  has been inserted. The maximum temperatures in the fuel and cladding of the HEU and LEU cores increase by only about 1°C, and remain well below the incipient melting temperatures of the claddings.

Figures 13-1 and 13-2 show the core power and maximum clad temperatures for this hypothetical accident scenario for the HEU and LEU cores, respectively. The core power trace shows almost no impact after increasing then blade drop time from the current 1.0 second specified in the current Technical Specifications to 1.5 seconds. The effect on the maximum fuel and clad temperatures in the HEU and LEU cores is similarly negligible.

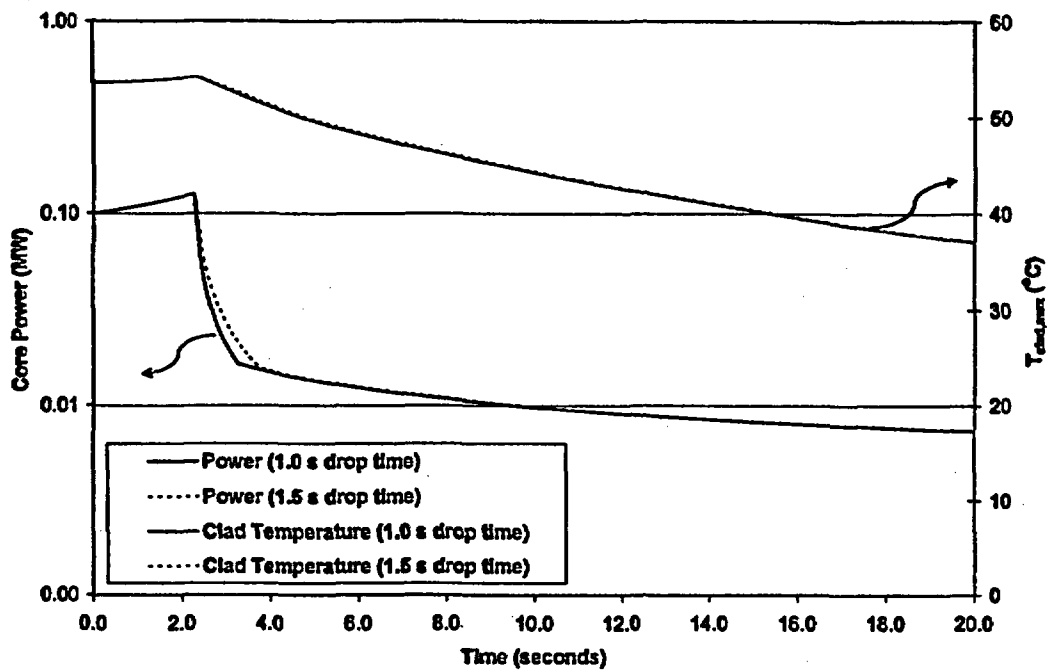


Figure 13-1 Power and Clad Temperature Response to Slow Insertion of 0.06%  $\Delta k/k/s$  with SCRAM in HEU Core

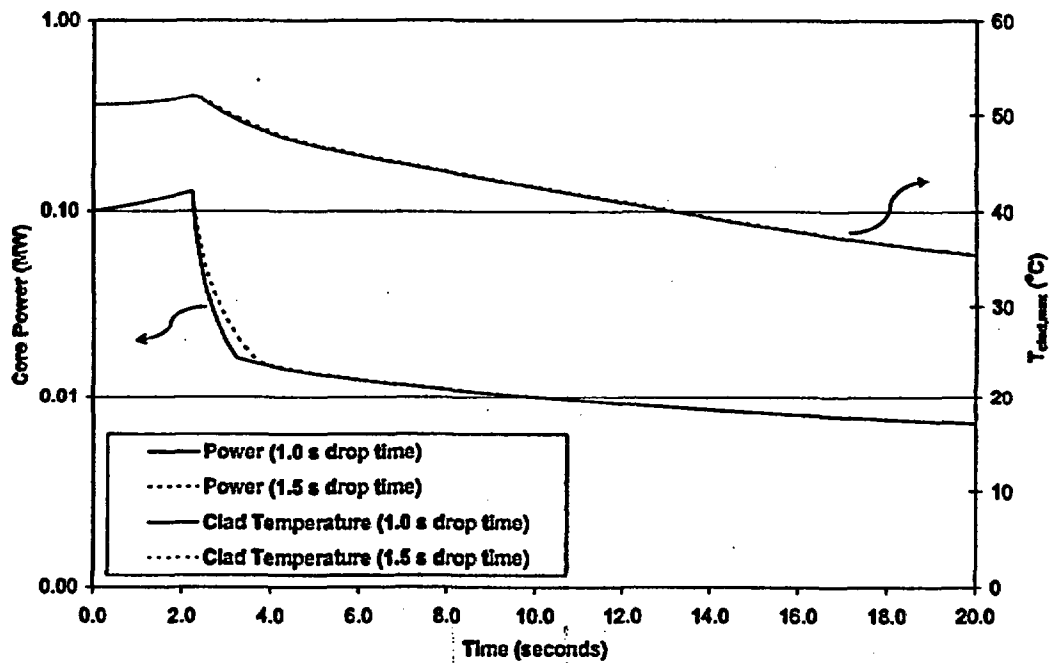


Figure 13-2 Power and Clad Temperature Response to Slow Insertion of 0.06%  $\Delta k/k/s$  with SCRAM in LEU Core

### 13.1.3 Sudden Insertion of the Maximum Allowed Excess Reactivity

The UFTR Technical Specifications for the current HEU core allow a maximum excess reactivity of 2.3%  $\Delta k/k$  based on analysis of the BORAX experiments in Ref. 1 and on analysis of the D12/25 SPERT I experiments in Ref. 18.

For the analysis of a sudden insertion of the maximum allowed excess reactivity, an approach is used similar to that described in Ref. 18. That analysis concluded that for a reactor like the UFTR operating at low power, a sudden insertion of 2.6%  $\Delta k/k$  would result in a peak fuel temperature of 586°C, which is 74°C below the melting temperature of the fuel meat. The analysis methodology that was used to obtain this result is described below, followed by a comparison of results from the D12/25 SPERT-I tests, computations for a generic Argonaut-UTR, and computations specific to the UFTR.

The analysis methodology (Refs. 18 and 19) is based upon predicting the total energy release that results from the initial power spike before the transient is suppressed by reactivity feedback effects. The total energy release is predicted by the relationship

$$E_{total} = 2\alpha / b \quad (13.1)$$

where  $\alpha$  is the inverse or reciprocal period in  $s^{-1}$  and  $b$  is a reactivity feedback coefficient in units of  $s^{-1}/MWs$ . The inverse period can be calculated using the relationship:

$$\alpha = \frac{\rho - \beta_{eff}}{l} \quad (13.2)$$

where  $\rho$  is the reactivity insertion,  $\beta_{eff}$  is the effective delay neutron fraction, and  $l$  is the prompt neutron lifetime.

The reactivity feedback coefficient,  $b$ , used to calculate  $E_{total}$  in Eq. 13.1 depends on the inverse period, and can be determined from the SPERT-I test results. Figure 13-3 illustrates the relationship between  $b$  and  $\alpha$  using data from Ref. 19 for the D12/25 core and then fit with a 3<sup>rd</sup> order polynomial to derive the relationship:

$$b = 2 \times 10^{-6} \alpha^3 - 1.2 \times 10^{-3} \alpha^2 + 0.28 \alpha + 3.17 \text{ [s}^{-1}/MWs\text{]}. \quad (13.3)$$

Combining Eqs. 13.1 and 13.3 gives a relationship between the total energy release and the inverse period:

$$E_{total} = (1 \times 10^{-6} \alpha^2 - 6.0 \times 10^{-4} \alpha + 0.14 + 1.585 \alpha^{-1})^{-1} \text{ [MWs]}. \quad (13.4)$$

The maximum clad or fuel temperature can then be predicted by scaling results from the SPERT-I tests:

$$T_{max} = T_{max, SPERT-I} \cdot \frac{E_{total}}{E_{total, SPERT-I}} \quad (13.5)$$

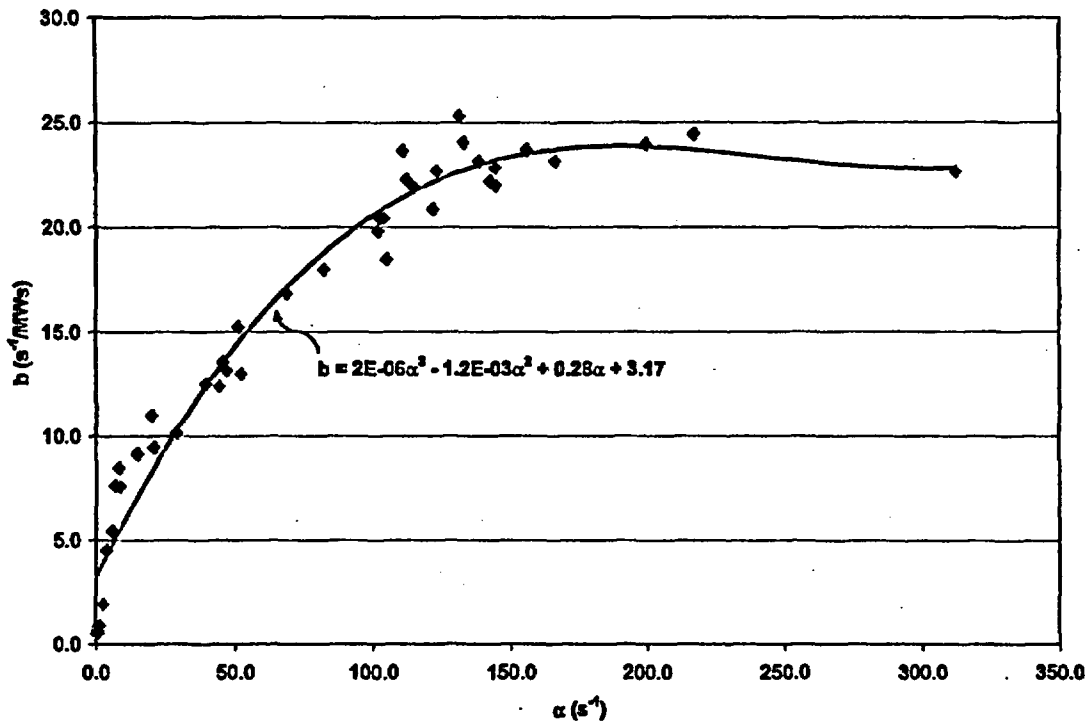


Figure 13-3 Relationship Between Reactivity Coefficient and Inverse Period from D12/25 SPERT-I Tests

The data used for Figure 13-3 is obtained from Ref. 19. Table 13-5 provides a comparison of the transient response from a sudden reactivity insertion in the SPERT-I destructive test, computations for a generic UTR, and computations specific to the UFTR following the methodology outlined above. One of the key parameters in this analysis is the reciprocal period  $\alpha$ , related to the prompt-neutron lifetime as shown in equation 13.2. From the measured value of  $\beta_{eff}/l$  in the water-reflected D12/25 SPERT I tests, the prompt-neutron lifetime is estimated to be about 60  $\mu\text{s}$ , using a  $\beta_{eff}$  of 0.0075. The prompt-neutron lifetime in the graphite-reflected HEU core of the UFTR was calculated here to be 187  $\mu\text{s}$ . A 2.6%  $\Delta k/k$  reactivity insertion in the SPERT reactor resulted in 35% fuel melting and destruction of the core from a coolant pressure burst. As shown in Table 13-5, increasing the lifetime by a factor of 3 significantly reduces the severity of the unprotected transient that results from the reactivity insertion. Furthermore, a 2.3%  $\Delta k/k$  reactivity insertion in the HEU-fueled UFTR is predicted to yield an energy release of 8.5 MWs and a peak temperature of 415°C, or about 245°C below the melting temperature of the Al-1100 clad.

The reference LEU core has a calculated prompt-neutron lifetime of 177  $\mu\text{s}$ , which is very close to the 187  $\mu\text{s}$  lifetime calculated for the HEU core. Likewise, the temperature reactivity coefficients for water and coolant void are similar for the HEU and LEU cores, as shown in Table 13-1. The SPERT tests were performed with HEU fuel, so very little of the reactivity feedback was associated with the fuel temperature. Since the LEU fuel has a much larger prompt fuel temperature (Doppler) feedback coefficient than the HEU fuel, the energy release and hence the maximum clad temperature resulting from a reactivity insertion of 2.3%  $\Delta k/k$  will be much lower than the 428°C value predicted for the LEU fuel in Table 13-5 using the methodology outlined above.

The maximum temperatures in the UFTR are predicted to be well below the incipient melting temperature of 660°C for the Al-1100 cladding of the HEU fuel and the incipient melting temperature of 582°C for the Al-6061 cladding of the LEU fuel. Thus, insertion into the UFTR LEU core of the maximum allowed excess reactivity of 2.3%  $\Delta k/k$  specified in the current Technical Specifications without action of the reactor protection system would result in maximum fuel and cladding temperatures that are well below the incipient melting temperature of the cladding.

Table 13-5 Transient Response from a Sudden Reactivity Insertion

	SPERT-I	Argonaut-UTR <sup>2</sup>	UFTR HEU Core		UFTR LEU Core
$\rho$ (% $\Delta k/k$ )	2.63%	2.6%	2.6%	2.3%	2.3%
$l$ ( $\mu s$ )	60	140	187.4	187.4	177.5
$\beta_{eff}$	0.0075	0.0065	0.00791	0.00791	0.00771
$\alpha$ ( $s^{-1}$ )	313	138	96.5	80.5	86.1
$E_{total}$ (MWs)	30.7	12	9.3	8.5	<8.8
$T_{max}$ (°C)	1500 <sup>1</sup>	586	453	415	<428

<sup>1</sup> Estimated maximum temperature; from NUREG/CR-2079 (Ref. 17).

<sup>2</sup> From analysis summarized in NUREG/CR-2079.

Nonetheless, it is proposed that the maximum allowed excess reactivity in the Technical Specifications of the LEU UFTR core be reduced from 2.3%  $\Delta k/k$  to 1.4%  $\Delta k/k$  since the facility does not require an excess reactivity larger than 1.4%  $\Delta k/k$  and has never had this much excess reactivity. For a step insertion of 1.4%  $\Delta k/k$  the total energy release would be < 6.1 MWs and the maximum temperature of the cladding would be less than 300°C providing much conservatism.

## 13.2 Loss-of-Coolant Accident

The UFTR FSAR (Ref. 1) evaluated a loss-of-coolant accident during full-power operation. The increase in fuel temperature following a loss-of-coolant and shutdown of the reactor either by the negative void coefficient of reactivity or by the insertion of control blades into the reactor showed that the fuel temperature will increase by less than 17°C (30°F) following a full trip event (blade drop with coolant dump).

This loss-of-coolant accident was not re-evaluated here for the LEU core because the average power per fuel plate in the fuel element with highest power in the LEU core (Table 4-11, position 2-3) is only 75% of the average power per plate in the corresponding fuel element (position 5-1) in the HEU core. This is mostly because an LEU element contains 14 fuel plates and an HEU fuel element contains 11 fuel plates. In addition, the volume fraction of air available for cooling after the water is lost is slightly larger in an LEU fuel element than in an HEU fuel element. These two effects, the lower power per plate and the slightly larger coolant volume fraction, will result in a fuel temperature increase in the LEU core that is less than the approximate 17°C temperature increase in the HEU core.

Consequently, a loss-of-coolant accident from operation at 100 kW power in either the HEU or LEU cores will result in maximum clad temperatures that are far below the melting temperatures of either the 1100 Al cladding of the HEU fuel (660°C) or the 6061 Al cladding of the LEU fuel (582°C). Integrity of the cladding will be maintained with both the HEU fuel and the LEU fuel and there will be no release of radioactivity.

### **13.3 Fuel Handling Accident (FHA)**

This hypothetical accident assumes that one fuel element is dropped during a core reload or other fuel handling operation. Fuel handling operations allow moving only one bundle at a time and it must be secured before proceeding to move another. For this event, assumptions were made based on credible operation of the reactor. Typically, the UFTS is shutdown from power operation for more than seven days prior to commencing fuel-handling operations. In all cases, the reactor would be shutdown from power operation for at least three days to allow substantial decay of fission product inventory. Since the coolant water may be drained from the core immediately after shutdown, any fission product release would be directly to the air of the reactor cell as a conservative measure.

The following data and assumptions were used to evaluate the source term associated with this accident:

- (1) The reactor is operated at 100 kW steady-state power for 4 hours per day for 30 days.
- (2) The fuel elements with highest power in the HEU and LEU cores based on MCNP5 calculations were selected for evaluation. These were bundle 5-1 with a power of 5.77 kW in the HEU core and bundle 2-3 with a power of 5.45 kW in the LEU core. These bundle powers were derived from an MCNP tally that assumes that all of the energy produced is deposited locally. This results in maximum bundle powers that are slightly larger than those shown in Table 4-14, which accounts for energy deposited in the fuel plates and gamma energy deposited in the coolant, moderator, and structural materials.
- (3) Radioisotope inventories were calculated three days after shutdown from power operation.
- (4) The radioisotopes of greatest significance for release in case of an accident are the radio-iodines and the noble gases, krypton and xenon.
- (5) It is postulated that the fuel element would undergo severe mechanical damage due to being dropped during the fuel handling operation and that this damage would be sufficient to expose fuel surface areas equivalent to stripping the aluminum cladding from one fuel plate out of 11 plates in an HEU element and one fuel plate out of 14 fuel plates in an LEU element. It is further assumed that 100% of the gaseous activity produced within the recoil range of the particles ( $1.37 \times 10^{-3}$  cm) or 2.7% of the total volatile activity instantaneously escapes from the fuel plate into the reactor cell.

#### **13.3.1 Radionuclide Inventories**

Radionuclide inventories for the highest power fuel element in the HEU and LEU cores were calculated using the ORIGEN-S code (Ref. 6) under the assumptions in the previous paragraph. Additional calculations verified that all of the gaseous fission products except  $^{85}\text{Kr}$  (half-life 11 years) reach their equilibrium concentrations based on this operating assumption.

The activities of the krypton, iodine, and xenon isotopes in one fuel plate of the HEU and LEU cores are given in Table 13-6 along with the inventory (2.7% of the total) that is assumed to escape from the damaged fuel plate into the air of the reactor cell.

Table 13-6 Calculated Radionuclide Inventories (Ci) Released into the Reactor Cell from the FHA in the HEU and LEU Cores

Isotope	HEU Core		LEU Core	
	Ci in One Plate Three Days after Shutdown	Ci in 2.7 % of One Plate Three Days after Shutdown	Ci in One Plate Three Days after Shutdown	Ci in 2.7 % of One Plate Three Days after Shutdown
Kr 85				
Kr 85m				
Kr 88				
I 130				
I 131				
I 132				
I 133				
I 135				
Xe 133				
Xe133m				
Xe 135				

### 13.3.2 Methodology for Dose Calculations

The following assumptions and methods were used to calculate the doses for occupational exposure at the site boundary and public exposure at the urban boundary. As explained in NUREG 1537 Part 2 (Ref. 20), the accidental dose limits found acceptable to the NRC staff for reactors initially licensed before January 1, 1994, has been 5 rem to the whole body and 30 rem to the thyroid for occupational exposure and 500 mrem to the whole body and 3 rem to the thyroid for members of the public.

#### Site Boundary (Occupational Exposure)

For Research Reactor Site Evaluation, the ANSI/ANS (Ref. 21) provides guidance on the location of the site boundary. According to this guidance, the location of the site boundary for the UFTR is 30 m from the outside wall of the reactor building. This represents the immediate surrounding of the UFTR reactor building which could be rapidly evacuated and controlled.

The calculation methodology for the site boundary assessment is based on the analysis presented in NUREG/CR-2079. The following assumptions were used in the analysis:

1. Breathing rate:  $3.33 \times 10^{-4} \text{ m}^3/\text{sec}$ .
2.  $\chi/Q$ , atmospheric dispersion factor:  $0.01 \text{ sec}/\text{m}^3$  for the 30m distance.
3. Inhalation activity fraction to the thyroid: 0.23.
4. Fractional release from the fuel plate inventory scenario: 2.7%.
5. Fractional release of Iodine from the building: 0.25(based on ANSI/ANS-15.7, Ref. 21).



### Urban Boundary (Public Exposure)

In regard to Research Reactor Site Evaluation, the ANSI/ANS (Ref. 21) provides guidance on the location of the urban boundary. According to this guidance, the location of the urban boundary for the UFTR is 400 m from the outside wall of the reactor building to the closest residential area. Between the site boundary and urban boundary doses were also evaluated for the following point of interests: East Hall Housing (190m), Ben Griffin Stadium (230m), Weaver Hall Housing (250m), Riker Hall Housing (275m), O'Connell Center (300m), and Tolbert Hall Housing (310m). Distances from the reactor building to the respective point of interest are shown in parentheses.

The calculation methodology used for the urban boundary assessment is based on the analysis shown in the UFTR Final Safety Analysis Report (Ref. 1). The assumptions for the analysis are based on the following:

1. Breathing rate:  $3.47 \times 10^{-4} \text{ m}^3/\text{sec}$  for 0 to 8 hours based on Ref. 22
2. Breathing rate:  $1.75 \times 10^{-4} \text{ m}^3/\text{sec}$  for 8 to 24 hours based on Ref. 22
3.  $\chi/Q$ , atmospheric dispersion factor is based on Reg. Guide 1.3 (Ref. 22) for ground release.
4. Fractional release from the fuel accident inventory scenario: 2.7%.
5. Fractional Iodine release from the building: 0.25.
6. Reactor cell leak rate: 0.2% volume/ hour.
7. Dose coefficients for Iodine taken from Federal Guidance Report (FGR) No. 11 (Ref. 23) based on inhalation.
8. Dose coefficients for Xenon and Krypton taken from FGR No. 12 (Ref. 24) based on dose coefficients for air submission.
9. Dose calculations are calculated for a 1 day (24 hours) exposure.

The dose conversion factors that were used to calculate thyroid and whole body doses at the site and urban boundaries are shown in Table 13-7.

**Table 13-7 Dose Conversion Factors Utilized for Site and Urban Boundary Analyses**

Isotope	Exposure-to- Dose Conversion Factors <sup>20</sup> for Inhalation of the Thyroid <sup>a,b</sup> (rem/Ci)	Effective Absorbed Energy per Disintegration <sup>12,13</sup> for the Whole Body <sup>a</sup> (MeV)	Dose Coefficients for Air Submersion <sup>21</sup> for the Effective Whole Body <sup>b</sup> (rem-s/Ci-m <sup>3</sup> )
Kr 85		1.20E-04	4.40E-04
Kr 85m		1.60E-04	2.77E-02
Kr 88		6.84E-04	3.77E-01
I 129	5.77E+06		
I 130	7.36E+04		
I 131	1.08E+06		
I 132	6.44E+03		
I 133	1.80E+05		
I 133m	1.80E+05		
I 134	1.07E+03		
I 134m	1.07E+03		
I 135	3.13E+04		
I 135m	3.13E+04		
Xe 133		6.44E-05	5.77E-03
Xe 133m		1.01E-04	5.07E-03
Xe 135		2.41E-04	4.40E-02
Xe 135m		1.55E-04	7.55E-02

<sup>a</sup> Site Boundary

<sup>b</sup> Urban Boundary

### 13.3.3 Dose Calculation Results for Fuel Handling Accident

The calculated thyroid doses and whole body doses at the site boundary and at the urban boundary for the fuel handling accident are shown in Tables 13-8 and Table 13-9, respectively.

**Table 13-8 Thyroid Doses and Whole Body Doses Calculated at the Site Boundary (30 m) for the FHA in the HEU and LEU Cores**

Isotope	HEU Core		LEU Core	
	Thyroid Dose, rem	Whole Body Dose, rem	Thyroid Dose, rem	Whole Body Dose, rem
Kr 85				
Kr 85m				
Kr 88				
I 130				
I 131				
I 132				
I 133				
I 135				
Xe 133				
Xe133m				
Xe 135				
<b>Total Doses</b>	<b><math>1.10 \times 10^{-3}</math></b>	<b><math>7.60 \times 10^{-3}</math></b>	<b><math>8.14 \times 10^{-3}</math></b>	<b><math>5.63 \times 10^{-3}</math></b>

These doses are significantly less than the accidental dose limits of 30 rem to the thyroid and 5 rem to the whole body at the site boundary for occupational exposure.

**Table 13-9 Thyroid Doses and Whole Body Doses Calculated at the Urban Boundary (400 m) for the FHA in the HEU and LEU Cores**

Isotope	HEU Core		LEU Core	
	Thyroid Dose, rem	Whole Body Dose, rem	Thyroid Dose, rem	Whole Body Dose, rem
Kr 85				
Kr 85m				
Kr 88				
I 130				
I 131				
I 132				
I 133				
I 135				
Xe 133				
Xe133m				
Xe 135				
<b>Total Doses</b>	<b><math>1.39 \times 10^{-4}</math></b>	<b><math>3.92 \times 10^{-4}</math></b>	<b><math>1.03 \times 10^{-4}</math></b>	<b><math>2.90 \times 10^{-4}</math></b>

These doses are extremely small in comparison with the dose limits of 3 rem to the thyroid and 0.5 rem to the whole body at the urban boundary for public exposure. Thyroid doses and whole body doses calculated at points of interest between the site

boundary (30 m) and the urban boundary (400 m) for the fuel-handling accident in the HEU and LEU Cores are given in Table 13-10 and shown in Figure 13-4.

Table 13-10 Thyroid and Whole Body Doses Calculated at Points of Interest Between the Site (30 m) and the Urban Boundary (400 m) for the FHA in the HEU and LEU Cores.

Distance from Source and Location	Thyroid Dose (rem)		Whole Body Dose (rem)	
	HEU Core	LEU Core	HEU Core	LEU Core
30 m Site Boundary	1.10E-02	8.14E-03	7.60E-05	5.63E-05
190 m East Hall Housing	5.17E-04	3.83E-04	1.46E-07	1.08E-07
230 m Ben Griffin Stadium	3.72E-04	2.75E-04	1.05E-07	7.73E-08
250 m Weaver Hall Housing	3.20E-04	2.37E-04	8.98E-08	6.63E-08
275 m Weaver Hall Housing	2.70E-04	2.00E-04	7.65E-08	5.65E-08
300 m Riker Hall Housing	2.38E-04	1.76E-04	6.72E-08	4.97E-08
310 m O'Connell Center	2.21E-04	1.64E-04	6.24E-08	4.61E-08
400 m Urban Boundary	1.39E-04	1.03E-04	3.92E-08	2.90E-08

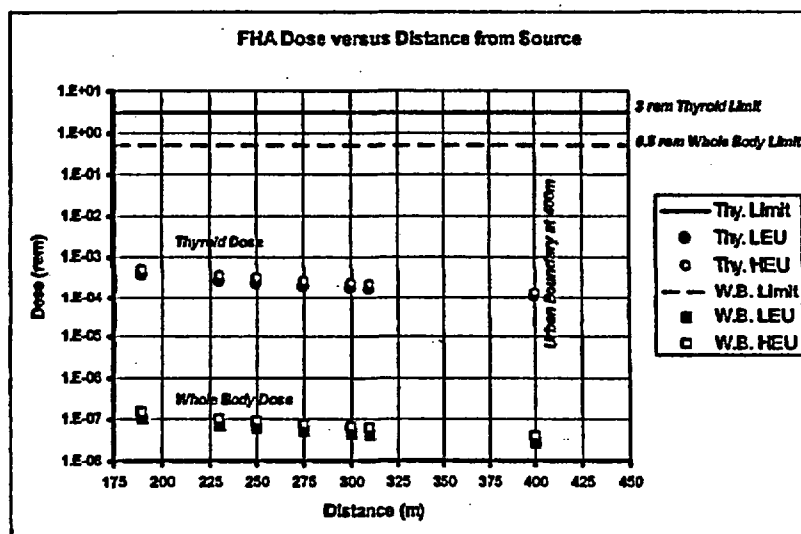


Figure 13-4 Thyroid Doses and Whole Body Doses for the Fuel Handling Accident

### 13.4 Maximum Hypothetical Accident (MHA)

The maximum hypothetical accident for the UFTR is a core-crushing accident in which the core is assumed to be severely crushed in either the horizontal or vertical direction by postulating that a concrete shield block is inadvertently dropped onto the core. Based on the design of the facility and the size and weight of the concrete blocks, it is difficult to conceive of how the core would actually be crushed. Nevertheless, even though the possibility of this hypothetical accident is extremely remote, the hypothesis is

made that dropping of a **concrete** shield block would result in severe mechanical damage to the fuel and a significant release of fission products.

The following data and assumptions were used to evaluate the source term associated with this accident:

- (1) The reactor is operated at 100 kW steady-state power with an equilibrium concentration of fission products.
- (2) The fuel elements with highest power in the HEU and LEU cores based on MCNP5 calculations were selected for evaluation. These were element 5-1 with a power of 5.77 kW in the HEU core and bundle 2-3 with a power of 5.45 kW in the LEU core.  
  
These bundle powers were derived from an MCNP tally that assumes that all of the energy produced is deposited locally. This results in maximum bundle powers that are slightly larger than those shown in Table 4-14, which accounts for energy deposited in the fuel plates and gamma energy deposited in the coolant, moderator, and structural materials.
- (3) Radioisotope inventories were calculated at 100 kW just before the accident.
- (4) The radioisotopes of greatest significance for release in case of an accident are the radio-iodines and the noble gases, krypton and xenon.
- (5) All of the water is assumed to drain out of the core in less than one second, so that any fission product release would be directly to the air of the reactor cell.
- (6) It is postulated that the core would undergo severe mechanical damage due to the core crushing accident and that this damage would be sufficient to expose fuel surface areas equivalent to stripping the aluminum cladding from one entire HEU element in the HEU core and one LEU element in the LEU core. It is further assumed that 100% of the gaseous activity produced within the recoil range of the particles ( $1.37 \times 10^{-3}$  cm) or 2.7% of the total gaseous activity instantaneously escapes from the fuel element into the reactor cell.

#### **13.4.1 Radionuclide Inventories**

Radionuclide inventories for the highest power fuel element in the HEU and LEU cores were calculated using the ORIGEN-S code using the assumptions in the previous paragraph. The activity of the krypton, iodine, and xenon isotopes in the HEU and LEU cores are shown in Table 13-11 along with the inventory (2.7% of the total) that is assumed to escape from the damaged fuel into the air of the reactor cell.

**Table 13-11 Calculated Radionuclide Inventories (Ci) Released into the Reactor Cell from the Maximum Hypothetical Accident in the HEU and LEU Cores**

Isotope	HEU Core		LEU Core	
	Ci in One Fuel Element Immediately after Shutdown	2.7% of Previous Column	Ci in One Fuel Element Immediately after Shutdown	2.7% of Previous Column
Kr 85				
Kr 85m				
Kr 88				
I 129				
I 130				
I 131				
I 132				
I 133				
I 133m				
I 134				
I 134m				
I 135				
I 135m				
Xe 133				
Xe 133m				
Xe 135				
Xe 135m				

#### **13.4.2 Methodology for Dose Calculations**

The methodology that was used for the Maximum Hypothetical Accident is the same as described in Section 13.3.2 for the Fuel-Handling Accident.

#### **13.4.3 Dose Calculations for Maximum Hypothetical Accident**

The calculated thyroid and whole body doses at the site boundary and at the urban boundary for the Maximum Hypothetical Accident are given in Tables 13-12 and 13-13, respectively.

The doses in Table 13-12 for the occupational exposure at the site boundary are significantly less than the dose limits of 30 rem to the thyroid and 5 rem to the whole body. Similarly, the doses in Table 13-13 for public exposure at the urban boundary are significantly less than the dose limits of 3 rem to the thyroid and 0.5 rem to the whole body.

Table 13-12 Thyroid Doses and Whole Body Doses Calculated at the Site Boundary (30 m) for the MHA in the HEU and LEU Cores.

Isotope	HEU Core		LEU Core	
	Thyroid Dose, rem	Whole Body Dose, rem	Thyroid Dose, rem	Whole Body Dose, rem
Kr 85				
Kr 85m				
Kr 88				
I 129				
I 130				
I 131				
I 132				
I 133				
I 133m				
I 134				
I 134m				
I 135				
I 135m				
Xe 133				
Xe 133m				
Xe 135				
Xe 135m				
Total Dose	1.13	0.060	1.07	0.057

Table 13-13 Thyroid Doses and Whole Body Doses Calculated at the Urban Boundary (400 m) for the MHA in the HEU and LEU Cores.

Isotope	HEU Core		LEU Core	
	Thyroid Dose, rem	Whole Body Dose, rem	Thyroid Dose, rem	Whole Body Dose, rem
Kr 85				
Kr 85m				
Kr 88				
I 129				
I 130				
I 131				
I 132				
I 133				
I 133m				
I 134				
I 134m				
I 135				
I 135m				
Xe 133				
Xe 133m				
Xe 135				
Xe 135m				
Total Dose	$1.51 \times 10^{-3}$	$3.94 \times 10^{-5}$	$1.43 \times 10^{-3}$	$3.72 \times 10^{-5}$

Thyroid doses and whole body doses calculated at points of interest between the site boundary (30 m) and the urban boundary (400 m) for the Maximum Hypothetical Accident in the HEU and LEU Cores are shown in Table 13-14 and are plotted in Figure 13-5.

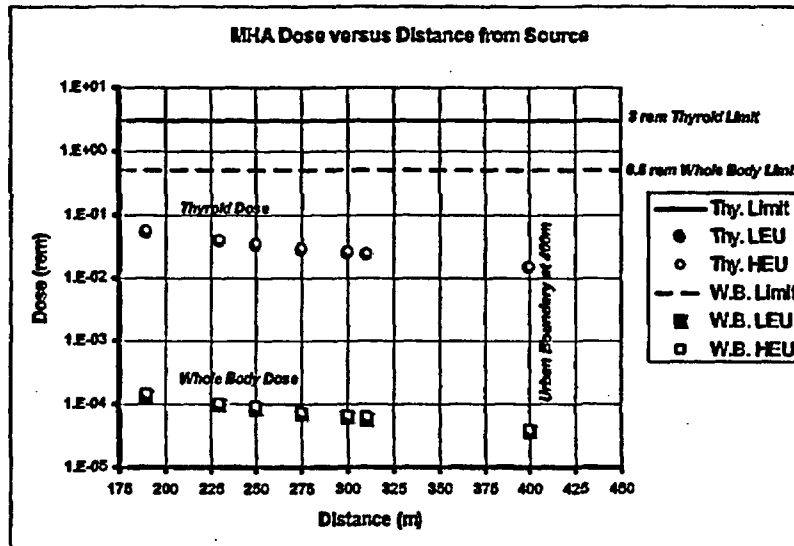


Figure 13-5 Thyroid Doses and Whole Body Doses for the Maximum Hypothetical Accident

Table 13-14 Thyroid and Whole Body Doses Calculated at Points of Interest Between the Site Boundary (30 m) and the Urban Boundary (400 m) for the MHA in the HEU and LEU Cores.

Distance from Source and Location	Thyroid Dose (rem)		Whole Body Dose (rem)	
	HEU Core	LEU Core	HEU Core	LEU Core
30 m Site Boundary	1.13E+00	1.07E+00	6.01E-02	5.67E-02
190 m East Hall Housing	5.59E-02	5.29E-02	1.46E-04	1.37E-04
230 m Ben Griffin Stadium	4.02E-02	3.81E-02	1.05E-04	9.93E-05
250 m Weaver Hall Housing	3.46E-02	3.28E-02	9.10E-05	8.59E-05
275 m Weaver Hall Housing	2.92E-02	2.76E-02	7.49E-05	7.07E-05
300 m Riker Hall Housing	2.57E-02	2.44E-02	6.68E-05	6.30E-05
310 m O'Connell Center	2.39E-02	2.27E-02	6.23E-05	5.88E-05
400 m Urban Boundary	1.51E-02	1.43E-02	3.94E-05	3.72E-05



## 14. Technical Specifications

For the UFTR HEU to LEU conversion, the only changes required for the UFTR Technical Specifications involve the fuel type and certain related specifications.

First, on page 4 of the Tech Specs, in Section 2.1, Safety Limits, specifications (1), (2) and (3), the safety limits on power level, primary coolant flow rate, and primary coolant outlet temperature from any fuel box are changed from their current specifications quoted as follows:

- (1) The steady-state power level shall not exceed 100 kWt.
- (2) The primary coolant flow rate shall be greater than 18 gpm at all power levels greater than 1 watt.
- (3) The primary coolant outlet temperature from any fuel box shall not exceed 200° F.

to new specifications on power level, flow rate, and primary coolant outlet temperature from any fuel box, correlated with the existing limiting safety system setting (LSSS) (trip points) on power level of 125 kW, flow rate of 30 gpm and primary coolant outlet temperature of 200° F and the accident analysis results presented to assure conservative limits in Section 4.7 as follows:

- (1) The power level shall not exceed 190 kW.
- (2) The primary coolant flow rate shall be greater than 23 gpm at all power levels greater than 1 watt.
- (3) The primary coolant outlet temperature from any fuel box shall not exceed 160° F.

As noted in the Section 4.7 analyses, the three parameters of power level, flow rate and primary coolant outlet temperature are interdependent so the safety limits are based on nominal as well as conservative analyses. For the nominal analyses, any two parameters are varied from nominal operating conditions to reach onset of nucleate boiling in the LEU core. In the conservative approach, any two parameters are varied from the LSSS point to reach onset of nucleate boiling. The actual proposed safety limits are based on a linear average of the two approaches as detailed in Section 4.7. In addition, the steady-state reference in specification (1) is removed as not applicable and the change from kWt to kW in specification (1) is simply to be consistent with the remainder of the Tech Specs. The resulting bases for specifications (1), (2) and (3) are then addressed together after the specifications in Section 2.1 as all three are interdependent with the objective now to prevent onset of nucleate boiling as a conservative objective and, as previously, to assure the fuel remains below temperatures at which fuel degradation would occur.

Second, on page 6 of the Tech Specs, in Section 3.1, Reactivity Limitations, paragraph (2), the core excess reactivity at cold critical, without xenon poisoning, is changed from not exceeding 2.3%  $\Delta k/k$  to not exceeding 1.4%  $\Delta k/k$ , again based on the accident analysis results presented in Section 13 and considering the actual realistic excess reactivity needed for operations.

Third, on page 13 of the Tech Specs, in Section 3.5, Limitations on Experiments, paragraph (3)(b), the limit on total absolute reactivity worth of all experiments is changed

from not exceeding 2.3%  $\Delta k/k$  to not exceeding 1.4%  $\Delta k/k$  to be consistent with the change made on overall reactivity limitations per the previous paragraph.

Fourth, on page 15 of the Tech Specs, in Section 3.7, Fuel and Fuel Handling, paragraph (1), the description of fuel elements is changed from "fuel elements consisting of 11 plates each . . ." to "fuel elements consisting of 14 plates each . . ." This change is necessitated by the basic LEU fuel assembly design selected for the conversion as described in Section 4 for the LEU fuel.

Fifth, on page 23 of the Tech Specs, in Section 5.3, Reactor Fuel, in the first paragraph, line 2, the enrichment is changed to specify "no more than about 19.75% U-235" based on the LEU fuel selections. In lines 4 through 6, the allowable fabrication methodology is changed to allow high purity uranium silicide-aluminum dispersion fuel in addition to the currently allowed high purity aluminum-uranium alloy. In the last line of the paragraph, the loading of U-235 per plate is changed to "nominally 12.5 g of U-235 per fuel plate." Again, these specifications are in agreement with the analysis provided in Section 4 for the LEU fuel.

Sixth, on page 23 of the Tech Specs, in Section 5.4, Reactor Core, in the first paragraph, in line 1, the number of plates per assembly becomes 14 for LEU bundles versus 11 for HEU bundles. Similarly, in line 4, a full assembly shall be replaced with no fewer than 13 plates in a pair of partial assemblies versus 10 plates for the HEU core. Finally, in the second paragraph, the table giving the required nominal fuel element specifications is updated to provide the parameters for the LEU fuel per the analysis summarized in Section 4.

Table 14-1 Summary of LEU Fuel Parameters to be Updated in the Technical Specifications

Item	Specification
Overall size (bundle)	2.845 in. x 2.26 in. x 25.6 in.
Clad thickness	0.015 in.
Plate thickness	0.050 in.
Water channel width	0.111 in.
Number of plates	Standard fuel element – 14 fueled plates; Partial element – no fewer than 11 plates in a pair of partial assemblies
Plate attachment	Bolted with spacers
Fuel content per plate	12.5 g U-235 nominal

## 15. Other License Considerations

The necessary documentation of reactor parameters and status will be provided after the conversion from HEU to LEU fuel.

## Appendix A

### A.1 Determination of Material Composition

This section includes information on material composition, and discusses the methodology used to accurately determine isotopic concentrations for the depleted cores.

Table A.1-1 presents the fuel concentrations for the HEU fresh core.

Table A.1-1 UFTR HEU Core Fuel Loading at Beginning-of-Life

Box	Bundle	Rx ID	U <sup>235</sup> Grams	U grams	U <sup>235</sup> wt%	U <sup>234</sup> wt%	U <sup>238</sup> wt%	U/plate grams	U-density g/cm <sup>3</sup>	Al-density g/cm <sup>3</sup>	Total g/cm <sup>3</sup>
1	1	UF-40									
1	2	UF18									
1	3	UF-26									
1	4	UF-24									
2	1	UF-10									
2	2	UF-13									
2	3	UF-25									
2	4	UF-12									
3	1	UF-99									
3	2	UF-36D									
3	3	UF-20									
3	4	UF-33									
4	1	UF-27									
4	2	UF-28									
4	3	UF-32									
4	4	UF-29									
5	1	UF-23									
5	2	UF-16									
5	3	UF-22									
5	4	UF-17									
6	1	UF-11									
6	2	UF-14									
6	3	UF-19									
6	4	UF-34D									

Table A.1-2 presents the power peak-to-average ratios that are used for the determination of material concentrations in the HEU core.

**Table A.1-2 HEU Power Peak-to-Average Ratio for Core at Beginning-of-Life**

<b>Bundle Number</b>	<b>Axial Segment</b>	<b>Peak to Average Ratio</b>	<b>Bundle Number</b>	<b>Axial Segment</b>	<b>Peak to Average Ratio</b>
1-1	1	4.26E-01	4-1	1	1.01E+00
1-1	2	5.44E-01	4-1	2	1.27E+00
1-1	3	4.02E-01	4-1	3	9.57E-01
1-2	1	9.18E-01	4-2	1	1.15E+00
1-2	2	1.14E+00	4-2	2	1.42E+00
1-2	3	8.36E-01	4-2	3	1.05E+00
1-3	1	8.89E-01	4-3	1	9.21E-01
1-3	2	1.12E+00	4-3	2	1.15E+00
1-3	3	8.40E-01	4-3	3	8.59E-01
1-4	1	1.03E+00	4-4	1	1.05E+00
1-4	2	1.27E+00	4-4	2	1.30E+00
1-4	3	9.55E-01	4-4	3	9.46E-01
2-1	1	9.86E-01	5-1	1	1.20E+00
2-1	2	1.22E+00	5-1	2	1.46E+00
2-1	3	8.87E-01	5-1	3	1.07E+00
2-2	1	9.62E-01	5-2	1	1.14E+00
2-2	2	1.19E+00	5-2	2	1.38E+00
2-2	3	8.68E-01	5-2	3	9.37E-01
2-3	1	1.11E+00	5-3	1	1.08E+00
2-3	2	1.37E+00	5-3	2	1.32E+00
2-3	3	1.02E+00	5-3	3	9.40E-01
2-4	1	1.08E+00	5-4	1	1.03E+00
2-4	2	1.33E+00	5-4	2	1.26E+00
2-4	3	9.89E-01	5-4	3	8.30E-01
3-1	1	8.17E-01	6-1	1	9.35E-01
3-1	2	1.02E+00	6-1	2	1.13E+00
3-1	3	7.44E-01	6-1	3	7.63E-01
3-3	1	8.96E-01	6-2	1	8.10E-01
3-3	2	1.11E+00	6-2	2	1.01E+00
3-3	3	8.31E-01	6-2	3	7.38E-01
3-4	1	7.85E-01	6-3	1	8.58E-01
3-4	2	9.82E-01	6-3	2	1.05E+00
3-4	3	7.45E-01	6-3	3	6.89E-01

The masses of the fuel matrix, impurities in the silicide, and impurities in Al are given in Tables A.1-3a to A.1-3c.

**Table A.1-3a Weights of major elements and isotopes in a LEU fuel plate**

Isotope	Mass per fuel plate (g)
U-234	1.03E-01
U-235	1.25E+01
U-236	6.57E-02
U-238	5.08E+01
Si	5.00E+00
Al	3.23E+01

**Table A.1-3b Impurities in U<sub>3</sub>Si<sub>2</sub> Powder**

Isotope	Concentration (ppm)	Mass (per Gram Fuel Meat)
Al	131.67	8.95E-05
Ba	2.00	1.36E-06
Be	0.50	3.40E-07
B	1.33	1.82E-07
Cd	0.50	3.40E-07
Ca	20.00	1.36E-05
C	244.00	1.66E-04
Cr	18.33	1.25E-05
Co	5.00	3.40E-06
Cu	100.83	6.85E-05
Eu	0.20	1.36E-07
Gd	0.20	1.36E-07
Fe	608.50	4.13E-04
Pb	0.50	3.3974E-07
Li	0.10	6.80E-08
Mg	10.00	6.80E-06
Mn	8.67	5.89E-06
Mo	3.00	2.04E-06
Ni	43.33	2.94E-05
N	55.00	3.74E-05
P	20.00	1.36E-05
Sm	0.20	1.36E-07
Ag	1.00	6.79E-07
Na	10.00	6.79E-06
Sn	1.00	6.79E-07
W	21.67	1.47E-05
V	4.50	3.06E-06
Zn	20.00	1.36E-05
Zr	3.83	2.60E-06

**Table A.1-3c Impurities in Aluminum Powder Used in Fuel**

Isotope	Mass Fraction (wt %)	Mass (per Gram Fuel Meat)
Zn	0.02	6.41E-05
Cu	0.001	3.21E-06
Cd	0.001	3.21E-06
Li	0.001	3.21E-06
B	0.001	3.21E-06
Fe	0.167	5.35E-04
O	0.097	3.11E-04

It is also important to mention that an effort was made in using realistic local parameters. Using coolant temperature profiles in the UFTR FSAR, a power shape was constructed to obtain an initial axial power peaking function for a generic fuel bundle. Average fuel and cladding temperatures as well as coolant temperature and density were calculated and used in an initial core physics calculation. The resulting power peak-to-average ratios were used to recalculate more accurate local parameters for each fuel bundle. Three average axial fuel temperatures are used for the whole core while an average coolant density per fuel box is considered. Tables A.1-5 and A.1-6 present the data local parameters for the HEU and LEU, respectively.

**Table A.1-5 UFTR LEU Core Average Coolant Densities per Fuel Box**

Coolant Box	Average Coolant Density Across Bundle Region (g/cc)
Box 1	0.99395
Box 2	0.99373
Box 3	0.99419
Box 4	0.99409
Box 5	0.99397
Box 6	0.99462

**Table A.1.7 UFTR LEU Average Fuel Temperature**

Axial Segment <sup>1</sup>	Average Fuel Temperature (K)
1	309.32
2	316.74
3	316.15

<sup>1</sup> Each axial segment represents a third of the bundle length with segment #1 being at the bottom

The peak-to-average power ratios for the LEU core are given in Table A.1-4.

**Table A.1-4 LEU Peak-to-Average Power Ratio for Core at Beginning-of-Life**

Bundle Number	Axial Segment	Peak to Average Ratio	Bundle Number	Axial Segment	Peak to Average Ratio
1-1	1	8.87E-01	4-1	1	9.14E-01
1-1	2	1.11E+00	4-1	2	1.14E+00
1-1	3	8.05E-01	4-1	3	8.49E-01
1-2	1	1.03E+00	4-2	1	1.05E+00
1-2	2	1.26E+00	4-2	2	1.28E+00
1-2	3	8.49E-01	4-2	3	9.27E-01
1-3	1	9.68E-01	4-3	1	8.19E-01
1-3	2	1.21E+00	4-3	2	1.03E+00
1-3	3	9.00E-01	4-3	3	7.46E-01
1-4	1	1.12E+00	4-4	1	9.36E-01
1-4	2	1.38E+00	4-4	2	1.15E+00
1-4	3	9.93E-01	4-4	3	7.77E-01
2-1	1	1.10E+00	5-1	1	1.10E+00
2-1	2	1.34E+00	5-1	2	1.34E+00
2-1	3	8.89E-01	5-1	3	9.51E-01
2-2	1	1.09E+00	5-2	1	1.06E+00
2-2	2	1.33E+00	5-2	2	1.28E+00
2-2	3	8.80E-01	5-2	3	8.85E-01
2-3	1	1.20E+00	5-3	1	9.82E-01
2-3	2	1.47E+00	5-3	2	1.19E+00
2-3	3	1.05E+00	5-3	3	7.95E-01
2-4	1	1.19E+00	5-4	1	9.41E-01
2-4	2	1.46E+00	5-4	2	1.14E+00
2-4	3	1.04E+00	5-4	3	7.51E-01
3-1	1	9.57E-01	6-1	1	8.78E-01
3-1	2	1.17E+00	6-1	2	1.07E+00
3-1	3	7.88E-01	6-1	3	7.41E-01
3-2	1	6.21E-01	6-2	1	7.70E-01
3-2	2	7.85E-01	6-2	2	9.54E-01
3-2	3	5.67E-01	6-2	3	7.12E-01
3-3	1	1.04E+00	6-3	1	7.86E-01
3-3	2	1.27E+00	6-3	2	9.63E-01
3-3	3	9.18E-01	6-3	3	6.41E-01
3-4	1	8.78E-01			
3-4	2	1.10E+00			
3-4	3	8.16E-01			

Note that, as in the FSAR, the average moderator temperature is assumed to be equal to the average coolant temperature (307.8K). To examine the validity of this assumption, we utilize Error! Objects cannot be created from editing field codes. to estimate the operating time required to reach the assumed temperature. To solve for  $t$ , we determine the deposited power  $P$  ( $3.69\text{E}+03 \pm 0.0002$  J/s) in graphite at full power using MCNP5 (in neutron-photon mode for a more accurate energy deposition), assume an initial temperature of 298K, and a graphite heat capacity of 0.711 J/g/K. Based on these parameters, this initial scoping calculation estimates that this assumption corresponds to the temperature reached after 2 hours of operation at full power. We believe this constitutes an acceptable assumption.



## A.2 Power History for the HEU Core

The power history given in Table A.2-1 includes a 1 kW-hr run at the end to account for any short lived isotopes generated during the experiment. The current experiments were run after the reactor was shut down for 5 days and therefore no power history was included for the days leading up to the experiment.

Table A.2-1 Power History for the 20 Oldest Bundles

Year	kW-hr	Full Power Days	Down time in Days	Year	kW-hr	Full Power Days	Down time in Days
1982	14480	1.51	89.74	1994	27599	11.50	353.50
1983	47287	19.70	345.30	1995	21347	8.89	356.11
1984	35879	14.95	350.05	1996	16904	7.04	357.96
1985	19288	8.04	356.96	1997	11615	4.84	360.16
1986	29749	12.40	352.60	1998	3429	1.43	363.57
1987	26677	11.12	353.88	1999	19387	8.08	356.92
1988	35199	14.67	350.33	2000	21744	9.06	355.94
1989	24700	10.29	354.71	2001	11173	4.66	360.34
1990	17519	7.30	357.70	2002	10761	4.48	360.52
1991	21904	9.13	355.87	2003	14536	6.06	358.94
1992	33943	14.14	350.86	2004	14995	6.25	448.75
1993	28798	12.00	353.00	Exp.	1	0.0004	n/a

Note that bundle UF-40 (bundle1-1 in the model) is a half-bundle which was added in 1986 and UF-99 (bundle 3-1 in the model) is a full bundle replacement added in 1990. These bundles have different power histories as shown in Tables A.2-2 and A.2-3.

Table A.2-2 Power History for Bundle UF-40

Year	kW-hr	Full Power Days	Down time in Days	Year	kW-hr	Full Power Days	Down time in Days
1986	22311.75	9.30	264.45	1996	16904	7.04	357.96
1987	26677	11.12	353.88	1997	11615	4.84	360.16
1988	35199	14.67	350.33	1998	3429	1.43	363.57
1989	24700	10.29	354.71	1999	19387	8.08	356.92
1990	17519	7.30	357.70	2000	21744	9.06	355.94
1991	21904	9.13	355.87	2001	11173	4.66	360.34
1992	33943	14.14	350.86	2002	10761	4.48	360.52
1993	28798	12.00	353.00	2003	14536	6.06	358.94
1994	27599	11.50	353.50	2004	14995	6.25	448.75
1995	21347	8.89	356.11	Exp.	1	0.0004	n/a

**Table A.2-3 Power History For Bundle UF-99**

Year	kW-hr	Full Power Days	Down time In Days	Year	kW-hr	Full Power Days	Down time In Days
1990	8759.5	3.65	178.85	1998	3429	1.43	363.57
1991	21904	9.13	355.87	1999	19387	8.08	356.92
1992	33943	14.14	350.86	2000	21744	9.06	355.94
1993	28798	12.00	353.00	2001	11173	4.66	360.34
1994	27599	11.50	353.50	2002	10761	4.48	360.52
1995	21347	8.89	356.11	2003	14536	6.06	358.94
1996	16904	7.04	357.96	2004-	14995	6.25	448.75
1997	11615	4.84	360.16	Exp.	1	0.0004	n/a

### A.3 Impact of the Boron Content for the HEU Core

Due to the uncertainties in the concentrations of certain impurities, it is necessary to perform a small sensitivity study. Table A.3-1 presents changes in  $k_{eff}$  obtained for different concentrations boron-equivalent impurities for the HEU core.

**Table A.3-1 Impact of Impurities on the Excess Reactivity of the HEU Core**

Case (ppm of natural boron-equivalent)	$\Delta k/k$ (%) <sup>1</sup>
4 ppm in graphite	0.303
6 ppm in graphite	-0.133
0 ppm in cladding	0.254
20 ppm in cladding	-0.177
0 ppm in Al structure	0.146
20 ppm in Al structure	-0.015
Graphite/cladding/structure impurities at minimum	0.546
Graphite/cladding/structure impurities at maximum	-0.472
5.72ppm <sup>2</sup> in fuel aluminum alloy	-0.107

<sup>1</sup> The 1 $\sigma$  relative errors for these values is below 0.00025

<sup>2</sup> This value is taken from ANL intra-laboratory memo of June 30<sup>th</sup>, 2005

Among the tested parameters in above table, the consideration of the impurities in the fuel aluminum alloy compensate for the observed difference in the core excess reactivity. Note that using the 5.72ppm of natural boron-equivalent impurity in the fuel, the  $k_{eff}$  of the depleted core with the control blades at their critical positions is 0.99993 (+/-0.00013).

### A.4 Determination of the Critical LEU Core

We have prepared seven LEU fuel configurations to investigate the necessary number of fuel bundles and plates. The seven cases are:

- 24 bundles,
- 23 bundles,
- 22.5 bundles with half dummy bundle located at SE,
- 22.5 bundles with half dummy bundle located at NE,
- 22 bundles,
- 21.5 bundles (same as the current HEU core), and
- 22 bundles with 10 fuel plates at SE.

Figure A.4-1 below shows the variation of the  $K_{eff}$  for different configurations. The selected configuration based on this study is case 7 that includes 22 full bundles and a partially filled bundle with 10 fuel plates and 4 dummy aluminum plates. This case leads to a  $K_{eff}$  of  $1.00934 \pm 0.000663$  with an excess reactivity 0.925 %. This is very close to the excess reactivity of the HEU core with fresh fuel. Note that because of existing uncertainties in material composition, besides case 7, we have analyzed cases 2 and 3 (with 23 and 22.5 fuel bundles), and estimated the effect of variations in the material impurities. Further detail on the results is provided in Table A.4-1.

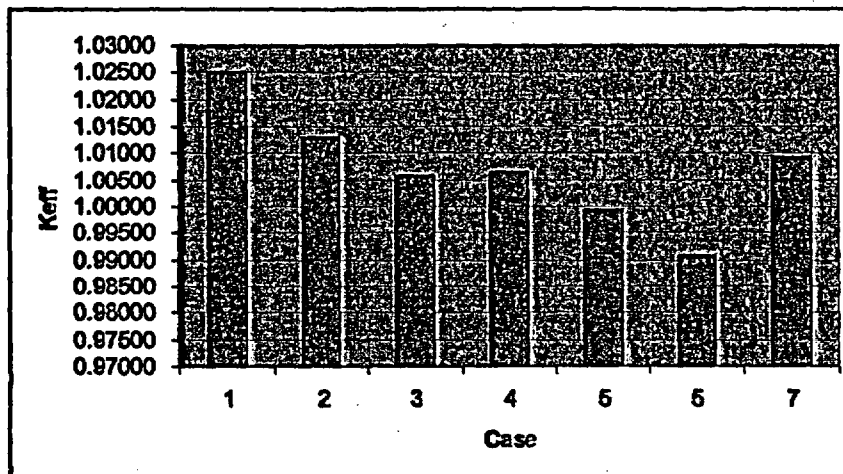


Figure A.4-1 Excess Reactivity for Different LEU Core ( $1-\sigma$  standard deviation is  $< 0.0007$ )

Table A.4-1 Comparison of the excess reactivity for different LEU Configurations

Case	Number of Bundles	Description	Blades Positions	$K_{eff}$	$1-\sigma$ Standard Deviation
1	24	all fuel bundles	all out (at 47.5 degree)	1.02510	0.000660
2	23	one dummy bundle at SE fuel box, (bundle number 3-2)	all out (at 47.5 degree)	1.01307	0.000600
3	22.5	one dummy bundle at NE fuel box (6-4); half dummy half fuel bundle at SE(3-2)	all out (at 47.5 degree)	1.00601	0.000620
4	22.5	one dummy bundle at SE fuel box (3-2); half dummy half fuel bundle at NE(6-4)	all out (at 47.5 degree)	1.00649	0.000620
5	22	two dummy bundles at NE (6-4) and SE (3-2)	all out (at 47.5 degree)	0.99936	0.000640
6	21.5	bundle layout same as HEU	all out (at 47.5 degree)	0.99076	0.000650
7	22b+10p	one dummy bundle at NE fuel box (6-4); 4 dummy plates 10 fuel plates for bundle at SE(3-2)	all out (at 47.5 degree)	1.00934	0.000630

It is clear that case 7 is the best case, considering the necessary excess reactivity.

## A.5 Detailed Flux Profiles for the HEU and LEU cores

In order to tally the axial and radial neutron flux profiles, it is necessary to determine an energy group structure. First, it is useful to evaluate the range of the "thermal" energy group, i.e., the energy group where the neutrons are in thermal equilibrium with their environment and follow a Maxwellian distribution. The Maxwellian distribution is often expressed in terms of neutron speed, as given by,

$$4\pi \left( \frac{1}{2\pi c} \right)^{3/2} v^2 e^{-v^2/2c} \quad (\text{A.5.1})$$

where  $v$  represents the neutron speed,  $c$  is  $kT/m$ ,  $k$  is the Boltzmann constant,  $T$  is the temperature of the gas and  $m$  is the mass of the neutron. Using three standard deviations from the average, we evaluate the "maximum" range of the distribution. This range for the UFTR is equal to 0.175eV. Another group boundary is set to 1eV since it is often used as the thermal boundary for reactors. The "epithermal" region is divided into three energy groups, and the "fast" region into two energy groups. Table A.5-1 gives the energy group upper boundaries.

Table A.5-1 Flux Energy Group Structure for UFTR

Spectrum Region	Group Number	Upper Energy (MeV)
Fast	1	2.00e1
	2	1.00e0
Epithermal	3	1.00e-1
	4	1.00e-2
	5	1.00e-4
Thermal	6	1.00e-6
	7	1.75e-7

Figures A.5-1 to A.5-7 show the detailed flux profiles for the HEU core obtained for each of the groups listed in Table A.5-1, while flux profiles for the LEU core are presented in Figures A.5-8 to A.5-13.

## A.5.1 HEU Detailed Flux Profiles

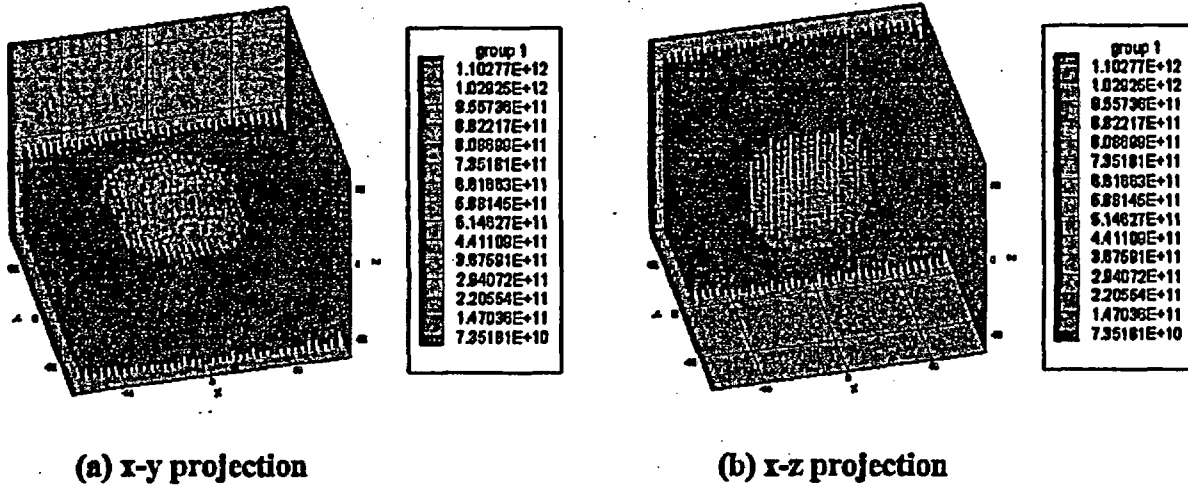


Figure A.5-1 Flux distribution for energy group 1 (1.0 – 20.0 MeV)

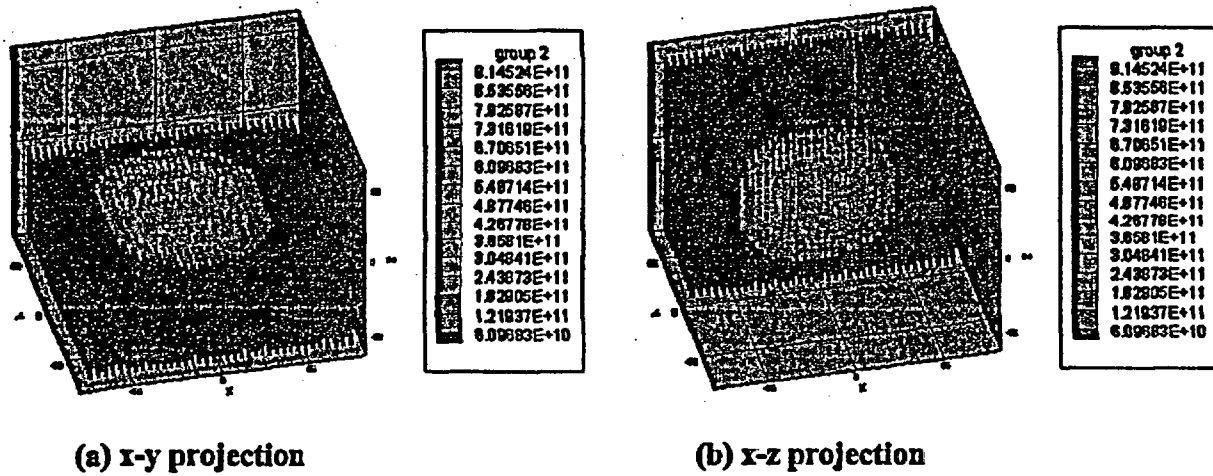
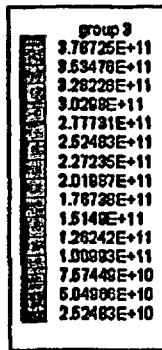
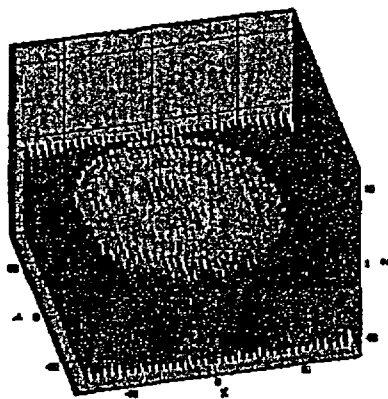
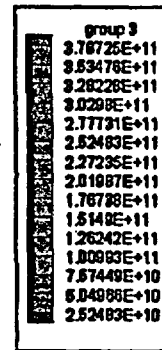
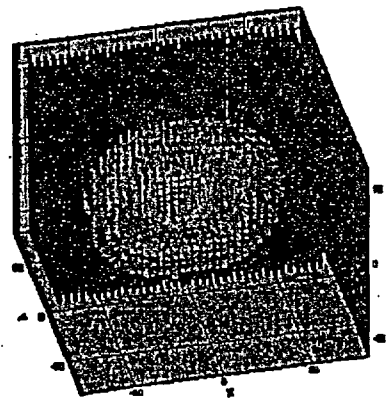


Figure A.5-2 Flux distribution for energy group 2 (0.10 – 1.0 MeV)

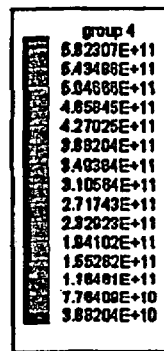
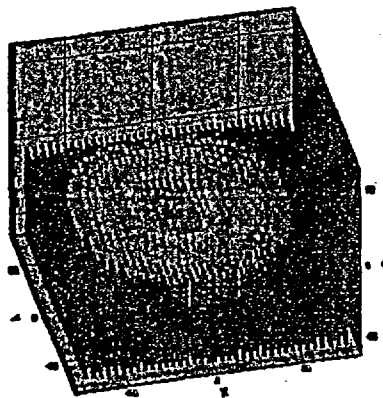


(a) x-y projection

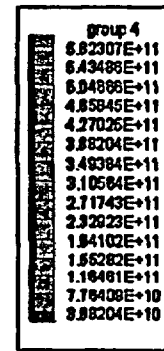
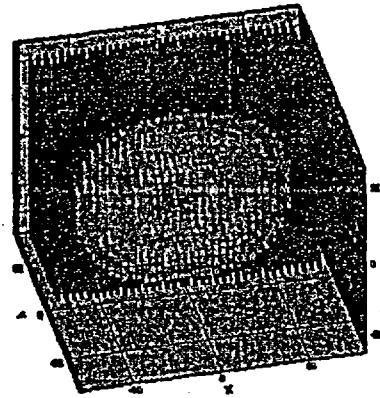


(b) x-z projection

Figure A.5-3 Flux distribution of energy group 3 (0.01 – 0.10 MeV)

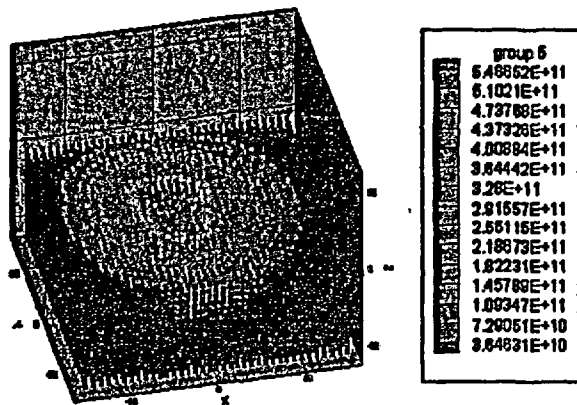


(a) x-y projection

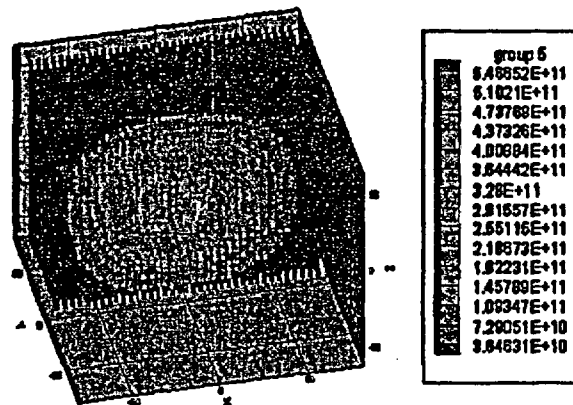


(b) x-z projection

Figure A.5-4 Flux distribution for energy group 4 (1.0 E-4 - .01 MeV)

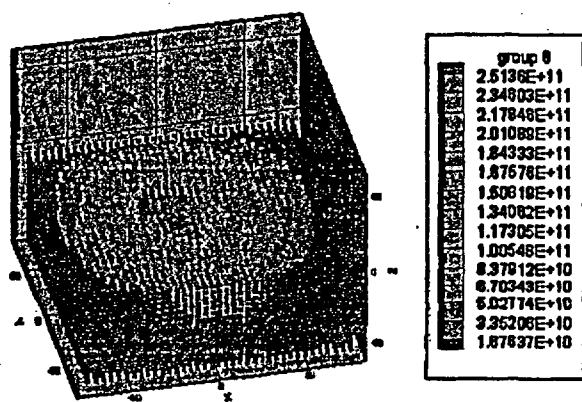


(a) x-y projection

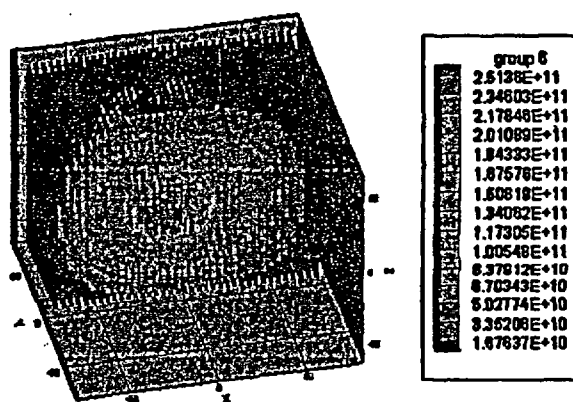


(b) x-z projection

Figure A.5-5 Flux distribution for energy group 5 ( $1.0E-6 - 1.0E-4$  MeV)

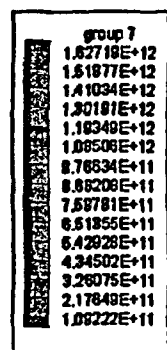
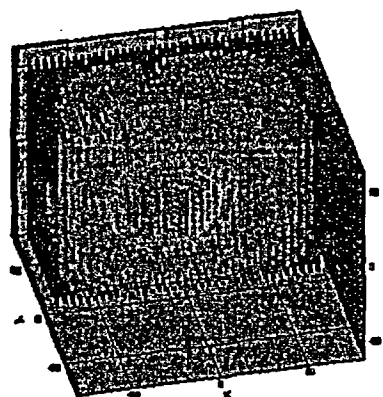
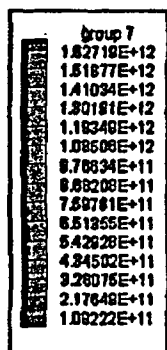
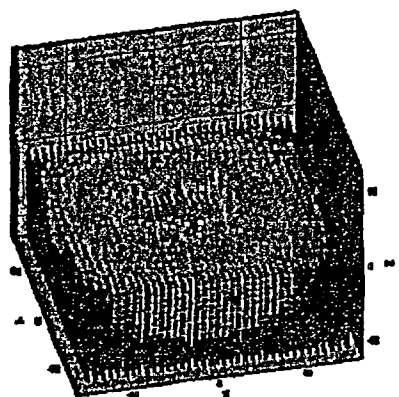


(a) x-y projection



(b) x-z projection

Figure A.5-6 Flux distribution for energy group 6 ( $1.0E-7 - 1.0E-6$  MeV)

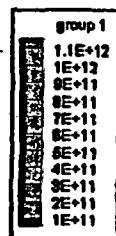
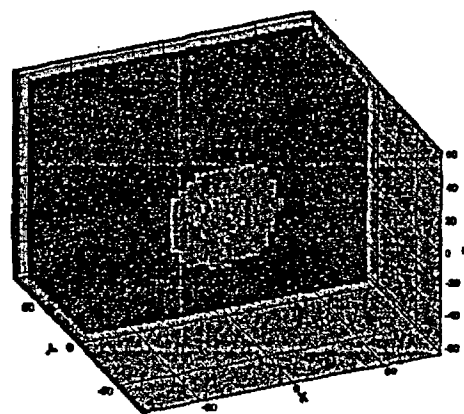
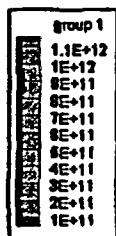
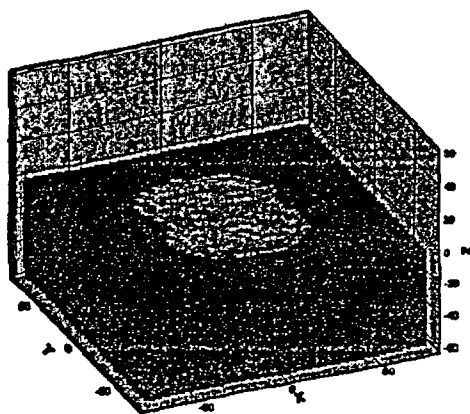


(a) x-y projection

(b) x-z projection

Figure A.5-7 Flux distribution for energy group 7 (0.0 -1.0E-7 MeV)

## A.5.2 LEU Detailed Flux Profiles

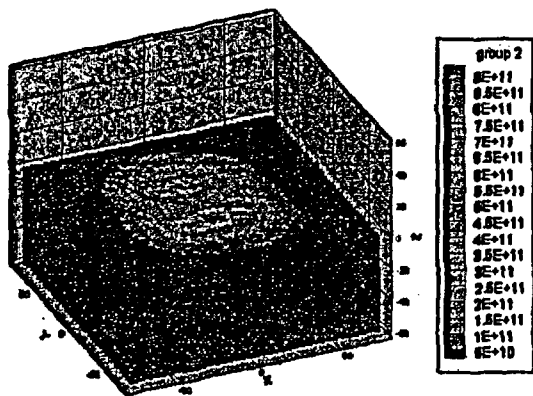


(a) x-y projection

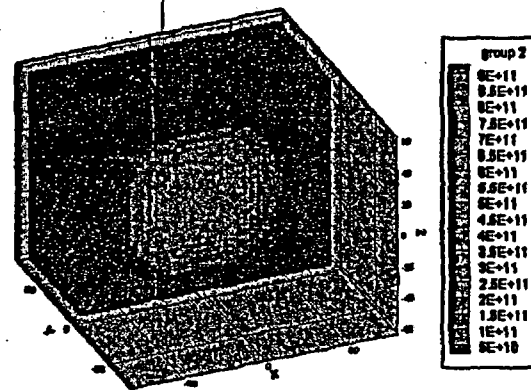
(b) x-z projection

Figure A.5-8 Flux distribution for energy group 1 (1.0 - 20.0 MeV)



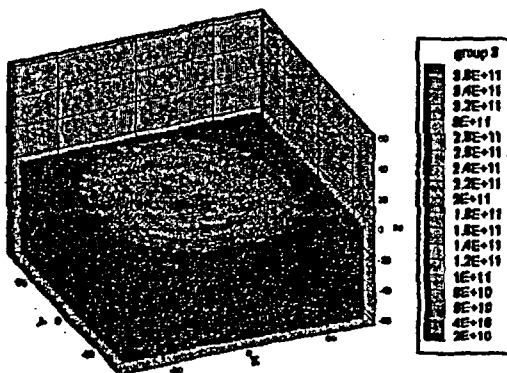


(a) x-y projection

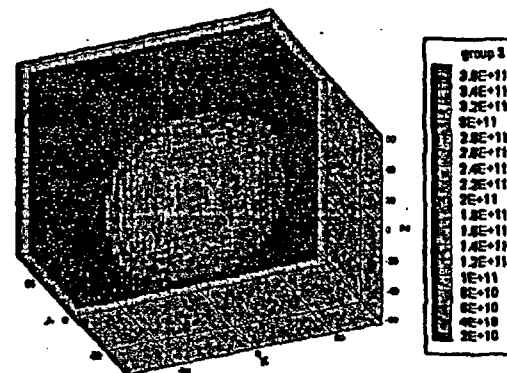


(b) x-z projection

Figure A.5-9 Flux distribution for energy group 2 (0.10 – 1.0 MeV)

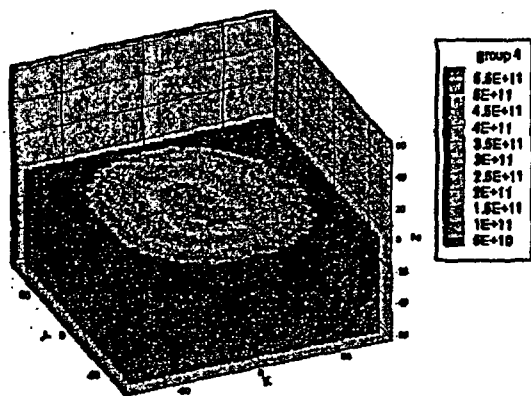


(a) x-y projection

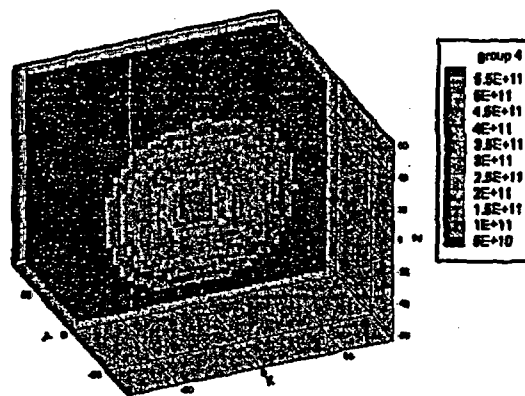


(b) x-z projection

Figure A.5-10 Flux distribution of energy group 3 (0.01 – 0.10 MeV)

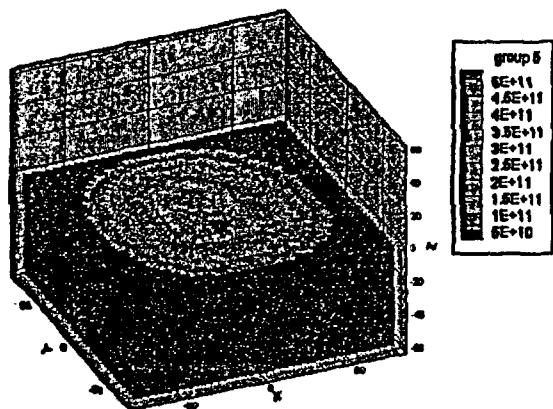


(a) x-y projection

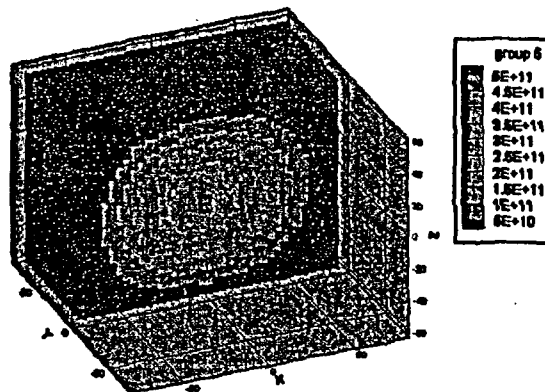


(b) x-z projection

Figure A.5-11 Flux distribution for energy group 4 ( $1.0 \text{ E-}4 - .01 \text{ MeV}$ )



(a) x-y projection



(b) x-z projection

Figure A.5-12 Flux distribution for energy group 5 ( $1.0\text{E-}6 - 1.0\text{E-}4 \text{ MeV}$ )

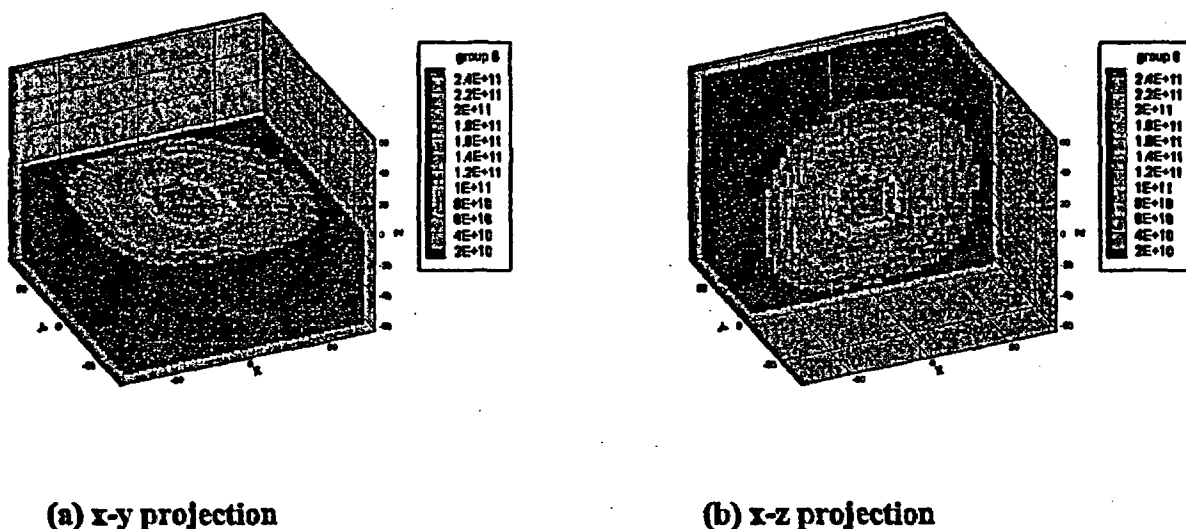


Figure A.5-13 Flux distribution for energy group 6 (1.0E-7 – 1.0E-6 MeV)

## A.6 Comparison of the parameters in the six-factor formula for HEU and LEU cores

The six-factor parameters provide an alternative way to characterize a reactor and provide insight into different physical processes occurring in the reactor core. Each factor represents a step in the "life cycle" of a neutron and is defined by specific parameters of the system, i.e. by compositions, cross sections and other nuclear properties. The six-factor formula is given by

$$k = \eta f \epsilon p P_{FNL} P_{TNL} \quad (\text{A.6.1})$$

The first of factor ( $\eta$ ) is the number of fission neutrons produced per absorption in the fuel. The second factor is the *thermal utilization* ( $f$ ); it represents the effectiveness of the fuel in competing with other materials in the reactor for the absorption of the thermal neutrons. Then to account for the process of slowing down, two other factors are introduced. The third factor, the *fast fission factor* ( $\epsilon$ ), take into account that some of the fissions are produce by fast neutrons. The fourth factor, the *resonance escape probability* ( $p$ ), represents the fraction of neutrons that managed to slow-down to the thermal energies without being absorbed. The last two factors are related to the probability of non-leakage and can be broken down  $P_{FNL}$  (*fast non-leakage*) and  $P_{TNL}$  (*thermal non-leakage*).

Table A.6-1 compares the calculated parameters of the six-factor formula for the HEU and LEU cores.

**Table A.6-1 Six Factors for the depleted HEU core and the reference LEU Core**

Factor	HEU Value	LEU Value	Relative Diff. (%)
$\eta$	1.987	1.889	-4.932%
<i>Thermal utilization f</i>	0.613	0.640	4.405%
<i>Fast fission factor <math>\epsilon</math></i>	1.057	1.067	2.156%
<i>Resonance escape probability p</i>	0.945	0.937	-0.847%
<i>Probability of non-leakage <math>P_{NL}</math></i> <sup>1</sup>	0.822	0.828	-0.730%

<sup>1</sup> Note that the fast and thermal non-leakage have been combine in one probability of non-leakage

A lower  $\eta$  value and a higher  $\epsilon$  value are expected for the LEU core because of the low enrichment of U-235.

## Appendix B

### **B.1 ENGINEERING UNCERTAINTY FACTORS**

This attachment addresses the engineering uncertainty factors (or hot channel factors) that were used to compute the thermal-hydraulic safety limits, safety margins, and safety system trip settings in HEU and LEU cores. The rationale for choosing these factors and the method used to combine them are outlined along with a summary of results.

The PLTEMP code (Ref. 11) used in the analyses allows for introduction of three separate engineering hot channel factors as they apply to the uncertainty in the various parameters (as opposed to a single lumped factor). The three hot channel factors are:

- $F_q$  for uncertainties that influence the heat flux  $q$
- $F_b$  for uncertainties in the temperature rise or enthalpy change in the coolant
- $F_h$  for uncertainties in the heat transfer coefficient  $h$ .

The code also allows introduction of nuclear peaking factors for the radial,  $F_r$ , and axial,  $F_z$ , distributions of the heat flux.

While there is no generally accepted method for the selection of hot channel factors, these factors are normally a composite of sub-factors, and the sub-factors can be combined either multiplicatively, statistically [ $F_b = 1 + \sqrt{\sum (1 - f_{bi})^2}$ ], or as a combination of the two. A detailed description of methods for calculating hot channel factors is contained in Ref. 25. The pure multiplicative method of combining the sub-factors is very conservative and somewhat unrealistic. The pure statistical method recognizes that all of these conditions do not occur at the same time and location and treats all of the uncertainties as random. The most realistic method is probably a combination of the multiplicative method for systematic uncertainties and the statistical method for the random uncertainties. The combined method is used for the analyses considered here.

The thermal and hydraulic design in Section 4.4 of the UFTR Final Safety Analysis Report dated January 1981 used a conservative method with "hot-channel factors" to calculate the fuel plate heat transfer data. In order to compare the HEU and LEU cores on a common basis using the methodology used in the PLTEMP code, the uncertainty factors shown in Table B-1 were identified for both the HEU and LEU cores. The systematic factors were combined multiplicatively and the random factors were combined statistically. The products of the two resulting factors were used for  $F_q$ ,  $F_b$ , and  $F_h$  in calculations of the HEU and LEU cores.

**Table B-1 HEU and LEU Engineering Uncertainty Factors**

Uncertainty	Type	HEU			LEU		
		F <sub>a</sub>	F <sub>b</sub>	F <sub>c</sub>	F <sub>a</sub>	F <sub>b</sub>	F <sub>c</sub>
Fuel Meat Thickness (local) <sup>a</sup>	random	1.07	-	-	1.07	-	-
<sup>235</sup> U Loading Per Plate <sup>b</sup>	random	1.03	1.015	-	1.03	1.03	-
<sup>235</sup> U Homogeneity (local) <sup>c</sup>	random	1.03	-	-	1.20	-	-
Coolant Channel Spacing <sup>d</sup>	random	-	-	1.01	-	1.067	-
Power Level Measurement <sup>e</sup>	systematic	1.05	1.05	-	1.05	1.05	-
Calculated Power Density <sup>e</sup>	random	1.10	1.05	-	1.10	1.10	-
Coolant Flow Rate <sup>e</sup>	systematic	-	1.10	-	-	1.10	-
Heat Transfer Coefficient <sup>e</sup>	systematic	-	-	1.20	-	-	1.20
Pure Multiplicative Combination		1.31	1.23	1.21	1.53	1.40	1.20
Pure Statistical Combination		1.14	1.12	1.20	1.24	1.17	1.20
Random Factors Combined Multiplicatively		1.13	1.05	1.01	1.24	1.12	1.00
Systematic Factors Combined Statistically		1.05	1.16	1.20	1.05	1.16	1.20
Product of Random & Systematic Factors		1.19	1.22	1.21	1.30	1.30	1.20

<sup>a</sup> HEU: Estimated from HEU fuel plate thickness data.

LEU: Derived from fuel plate thickness specification of 50 ± 2 mils.

<sup>b</sup> HEU: Assumed to be the same as for the LEU plate.

LEU: Derived from fuel plate loading specification of 12.5 ± 0.35 g <sup>235</sup>U.

<sup>c</sup> HEU: Estimated for U-Al alloy fuel meat.

LEU: From fuel plate homogeneity specification.

<sup>d</sup> HEU: Derived from tolerances on drawing UTR-103.

LEU: Derived from specification of 94 ± 2 mils for channel adjacent to fuel box and fuel plate thickness specification of 50 ± 2 mils.

<sup>e</sup> HEU and LEU: Assumed values.

## References

1. Diaz and Vernetson, "Final Safety Analysis Report (FSAR)," 1981 updated to Rev. 11, University of Florida, 1998.
2. U.S. Nuclear Regulatory Commission, "Safety Evaluation Report Related to the Evaluation of Low-Enriched Uranium Silicide-Aluminum Dispersion Fuel for Use in Non-Power Reactors," NUREG-1313, July 1988.
3. Shaber, Eric, and Hofman, Gerard, "Corrosion Minimization for Research Reactor Fuel," Idaho National Laboratory, RERTR Program, INL/EXT-05-00256, June 2005.
4. Idaho National Engineering and Environmental Laboratory (INEEL), "Specification For University of Florida LEU Standard and Dummy Fuel Plate Assemblies – Assembled for University of Florida Training Reactor," Document ID SPC-383, October 2003.
5. X-5 Monte Carlo Team, "MCNP-A General Monte Carlo N-Particle Transport Code, Version 5 Volume I, II and III," Los Alamos National Laboratory, Report LA-CP-03-0245 (2003).
6. "SCALE: A Modular Code System for Performing Standardized Computer Analyses for Licensing Evaluations," ORNL/TM-2005/39, Version 5, Vols. I-III, April 2005.
7. Letter, Scott T. Fairburn, BWXT Nuclear Products Division Transmission Package to Alireza Haghighat, University of Florida, June 23, 2005
8. International Atomic Energy Agency, "Research Reactor Core Conversion Guidebook", Volume 4: Fuels, IAEA-TECDOC-643, April 1992.
9. Letter, Meyer, Mitchell K., U.S. National Technical Lead for RERTR Fuel Development, INL Transmission Package to Alireza Haghighat, University of Florida, June 21, 2005.
10. The RELAP5-3D Code Development Team, "RELAP5-3D Code Manual", INEEL-EXT-98-00834, Revision 2.2, Idaho National Engineering and Environmental Laboratory, Idaho Falls, Idaho (October 2003).
11. A.P. Olson, "The PLTEMP V2.1 Code", Proc. 2003 International Meeting on Reduced Enrichment for Research and Test Reactors, Chicago, Illinois, October 5-10, 2003, pp. 367-376. The code was updated to include laminar forced convection in September 2005 and called Version 2.14.
12. ORNL Monthly Progress Report, ORNL/ANS/INT-5/V19, Oak Ridge National Laboratory, October, 1989. This is also used by RELAP5/3D.
13. B. S. Petukhov and V. N. Popov, "Theoretical Calculation of Heat Exchange in Turbulent Flow in Tubes of an Incompressible Fluid with Variable Physical Properties," High Temp., 1, No. 1, pp 69-83 (1963). See also Y. A. Hassan, and L. E. Hochreiter, Nuclear reactor thermal-hydraulics, presented at the Winter Annual Meeting of the American Society of Mechanical Engineers, Atlanta, Georgia, December 1-6, 1991, American Society of Mechanical Engineers, Heat Transfer Division, New York, N.Y., p. 63.
14. A. E. Bergles and W. M. Rohsenow, "The Determination of Forced-Convection Surface-Boiling Heat Transfers," Trans. ASME, J. Heat Transfer 86, 365 (1964).
15. D. C. Groeneveld et al., "Lookup Tables for Predicting CHF and Film-Boiling Heat Transfer: Past, Present, and Future," Nuclear Technology 152, Oct. 2005, p. 87.

16. NUREG-0913, "Safety Evaluation Report related to renewal of the operating license for research reactor of the University of Florida," US Nuclear Regulatory Commission, May 1982.
17. NUREG/CR-2079, "Analysis of Credible Accidents for Argonaut Reactors", prepared by Battelle Pacific Northwest Labs, Richland, WA for the Nuclear Regulatory Commission, Washington, DC, April 1981.
18. Miller, R.W., A. Sola, and R.K. McCardell, "Report of the SPERT I Destructive Test Program on an Aluminum, Plate-Type, Water Moderated Reactor", IDO-16285, Phillips Petroleum Co. NRTS, Arco, Idaho, 1964.
19. Zeissler, M. R., "Non-Destructive and Destructive Transient Tests of the SPERT I-D, Fully Enriched, Aluminum-Plate-Type Core: Data Summary Report," IDO-16886, Phillips Petroleum Co., November 1963. 5.
20. USNRC, "Guidelines for Preparing and Reviewing Applications for the Licensing of Non-Power Reactors, Standard Review Plan and Acceptance Criteria", NUREG 1537, Part 2, February 1996.
21. ANSI/ANS-15.7-1977;R1986;W1996: Research Reactor Site Evaluation, American Nuclear Society, La Grange Park, IL.
22. USNRC, "Assumptions Used for Evaluating the Potential Radiological Consequences of a Loss of Coolant Accident for Boiling Water Reactor," Regulatory Guide 1.3, Revision 2, June, 1974.
23. Federal Guidance Report 11, "Limiting Values of Radionuclide Intake and Air Concentration and Dose Conversion Factors for Inhalation, Submersion, and Ingestion," ORNL, 1988.
24. Federal; Guidance Report 12, "External Exposure to Radio nuclides in Air, Water, and Soil," ORNL, 1993.
25. W.L. Woodruff, "Evaluation and Selection of Hot Channel (Peaking) Factors for Research Reactor Applications," Proc. X International Meeting on Reduced Enrichment for Research and Test Reactors, Buenos Aires, Argentina, September 28 - October 1, 1987, pp. 443-452. This paper was also published as ANL/RERTR/TM-30, February 1997, and can be found on the RERTR Program website: [www.rertr.anl.gov](http://www.rertr.anl.gov) under Analysis Methods.